IS-T-707

GAMMA-RAY DECAY SCHEMES FOR ^{93}Kr, ^{93}Rb, AND ^{93}Sr

Charles Jacob Bischof

Ph.D. Thesis Submitted to Iowa State University

Ames Laboratory, ERDA
Iowa State University
Ames, Iowa 50011

January 1976

PREPARED FOR THE U.S. ENERGY RESEARCH AND DEVELOPMENT ADMINISTRATION UNDER CONTRACT NO. W-7405-eng-82

DISCLAIMER

Available from: National Technical Information Service
U. S. Department of Commerce
P.O. Box 1553
Springfield, VA 22161

Price: Microfiche $2.25

Gamma-ray decay schemes for ^{93}Kr, ^{93}Rb, and ^{93}Sr

by

Charles Jacob Bischof

An abstract of

A Dissertation Submitted to the

Graduate Faculty in Partial Fulfillment of

The Requirements for the Degree of

DOCTOR OF PHILOSOPHY

Approved:

W. L. Talbert, Jr.

In Charge of Major Work

C. A. Swenson

For the Major Department

D. J. Zaffarano

For the Graduate College

Iowa State University
Ames, Iowa

1975

Gamma-ray decay schemes for ^{93}Kr, ^{99}Rb, and ^{93}Sr[1]

Charles Jacob Bischof

Under the supervision of W. L. Talbert, Jr.
From the Department of Physics
Iowa State University

A study of the gamma-ray de-excitation following the beta decays of ^{93}Kr, ^{93}Rb, and ^{93}Sr using the TRISTAN on-line separator facility is reported. Gamma-ray singles and gamma-gamma coincidence measurements were made using Ge(Li) detectors. Of the 162 gamma rays observed in the decay of ^{93}Sr, 143, representing more than 99% of the total gamma-ray intensity observed, were placed in a level scheme containing 36 levels. For the decay of ^{93}Rb, 243 gamma rays were observed, of which 231 are placed in a level scheme consisting of 74 levels. This again represents a placement of over 99% of the total gamma-ray intensity measured. In the case of the ^{93}Kr decay approximately 98.5% of the observed gamma-ray intensity has been accounted for by the proposed level scheme. This results from the placement of 203 of the 217 gamma rays assigned to this decay in a level scheme comprising 56 levels. Beta-branching for these decays were determined from transition intensity balances. Spin and parity assignments were proposed, whenever possible, on the basis of gamma-ray tran-

---

[1]USERDA Report IS-T-707. This work was performed under contract W-7405-eng-82 with the U. S. Energy and Research Development Administration.

sition probabilities and deduced log*ft* values. A comparison is made with the available reaction data for the ^{93}Y level scheme. In all cases an attempt has been made to explain some of the levels in terms of the nuclear shell model and decay systematics.

Gamma-ray decay schemes for ^{93}Kr, ^{93}Rb, and ^{93}Sr

by

Charles Jacob Bischof

A Dissertation Submitted to the
Graduate Faculty in Partial Fulfillment of
The Requirements for the Degree of
DOCTOR OF PHILOSOPHY

Department: Physics
Major: Nuclear Physics

Approved:

W. L. Talbert, Jr.
In Charge of Major Work

C. A. Swenson
For the Major Department

D. J. Zaffarano
For the Graduate College

Iowa State University
Ames, Iowa

1975

TABLE OF CONTENTS

LIST OF FIGURES

LIST OF TABLES

I. INTRODUCTION

The discovery of fission occurred rather accidentally following Chadwick's discovery of the neutron in 1932 (1). In a series of experiments in 1934 Fermi (2) attempted to produce transuranic elements by irradiating natural uranium with neutrons. These irradiations resulted in the production of many different radioactivities, a fact that created much confusion. From 1934 through most of 1938 questions concerning the identities of these radioactive species went unanswered. Finally in 1939 Hahn and Strassman (3,4) provided conclusive proof that some of these radioactive species were isotopes of barium and lanthanum. This explanation was at first offered with some reservation because it seemed inconsistent with previously known nuclear properties.

A. Fission and Beta Decay

The first theoretical explanation for the fission process was proposed by Meitner and Frisch in 1939 (5). They assumed that the fissioning nucleus could be compared to the splitting of a vibrating liquid drop. In this liquid drop model there were two competing terms. The first is the surface potential resulting from the attractive short range nuclear force. The second is the Coulomb potential caused by the repulsive electrostatic force acting between protons. The total potential energy is the sum of these terms. The

overall potential will have a minimum value for a particular equilibrium shape of the nucleus. Any change from this shape results in an increase of the potential energy since the attractive nuclear force dominates. This increase continues until the longer range electrostatic force becomes the dominant factor. From that point on, the potential energy decreases. A potential energy barrier must therefore be overcome in order for fission to take place. In the case of ^{235}U this energy can be exceeded by the capture of a thermal neutron. Meitner and Frisch (5) predicted that the kinetic energy of these fission fragments should be around 200 MeV. Later that same year Frisch (6) offered experimental evidence that the radioactive species observed by Hahn and Strassman did have kinetic energies of this magnitude.

Although the liquid drop model describes the general features of the fission barrier it fails to explain the tendency for heavy nuclei to fission asymmetrically. The fission yield curve for ^{235}U illustrating this preference is shown in Figure 1. In a more recent model (7) it is assumed that as the time of scission is approached, nucleons are transferred between the two nascent fragments. The only restrictions on such a transfer are (1) the potential energy is always minimized and, (2) the two fragments remain in thermal equilibrium. The latter requirement tends to weaken the effects of shell structure by causing nucleons to be transferred in or-

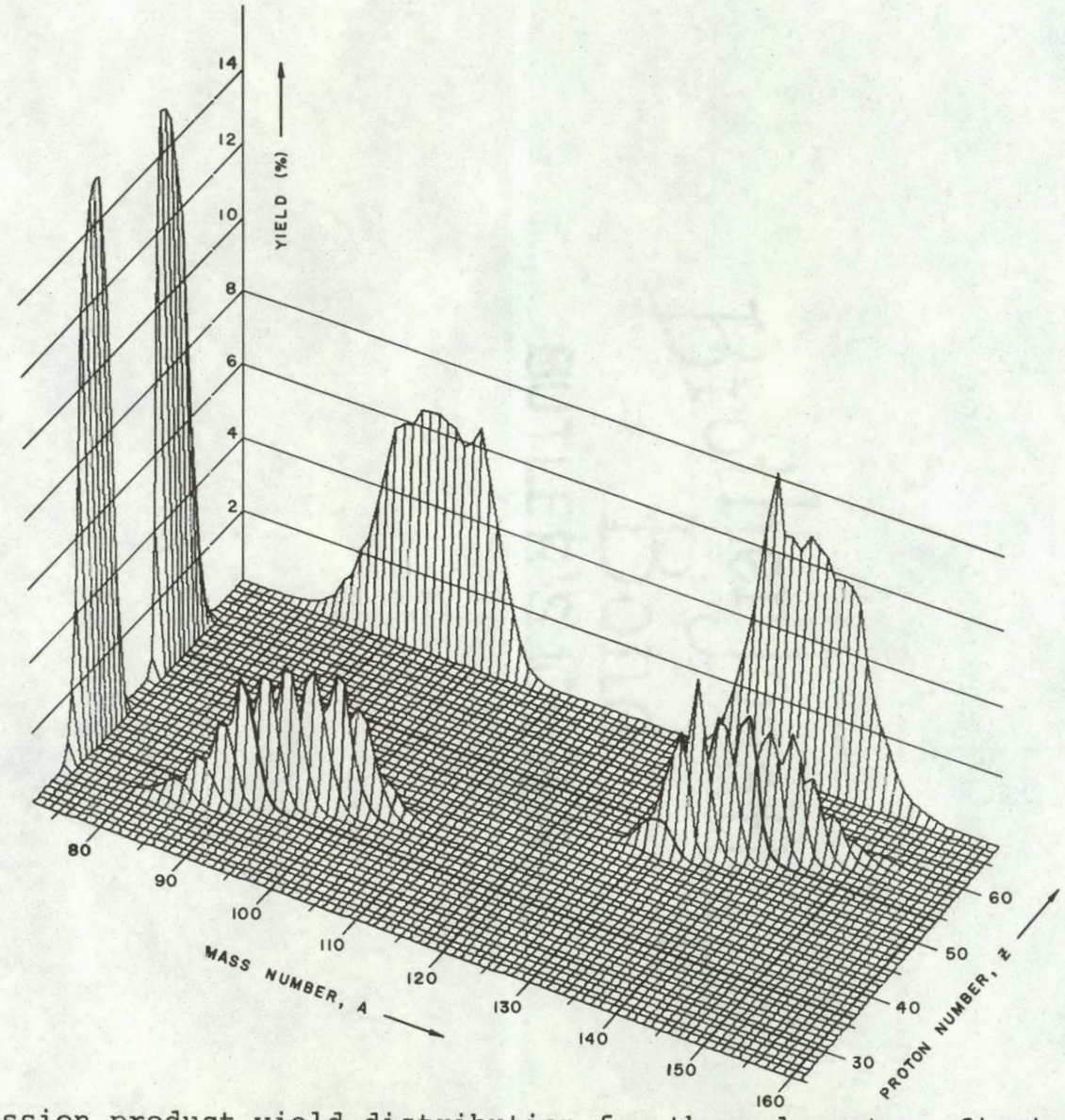

Figure 1. Fission product yield distribution for thermal neutron fission of ^{235}U

der to maintain thermal equilibrium. As the energy of the captured neutron increases this restriction dominates and heavy nuclei display a tendency to fission symmetrically. Such a model reproduces the fission yield curve quite well, except that one would expect the larger fragment yield to peak near A = 132 due to the shell closures for Z = 50 and N = 82. The broadening of the fission yield curve appears to be a result of the requirement that thermal equilibrium be maintained.

The nuclear decays studied in this work are those of ^{93}Kr and two of its daughters ^{93}Rb and ^{93}Sr. The difficulty involved in studying these nuclei is in large part due to their reduced fission yield. The A = 93 chain yield as seen in Figure 1 is 6.39% (8). Looking at the individual members in this chain, however, we see that the cumulative yield for ^{93}Kr is only 0.48% while the cumulative yields for ^{93}Rb and ^{93}Sr are 3.69% and 6.18% respectively (8,9). Further complication results from the fact that ^{93}Kr and ^{93}Rb are delayed neutron emitters, with delayed neutron emission probabilities of 2.6 ± 0.5% and 1.65 ± 0.30%, respectively (10). Furthermore, these two isobars have rather short half-lives as illustrated in Figure 2. Since the neutron number to proton number ratio increases with mass number for the stable nuclei, the fission fragments are extremely neutron rich. Such nuclei undergo a decay process known as beta decay. In

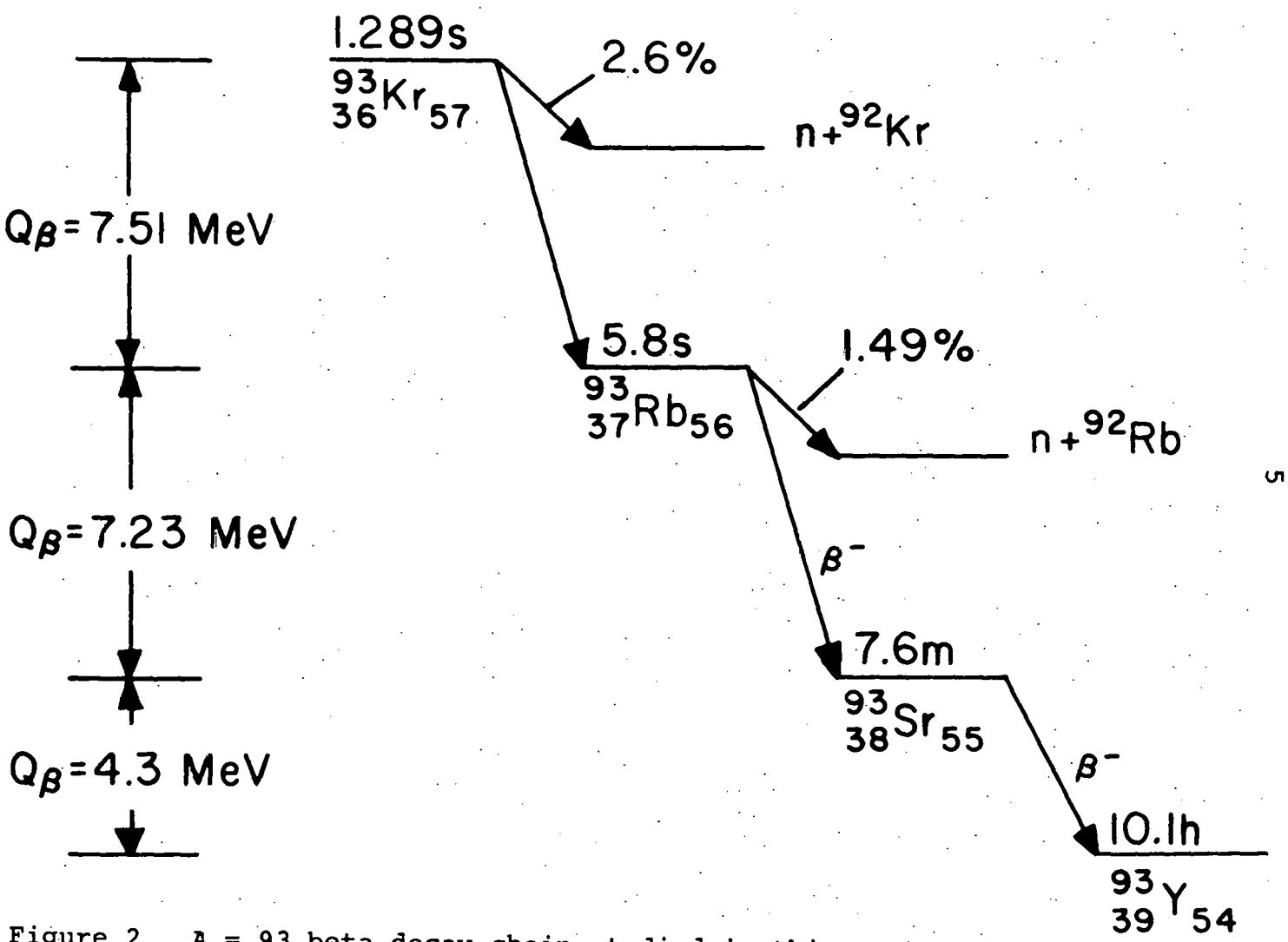

Figure 2. A = 93 beta decay chain studied in this work

this decay process an electron and an anti-neutrino are ejected from the nucleus. The mass number (A) thus remains the same but the number of protons present increases by one. These daughter nuclei may also undergo beta decay until the line of beta stability is reached. As a result of the beta decay process the daughter nucleus may be left either in some excited state or the ground state. The largest amount of energy is released in the decay if the daughter nucleus is left in the ground state and this energy is called the Q-value of the parent nucleus. The Q-values of the nuclei examined in the present work are also shown in Figure 2.

Whether or not states of the daughter nucleus are fed by beta decay is determined by the spins and parities of the initial and final states. Final states having the same parity as the ground state of the parent nucleus and a spin differing by one unit or less are most likely to be fed in beta decay. Transitions of this type are referred to as "allowed" transitions. "Forbidden" transitions are those cases in which a change of parity or any other change in spin occurs. "Allowed" transitions are more probable than "forbidden" transitions for comparable energy differences. Therefore, initial states decaying via a "forbidden" transition have longer lifetimes.

The simplest assumption that can be made for the electron wave function in the theory of beta decay is that it is

a constant equal to its free-particle value at the center of the nucleus. A correction can be made for the distortion of this wave function by the charge of the nucleus. This correction factor is called the Fermi function and is usually denoted by $f(Z,E)$ where E is the energy of the electron and Z is the proton number of the parent nucleus. For allowed transitions the theory predicts that the product $f(Z,E)t$, where t is the half-life of the parent nucleus, is energy independent and a function only of the spins and parities of the initial and final states. This result has also been extended to describe the electron wave functions leading to "forbidden" transitions and can be summarized in the beta decay selection rules shown in Table 1. Generally the log*ft* values are given rather than the *ft* values themselves because of the extreme variations present between "allowed" and "forbidden" processes.

Table 1. Beta decay selection rules

Beta-transition Category	Spin Change	Parity Change
Allowed	0,±1	No
First-forbidden, nonunique	0,±1	Yes
First-forbidden, unique	±2	Yes
Second-forbidden	0,±1,±2,±3	No
Third-forbidden	0,±1,±2,±3,±4	Yes

B. Gamma-Ray Transitions

After beta decay the daughter nucleus is often left in an excited state. This nucleus will then usually de-excite by means of an electromagnetic transition in which a gamma ray is emitted. The theory of such electromagnetic processes is contained in Maxwell's equations. These equations can be expressed in terms of a vector potential ($\bar{A}$) and a scalar potential (ϕ). Nuclear states have a definite angular momentum and parity because the nuclear Hamiltonian is invariant under rotations and reflections. Using this fact, it is advisable to carry out a multipole expansion of the vector potential ($\bar{A}$). Once this is done it is the multipole potential which will be responsible for the electromagnetic transitions between nuclear states. Each gamma ray emitted from the nucleus carries off a total angular momentum L. It can be shown that transitions of multipole order L are favored over those of order L + 1. This expansion can also be divided into electric and magnetic multipoles denoted by EL and ML respectively. It can be further shown that the ML strength is smaller than that of the EL transition. The selection rules for gamma-ray transitions resulting from this multipole expansion are listed in Table 2.

Table 2. Gamma-ray selection rules

Type	Symbol	Maximum Angular Momentum Change, L	Parity Change
Electric Dipole	E1	1	Yes
Magnetic Dipole	M1	1	No
Electric Quadrupole	E2	2	No
Magnetic Quadrupole	M2	2	Yes
Electric Octupole	E3	3	Yes
Magnetic Octupole	M3	3	No
Electric Hexadecapole	E4	4	No
Magnetic Hexadecapole	M4	4	Yes

The absolute transition probability for a given type of multipole radiation depends on the wave functions describing the initial and final states. In most cases the resulting level lifetimes are quite short (10^{-12} - 10^{-15} sec). However, in some cases large changes in angular momentum are required which can lead to extended lifetimes. In fact, measurements of such level lifetimes are useful in determining the multipole order of the transition observed. Using shell model wave functions and assuming single-particle transitions, Weisskopf has made estimates of transition lifetimes as a function of energy and multipole order. These estimates for proton number 40 are shown in Figure 3.

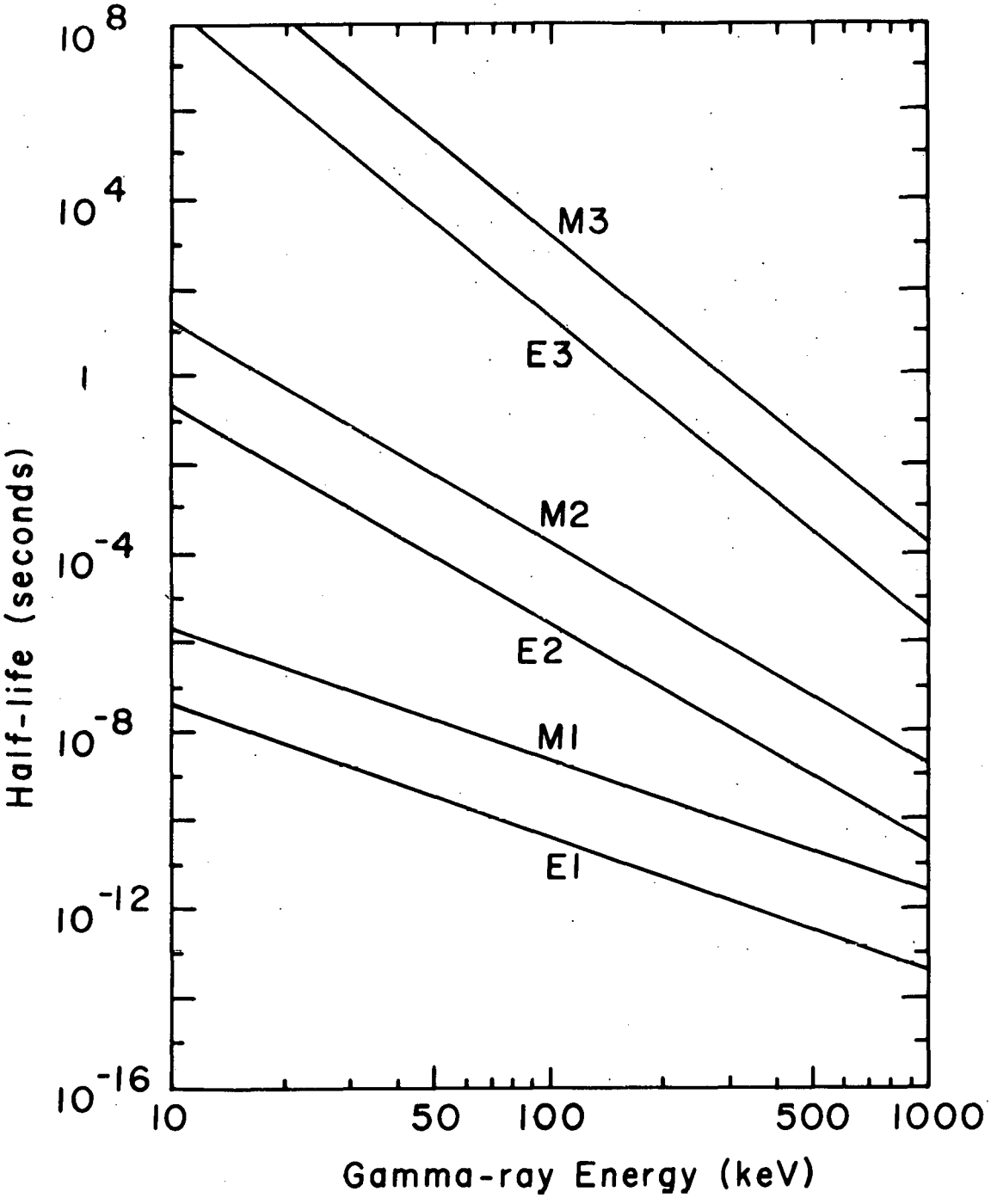

Figure 3. Weisskopf estimate of E1, M1, E2, M2, E3, M3 transition lifetimes for Z = 40

C. Internal Conversion

The internal conversion process competes with gamma-ray emission as a mode of de-excitation for excited states of nuclei. In this process, the nuclear transition energy is transferred to an atomic electron which is then ejected from the atom with an energy equal to the transition energy minus the electron binding energy. A measure of the probability of such an event occurring is the internal conversion coefficient, α. It is defined as the ratio of the number of atomic electrons emitted per unit time to the number of gamma rays emitted for the same transition per unit time, or symbolically, $\alpha = N_e / N_\gamma$. It is possible to distinguish the atomic electrons emitted from each atomic shell. Writing the internal conversion coefficient to accommodate this distinction, we find that

$$\alpha = \alpha_K + \alpha_L + \alpha_M + \cdots$$

This series converges rapidly since the overlap between the nucleus and the wave functions of the outer orbital electrons becomes very small. Furthermore, the probability of internal conversion decreases rapidly with increasing transition energy as well as decreasing angular momentum transfer. Thus it is usually only for the low-energy or high multipolarity gamma rays that internal ccnversion actually competes as a mode of de-excitation.

D. Motivation For This Study

Nuclei having a spherical shape have long been associated with closed shells and the corresponding "magic" numbers of nucleons. The closed shell for neutrons at N = 50 has long been established. Such evidence as the increase in binding energy per nucleon, the increased energy of the first 2^+ excited states, the discontinuity in neutron separation energies, and the decreased thermal neutron capture cross-sections, verifies the existence of shell closure for this neutron number.

For the case of proton configurations in this region there is a controversy concerning whether Z = 38 or Z = 40 should be considered a "semi-magic" number. Various authors (11,12,13) have calculated theoretical level schemes using ^{90}Zr as a stable core, while others (13,14,15,16) have used ^{88}Sr as the core configuration. In both cases the results have been consistent with the experimental data available. The energies of the first 2^+ excited states of the even-even isotones for various neutron numbers are shown in Figure 4. In each case the energy of this state is maximum for either Z = 38 or Z = 40. However, in each case where the energy peaks for Z = 40 there exists at moderately low energies a second 0^+ state. Configuration interaction between this state and the ground state would tend to lower the energy of the ground state.

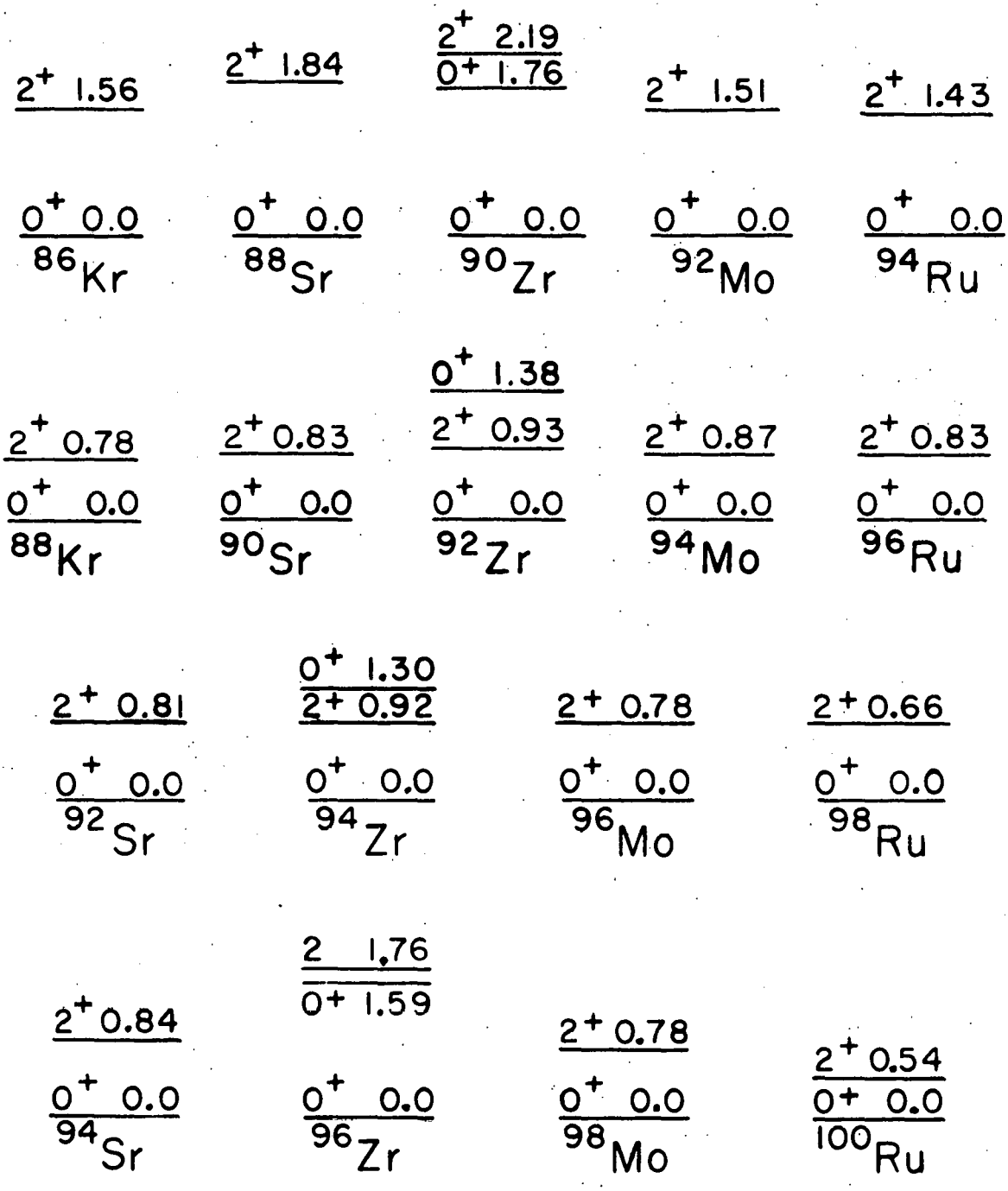

Figure 4. First 2^+ excited states of even-even isotones for N = 50, 52, 54, and 56

If correction is made for this energy shift it is likely that the energy of the first 2^+ state is greatest for Z = 38.

Although the above discussion fails to resolve the dilemma over which proton number is "semi-magic", the point that these nuclei should be described using the shell model is unaffected. Plotting the quadrupole moment versus Z indicates small or zero moments in the region of Z = 38,40 (17). The level schemes of these nuclei also agree well with the vibrational spectrum expected for oscillations about a spherical equilibrium shape. It seems reasonable then to assume that nuclei near A = 90 have a spherical shape.

In 1965, S. A. E. Johansson (18) reported the first evidence for deformed nuclei in the A $\sim$ 100 mass region. His study of the delayed gamma-ray spectra from ^{252}Cf fission fragments indicated similarities between these spectra and the spectra observed for the rare-earth nuclei, which had already been determined to be permanently deformed. As a result of his observations he predicted that nuclei with A $\sim$ 110 would be most likely tc be permanently deformed. Cther calculations performed later predicted stable deformations for $^{100-110}$Zr, $^{98-108}$Sr and $^{96-106}$Kr. Finally in 1970, Cheifetz, et al. (19) presented experimental evidence cf the rotation-like behaviour of ^{102}Zr and ^{106}Mo. They also noted that the E(4+)/E(2+) ratio as well as the B(E2)exp./B(E2)s.p. ratio undergo extreme changes between ^{98}Zr and ^{100}Zr. It

appears then that the existence of this new deformed region is quite well established. Examining this information, it becomes obvious that much might be learned by examining the transitional nuclei connecting the two regions of spherical nuclei around A = 90 and deformed nuclei around A = 100. The members of the A = 93 mass chain studied in this work represent such transitional nuclei.

In the history of nuclear physics much information has been gained through a systematic study of neighboring nuclei. Often, a significant trend was noted only after information on many neighboring nuclei was compared. In the absence of a unified model for the nuclear force the best approach is to accumulate as much experimental data as possible in hopes of providing some insight intc the properties of this force. The present work is also an attempt to supply such information for nuclei far from the line of beta stability.

In 1970 Grueter, et al. (20) reported the existence of a 257-keV gamma ray associated with a 57-μsec isomeric state in ^{93}Rb. Later Grueter (21) detected two 1.4-μsec gamma rays and assigned them to an isomeric state in ^{93}Sr. Earlier, Johansson (18) and others found that such isomeric states populated during fission were concentrated into a few narrow mass regions. Prior to this work Cavallini, Schussler, and Moussa (22) had already found that a 168-keV gamma-ray transition depopulated a 759-keV isomeric state in ^{93}Y.

Finally, the information on gamma-ray and beta-ray energies and the associated decay intensities of fission products such as those examined in this study is of interest to those involved in reactor physics calculations. Charged particles interact strongly with the structural material of the reactor. As a result, their energy is deposited in the form of heat very near the point of emission. Gamma rays, on the other hand, penetrate these materials to a much greater extent. Thus their energy can be deposited as heat far from the point of emission, provided their energies are large enough. In addition, beta particles having energies of several MeV or more will lose their energy by emitting intense bremstrahlung radiation. The relative strengths of such radiative processes must therefore be taken into consideration when designing the shielding and cooling structures of a workable reactor.

E. Previous Studies

The decay of ^{93}Sr was first identified by C. Lieber (23) in 1939. She identified this isotope as the 7-minute component observed in the Sr activity decay curves she was studying. Several measurements of this half-life have been reported but the most accurate appears to be 7.32 ± 0.10 min from Carlson, et al. (24). Q-values varying from 3.8 MeV to 4.8 MeV have been reported in the literature. The most con-

sistent value however, is probably 4.3 ± 0.2 MeV as reported by Bakhru and Mukherjee (25) and by Herzog and Grimm (26). It should be mentioned that, in the discussion of the ^{93}Y level scheme, evidence will be provided for favoring the upper limit on this Q-value. The first partial level scheme based on Ge(Li) detector gamma-ray spectra was proposed by Cavallini, Schussler, and Moussa (22). In this work 40 gamma rays were identified of which eight were placed in a level scheme composed of seven levels. These authors were also the first to note the existence of a 759-keV isomeric state. Later, using a similar approach, Herzog and Grimm (26) proposed a level scheme based on 55 transitions between 23 levels. They also assigned spins and parities to the six lowest levels based on the $^{94}Zr(d,^{3}He)$ reaction work of Preedom, et al. (27). The most recent comprehensive gamma study of this decay was performed by Achterberg, et al. (28). Besides placing 69 transitions within a scheme of 25 levels, Achterberg, et al. determined the conversion coefficients for the 168- and 590-keV transitions as well as a half-life of 85 ± 15 msec for the 759-keV isomeric state. However their value for the half-life is in great disagreement with a more recent determination of 820 ± 40 msec by Casella, Knight, and Naumann (29) which has been adopted in this work.

Experimental evidence for the existence of ^{93}Rb was first presented in 1960 by Fritze and Kennett (30). Never-

theless, its existence had been guaranteed in 1951 when Dillard, et al. (31) identified its gaseous fission product parent ^{93}Kr. The most accurate half-life measurement was performed by Carlson, et al. (24) who stated that the half-life was 5.86 ± 0.13 sec. Clifford, et al. (32) measured the Q-value to be 7.23 ± 0.10 MeV. This is in fairly good agreement with the value of 7.55 ± 0.15 MeV reported by Macias-Marques, et al. (33). A single beta-gamma coincidence gate was also reported by Clifford, et al. However, because a definitive decay scheme did not exist at the time of Clifford's experiment, he was not able to include in his analysis the various beta groups which contribute to the gated beta spectrum. This complication makes it inadvisable to adapt the end-point energy value for the gated spectrum reported in his study as a means of deducing the Q-value.

A Q-value of 5.75 ± 0.10 MeV has been proposed by Brissot, et al. (34) based on several coincidence gates. The level scheme proposed in the present work, however, has several well-established levels at energies greater than 6.0 MeV. Therefore a Q-value below this energy seems unlikely. This value is also much lower than the Q-values predicted by Garvey, et al. (35), Seeger (36) and Wapstra and Gove (37).

Until recently no level scheme existed for ^{93}Sr. In the last six months though, two articles have been published on this decay. Achterberg, et al. (34) provided a level

scheme of 20 levels connected by 37 transitions. They also determined the multipolarity of the three lowest-energy gamma rays on the basis of measured internal conversion coefficients. In an almost simultaneous publication Brissot, et al. (34) offered a quite different level scheme comprised of 69 transitions placed among 25 levels. There was also little agreement between the gamma intensities quoted in these two articles. The gamma-ray intensities obtained as a result of the present work should help to resolve this discrepancy.

Brady and Sugarman (38) first discovered that the 10-h ^{93}Y activity results from a gaseous parent. Unfortunately, at that time no mass assignment had been made for this yttrium isotope. Dillard, et al. (31) determined that the Kr parent had a half-life of 2.0 ± 0.5 sec but incorrectly assigned it to the mass 95 chain. Later Selikson and Siegel (39) examined the daughter activity resulting from the 10-h Y decay and noted that a negligible amount of ^{95}Zr was present. They argued that this 10-h Y activity should be credited to the mass 93 chain. This was also supported by cumulative fractional yield measurements performed by Glendenin, Coryell, and Edwards (40). The ^{93}Kr activity has thus been established as a direct fission product. As before, a reliable half-life measurement of 1.289 ± 0.012 sec has been made by Carlson, et al. (24).

Clifford, et al. have reported a Q-value of 8.3 ± 0.5 MeV for the beta decay of ^{93}Kr based on a beta singles spectrum. Beta decay endpoint energies were also quoted for four beta-gamma coincidence gates. However, since no decay scheme existed at the time of Clifford's study it was not possible for him to calculate a Q-value based on these spectra. Using the level scheme presented in this work, along with the beta endpoint energies reported by Clifford, a new value for the Q-value of this decay has been determined. A weighted average of the values obtained from the four gates yields a Q-value of 7.51 ± 0.05 MeV. This is in agreement with the Q-value of 7.3 ± 0.2 MeV reported by Brissot, et al.

As in the case of the ^{93}Rb decay, no decay scheme existed for ^{93}Kr prior to the publication of the studies by Achterberg, et al. and Brissot, et al. The two level schemes presented for ^{93}Rb are fairly consistent, but again there is disagreement in the reported gamma-ray intensities.

It should be noted that Achterberg, et al. proposed positive parity for the ground state and the first four excited states of the ^{93}Rb level scheme. This parity assignment seems unlikely because of the predominance of negative-parity shell-model states available in the region around Z = 37. The present study will indicate that the parity of these levels is probably negative in agreement with the predictions of the shell model.

II. EXPERIMENTAL METHODS

The A = 93 isobars reported on in this work are only a small part of a continuing study of ^{235}U gaseous fission products being carried out at the TRISTAN facility. This facility consists of an on-line isotope separator in conjunction with a switch magnet which directs the mass-selected ion beam to one of three stations. Each of these three stations is equipped with a different experimental apparatus to be used for nuclear spectroscopy studies. An overhead view of this facility is shown in Figure 5. An article by J. R. McConnell and W. L. Talbert (41), soon to be published, provides a thorough description of this installation. Consequently, only a sketch of the major components of the system will be reproduced here.

A. Isotopic Separation of ^{235}U Fission Products

The gaseous fission products are obtained by placing a sample of an average mass of 8 gm of uranium stearate in an external neutron beam provided by the Ames Lab Research Reactor. The uranium stearate is composed of approximately 25%, by weight, fully-enriched ^{235}U. The maximum neutron flux is around 3×10^9 thermal neutrons/cm^2/sec. After the fission products are released they are transferred to an ion source through a neoprene transport line with an inner liner of teflon. The diffusion of these fission products through the

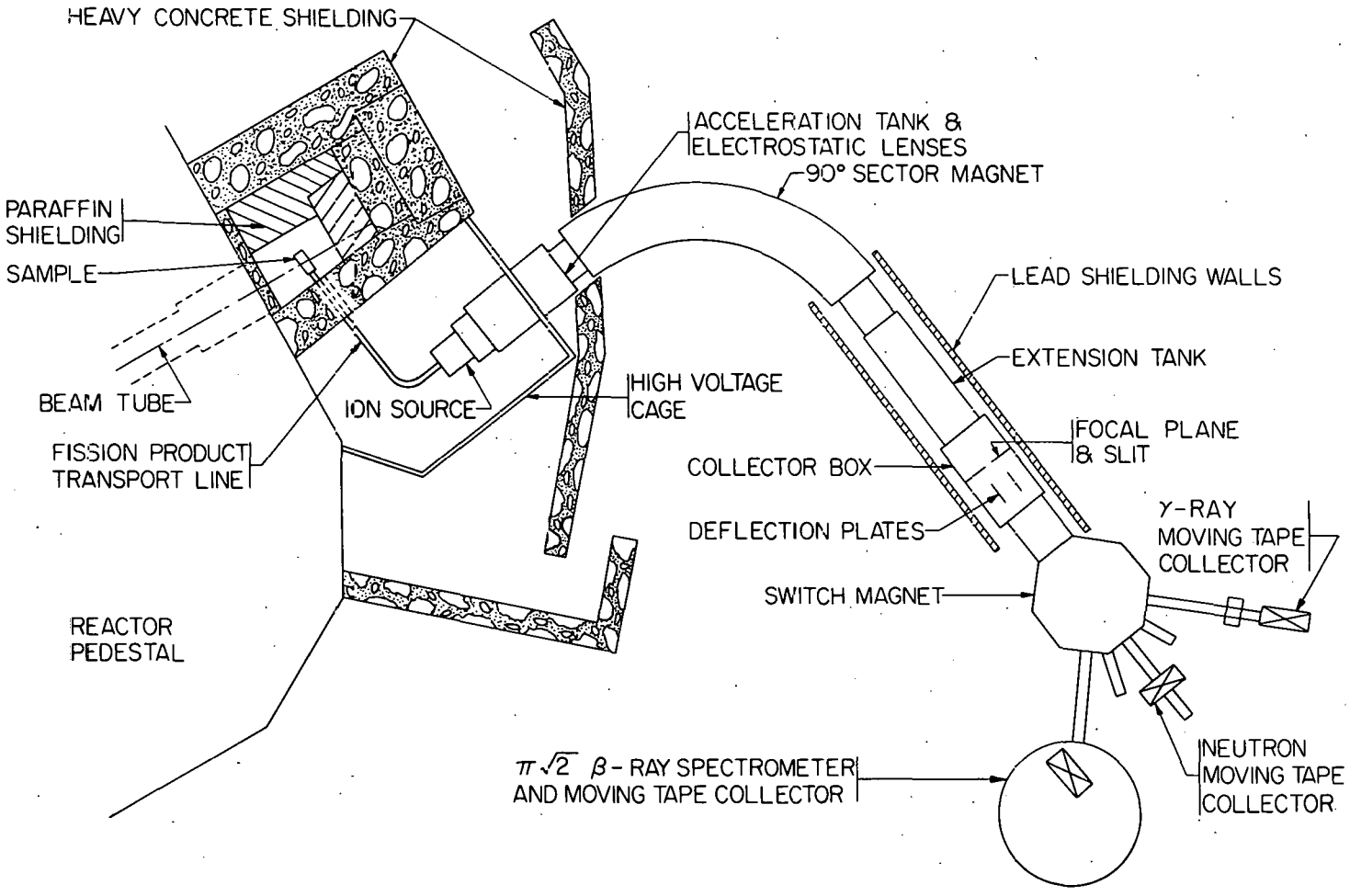

Figure 5. Schematic overhead view of TRISTAN facility

transport line is aided by the introduction of a mixture of He, Xe, and Kr gases. The Xe and Kr gases, representing only a few per cent of this mixture, are used as mass markers and a convenience for beam focusing adjustments.

An extractor lens, operating at approximately 5 kV, draws the ions out of the ion source. After extraction, the ions pass through acceleration and electrostatic focusing lenses. The acceleration potential was usually 55 kV during these experiments. Following passage through the focusing lens, the ions enter a 90° sector magnet of mean radius 160 cm. It is this magnetic field which actually provides the isotopic separation of these icnized fission products. The mass separation has been proven to be quite good with contamination from masses A ± 1 in the mass A deposit being on the order of 1 part in 5×10^5 (41). Extreme contamination can result, however, from the A - 1 mass chain in the form of KrH^+ molecular ions. This contamination is most evident in the study of low-yield, high-mass Kr chains, such as that in this work. The amount of hydride contamination appears to depend mostly on the age of the uranium stearate sample. In most cases after ten to twelve weeks of stearate exposure to the neutron beam, this hydride contamination was less than 1 or 2 per cent. For the ^{93}Rb and ^{93}Sr decay studies this contamination was of less importance due to additional circumstances. The ^{92}Rb decay proceeds almost entirely to the

ground state of ^{92}Sr. As a result there are very few gamma rays of sufficient intensity to contaminate the ^{93}Rb decay spectrum. Because ^{92}Sr and ^{93}Sr have very different half-lives, 2.69 h and 7.5 min respectively, the amount of ^{92}Sr activity accumulated during the usual beam collection time was very small.

After the mass dispersion by the magnet, the beam enters the collector box. Inside the collector box are located stabilization pins, a fluorescent screen, and a mass-defining slit. The fluorescent screen is an Al plate coated with KBr. The appearance of the stable Kr marker beam on this screen is used to find the initial separator control settings. The magnet current can then be adjusted such that the desired mass passes through the defining slit. When the beam is in position the stabilization pins are adjusted such that a neighboring mass is situated between the two pins. The beam position stabilizer then monitors the current striking each pin. If a current imbalance occurs the stabilizer makes a correction in the acceleration voltage in order to return the beam to its original position. Immediately following the mass slit is a pair of vertical deflection plates. The beam can be deflected at this point by applying a potential of 800 volts to these plates. This deflection voltage was usually utilized in conjunction with the moving tape collector (MTC) and the daughter analysis system.

The switch magnet deflects the beam through an angle of 45° along a path having a mean radius of curvature of 45 cm when using the MTC. This magnet also provides a second mass separation, thus helping tc reduce further the level of cross contamination.

B. Isobaric Separation of A = 93 Activities

The beam being deposited on the aluminum coated mylar tape of the MTC consists of the first member of the isobaric decay chain selected. The isobaric separation of the resulting activities is performed mechanically. Figures 6 and 7 are photographs of the previous and present models of the MTC. The ^{93}Sr and ^{93}Rb decays were studied using the clder model while the newer model was utilized for the ^{93}Kr decay work. The newer model was especially suited for the ^{93}Kr experiments for several reasons. First of all the tape drive system was reversible. Thus when studying short-lived activities it was possible to rewind the tape when the supply reel was empty. Since the beginning of the tape had not been exposed to the beam for about 12 hours or more the amount of contaminant activity was negligible relative to backgrcund activity. The rewind time was usually around one hour. This was much less than the time required to remove the shielding, open the "old" MTC, replace the tape, and pump down. Secondly, the new MTC has larger reels capable of holding four

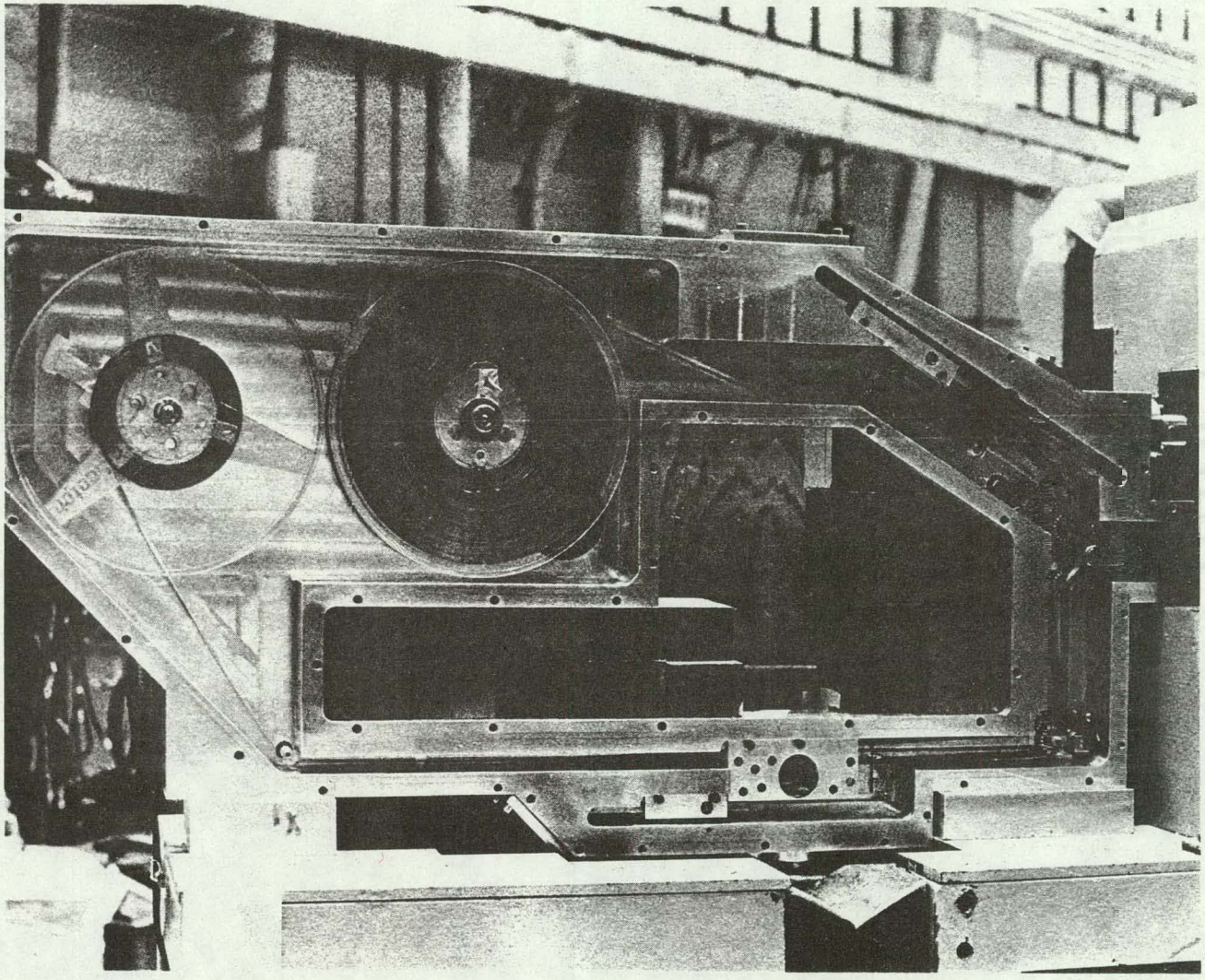

Figure 6. Photograph of second generation moving tape collector (MTC)

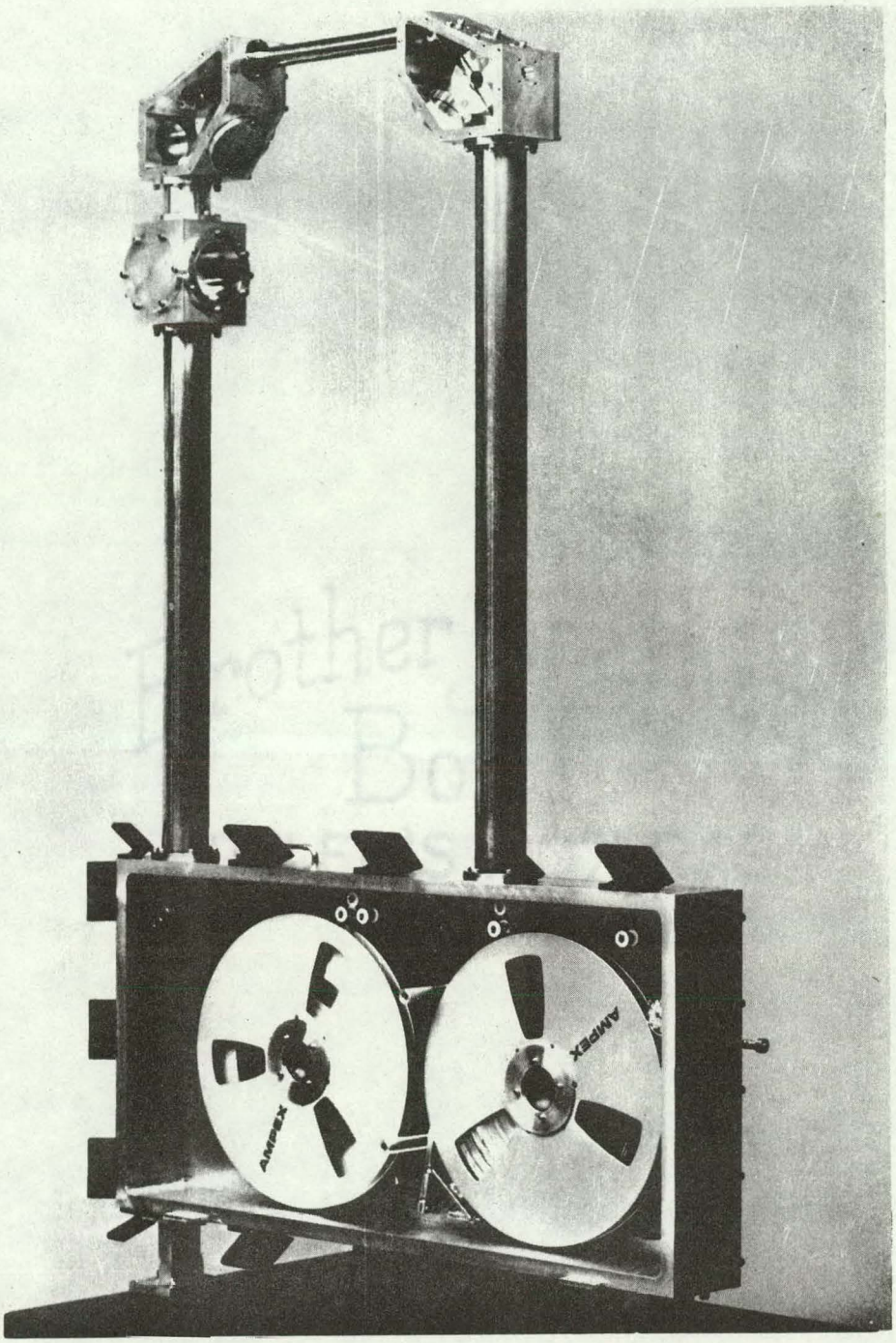

Figure 7. Photograph of third generation moving tape collector (MTC)

times as much tape. As a result, a smaller fraction of the total run time is spent in replenishing the tape. Finally, the takeup reel is further removed from the location of the Ge(Li) detectors. Because of this increased separation any activity buildup on the previously exposed tape was not detectable. This had previously been a problem on experiments involving low-yield mass chains.

"Parent" and "daughter" ports are present on both MTCs. During the ^{93}Kr experiments the "parent" port was used and the tape was moved every 7 seconds in order to reduce contamination by daughter activities. While the tape was in motion the beam was interrupted by applying a voltage to the deflection plates and the multichannel analyzer was gated off. Cycling of the tape, deflection voltage and the analyzer is controlled by the Daughter Analysis System (DAS). For the low energy gamma-ray studies a thin mylar window replaced the usual aluminum cover on the "parent" port.

The ^{93}Rb and ^{93}Sr data were collected using the "daughter" port. Using suitably chosen beam collection, delay, and accumulation times it is possible to enhance each daughter activity independently. The minimum delay time is the time needed to transfer the activity from the "parent" to the "daughter" port. The program ISOBAR (42) aids in deciding which collection, delay and accumulation times will yield optimum enhancement.

C. Ge(Li) Detectors Utilized

Singles and coincidence data were obtained using 60-cm^3 Ge(Li) detectors. Additional studies were made of the low energy gamma-ray spectrum cf ^{93}Kr. Both LEPS (Low Energy Photon Spectrometer) singles and LEPS - Ge(Li) coincidences experiments were performed on this decay. In fact, two separate LEPS measurements were made on the low energy gamma-ray spectrum of ^{93}Kr. The first was used to provide accurate energies and intensities for the region 0 - 400 keV. This was later repeated with a higher resolution LEPS detector in order to resolve the 253-keV multiplet. The final fit of this multiplet, reproduced in Figure 8, indicates the degree of resolution possible with this detector. The specifications for all of these Ge(Li) detectors are listed in Table 3.

Table 3. Ge(Li) detector specifications

Detector Geometry	Active Volume (cm^3)	Resolution @ Energy (keV)	Efficiency	Peak/Compton for 1332-keV Gamma Ray
true coaxial	57.3	2.7 @ 1332	11.8%	34/1
true coaxial	58.2	2.7 @ 1332	9.0%	28/1
planar	1.0	0.750 @ 122	N.A.	N.A.
planar	1.0	0.450 @ 122	N.A.	N.A.

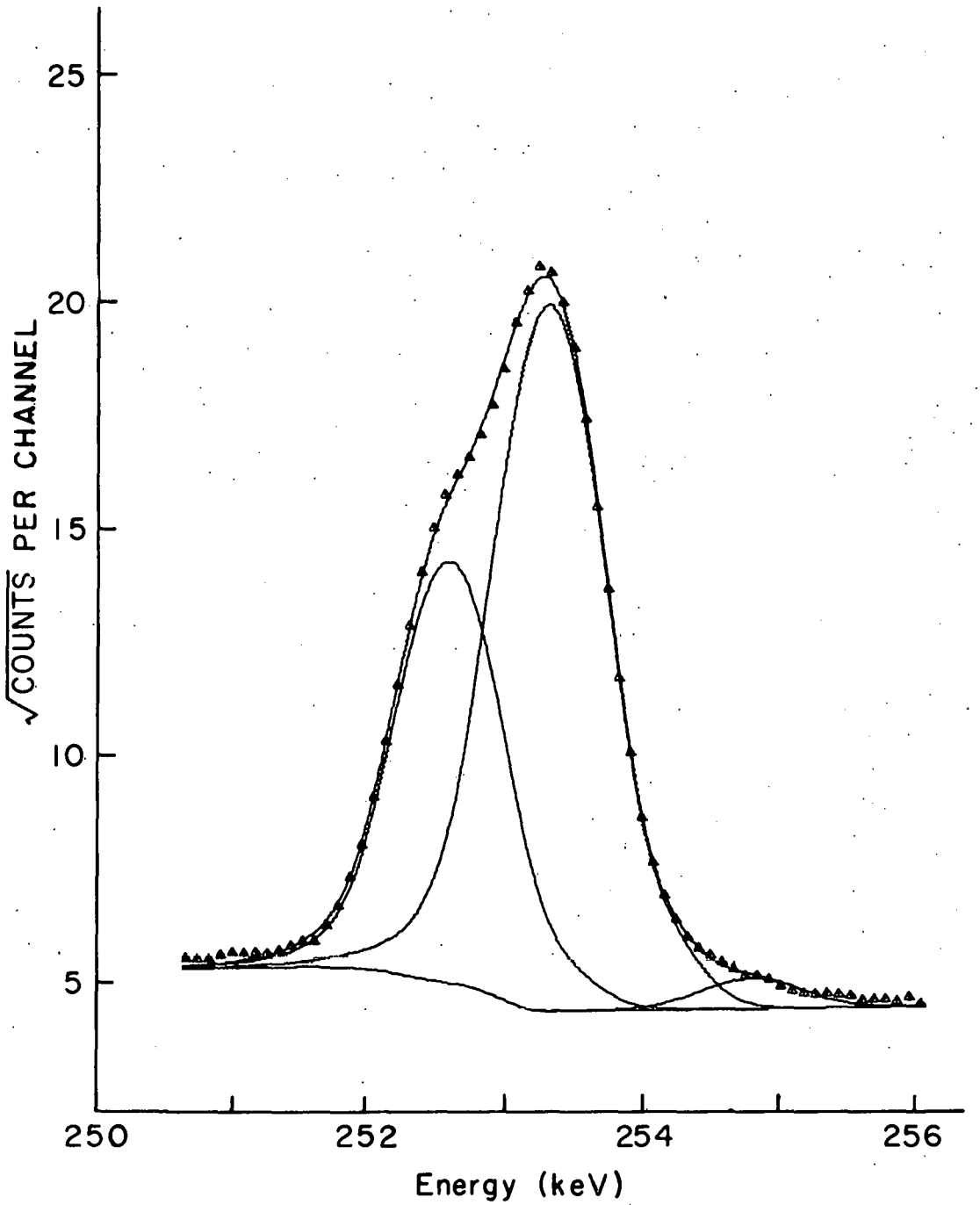

Figure 8. SKEWGAUS fit of 253-keV multiplet

D. Electronic Systems used for Data Accumulation

A block diagram of the electronic circuit used to accumulate the gamma-ray singles spectra is shown in Figure 9. This arrangement by itself was used only for the initial scan of the 93 mass chain. In all later experiments the singles data were accumulated in conjunction with gamma-gamma coincidence experiments. The section of the circuit responsible for simultaneous singles data accumulation was, however, unchanged from that presented in Figure 9. The discussion of this circuit will therefore pertain to both of these cases.

The detector chosen for singles studies was one of the 60-cm^3 detectors, or one of the 1-cm^3 LEPS detectors, depending on the energy region of interest. The linear amplifier was either an Ortec 452 or a Tennelec TC 203BLR. Both have internally compensated differentiation and integration time constants, base line restoration, and adjustable pole-zero cancellation. In the case of the Ortec (Tennelec) amplifier the DC bipolar output was used with a three microsecond (four microsecond) time constant. In all cases the amplifier was DC coupled to a Geoscience 8050 ADC having an 8K conversion capacity. Pile-up rejection for high counting rates was also handled by the Geoscience ADC. For all except the last ^{93}Kr LEPS study the signals were processed by a Technical Measurement Corporation 16K analyzer having a single channel capacity of 10^5 counts. A Geoscience Nuclear 5010 4K analyzer

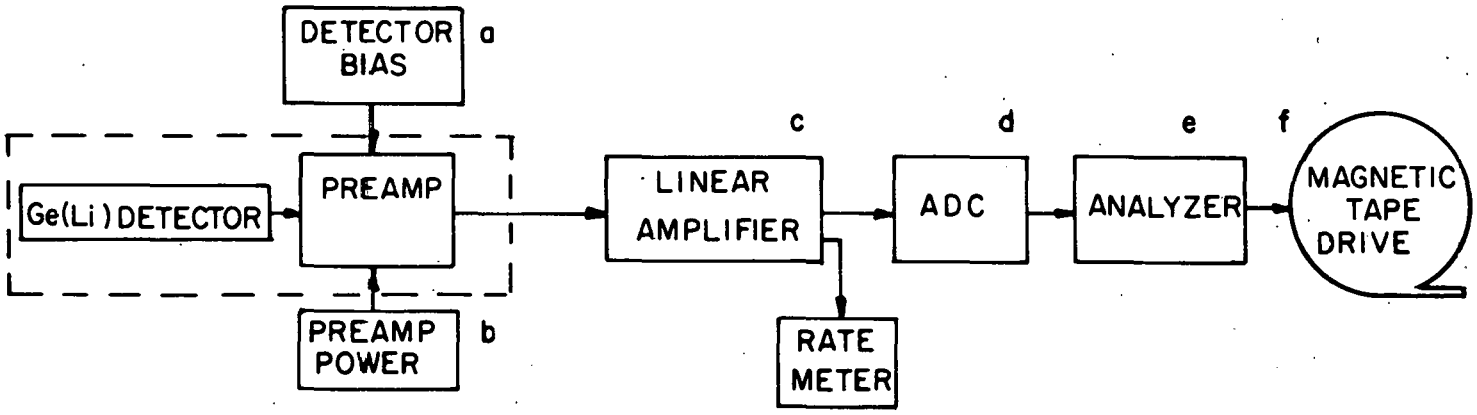

Figure 9. Block diagram of gamma-ray singles collection circuit

having a single channel capacity of 2^{20} counts was used in the special case mentioned above. As the number of counts in the most likely channel approached overflow the analyzer was stopped and the contents of the memory were destructively recorded on a seven-track tape. A Hewlett-Packard Tape Unit (Model 2020) recorded the memory output for the TMC analyzer. The memory content of the Geoscience analyzer was recorded by means of a Peripheral Equipment Corporation Tape Unit (Model 6860-75).

Since the activity available from the mass 93 chain is rather low, a circuit such as that shown in Figure 10 was used for almost all of the gamma-gamma coincidence experiments. This arrangement made it possible to collect singles and coincidence information simultaneously. Normally each of these experiments would require about six to seven days of data accumulation time so that performing them together was extremely time-saving.

Two Ge(Li) detectors separated by approximately four cm were positioned in 180° gecmetry for all coincidence studies. For the ^{93}Kr, ^{93}Rb, and ^{93}Sr studies, two 60-cm^3 Ge(Li) detectors were employed to observe coincidence events. Due to the complexity of the low energy gamma-ray spectrum for the ^{93}Kr decay, an additional coincidence study was made using a 60-cm^3 Ge(Li) detector and a 1-cm^3 Ge(Li) LEPS detector. Listed in Table 4 is the equipment used in the coincidence portion of the circuit.

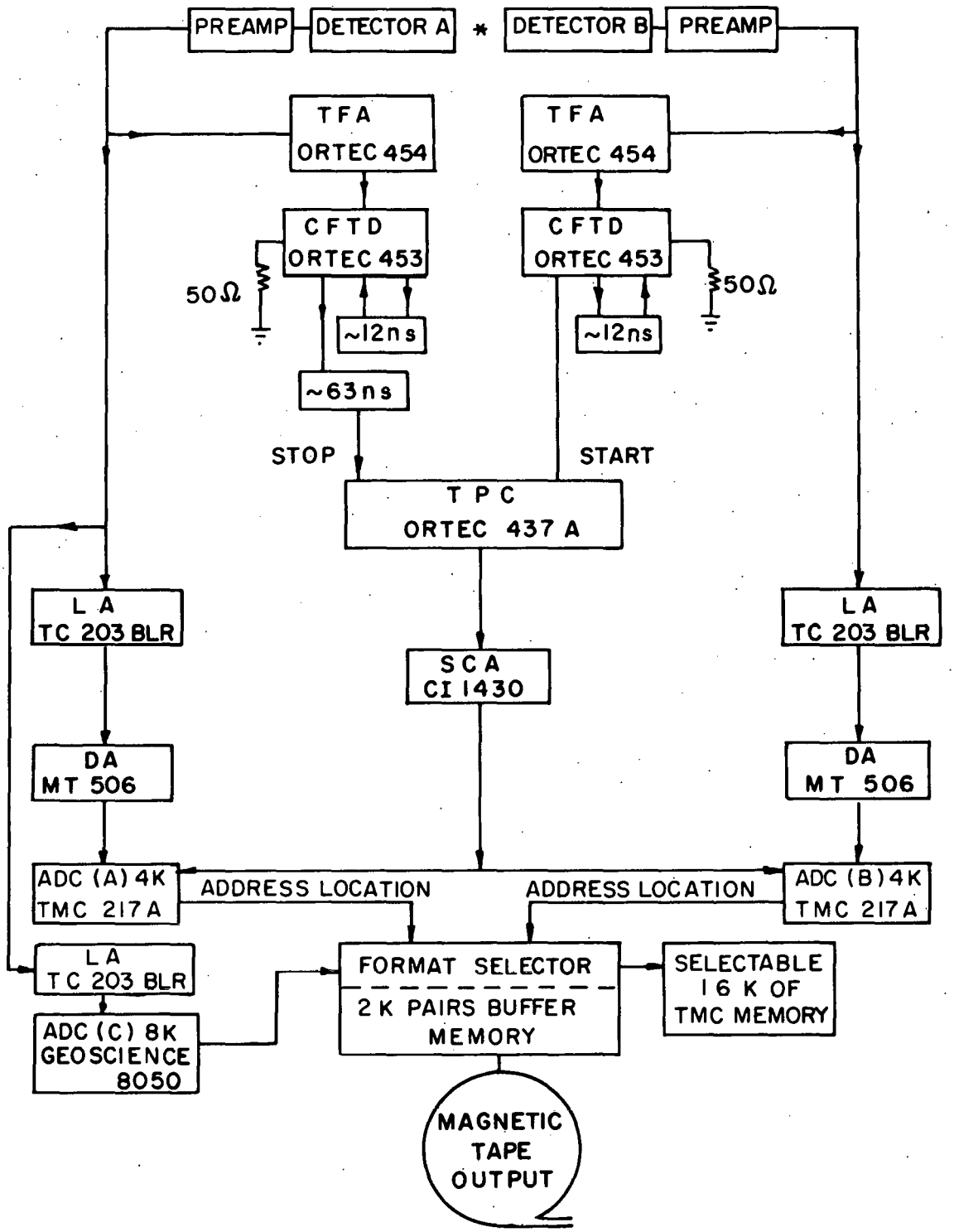

Figure 10. Block diagram of simultaneous singles and coincidence circuit

Table 4. Equipment utilized for gamma-gamma coincidence studies

Preamps: Ortec 117A(LEPS) and Ortec 120(60-cm^3)
Timing Filter Amplifiers: Ortec 454
Constant Fraction Timing Discriminators: Ortec 463
Delays: Measured delay cables
Time-to-Pulse-Height Converter: Ortec 437A
Single Channel Analyzer: Canberra 1430
Linear Amplifiers: Tennelec 203BLR
Delay Amplifiers: Mechtronics 506
ADC's: Geoscience 8050

A coincidence event is determined by the timing between signals from the two detectors. The signals from one detector are used as a start signal for the time-to-pulse-height converter (TPHC). The signals from the other detector are delayed by 63 ns and act as a stop signal for the TPHC. The single channel analyzer then selects a region of pulse heights (usually around 40 ns) which correspond to coincidence events. Whenever the output of the TPHC falls within this 40 ns "window" an output signal of fixed amplitude gates the ADC's to accept the two original signals. A block diagram of the coincidence timing circuit is shown in Figure 11.

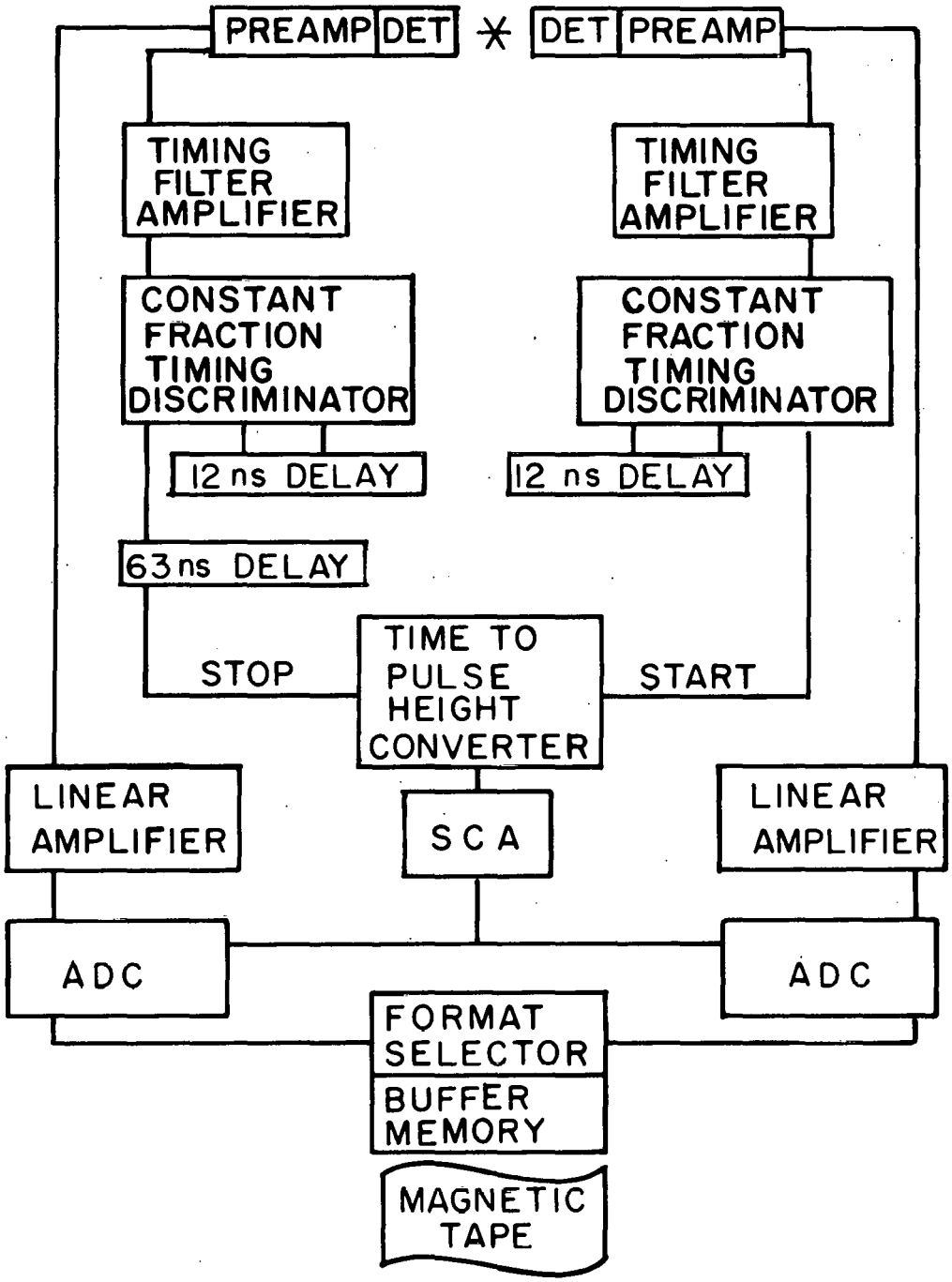

Figure 11. Block diagram of gamma-gamma coincidence timing circuit

The multiparameter Tape Buffer System storing the coincidence information is composed of three main components, the format selector, the 2 x 2K memory buffer and a Precision Instruments Model PI 1200 incremental tape drive. The format selector stores the coincidence information in the form of pairs of channels corresponding to the two coincident gamma-ray signals. These pairs are stored in the buffer memory until 2K such buffers have been observed. At that time the "buffer" of 2K coincident pairs are transferred to magnetic tape. Later the spectrum of gamma rays in coincidence with any gamma ray of interest can be obtained using the program BUFFTAPE. The user selects the upper and lower channels representing the gating gamma-ray limits. The program then searches and records the spectrum defined by the second member of all pairs whose first member falls in the increment defined by these two channels.

III. DATA ANALYSIS

A. Addition of Shifted Spectra

The relatively low counting rates observed with the A = 93 decay chain resulted in prolonged runs of six or seven days. During this time it was difficult to maintain a constant count rate and experimental environment. As a result, shifts in the gamma-ray spectrum peak locations were unavoidable. An option to the program DISKRITE was used to correct for such gain shifts. In some cases, large gain shifts were noted during the collection of a single spectrum. Because it is impossible tc correct for such a shift these spectra were discarded. Such circumstances were extremely rare, however, and in all cases the fine resolution afforded by Ge(Li) detectors was preserved.

B. Calculation of Energies and Intensities

In order to identify the unknown peaks of the decay being studied, three different types of spectra were examined. The first type was composed of gamma rays observed in the decay of known calibration sources plus the "unknown" source. The energies of these known calibration peaks were used to calculate the energies of the more intense "unknown" peaks. Above 3.55 MeV, the highest energy calibration peak available, the energies of the single- and double-escape peaks were used to obtain the energy of the corresponding

photopeak. In this way the energy calibration can be extended to the highest energy observed peak.

These previously-determined energies were then used as an internal calibration in the second type of spectrum, that of the "unknown" source alone. Such spectra were taken in order to remove the possibility of calibration peaks coinciding with weaker "unknown" peaks. The third type of spectrum consisted of background peaks alone. This background spectrum was used to eliminate any contaminant peaks which may have been present. The prcgram SKEWGAUS was used to determine peak locations and areas as well as their associated errors. These locations and areas were then converted tc energies and intensities by the program DRUDGE.

C. Determination cf Coincidence Events

The determination of coincidence events was facilitated by the use of the program BUFFTAPE. Two gates were set for each gamma ray whose coincident spectrum is desired. The first gate included the gamma ray of interest. The second gate included channels above and below this peak with the total number of channels equalling that of the first gate. This second gate was termed the "background" gate and was used to eliminate the coincidences resulting from Compton-scattered events of the same energy. Peaks having significantly greater areas in the first gate were considered to be "true" coincidences. The decisions concerning which peaks

have significant area differences were made either by visual inspection or with the aid of the program BRUTAL.

D. Construction of Level Schemes

The initial level scheme was built for each decay by attempting to place three or four of the most intense peaks. Once the first few excited states were verified, further levels were then constructed using available coincidence information and energy sums. Subsequent placement of gammas can best be accomplished through use of the program LVLSURCH. The final decision on whether or not a level should be kept depends on the number of gamma transitions feeding or depopulating a level as well as any possible or definite coincidences. Defining the confidence index (CI) as the sum of these respective occurrences the following expression results:

$$CI = n_{\gamma} + 2n_{c} + n_{pc}$$

The requirement for keeping a level is then expressed simply by stating that the confidence index must be equal to or greater than a certain value. In this work, this value has been chosen to be four.

E. Beta Branchings and Log*ft* Values

Following the placement of all possible gamma transitions the internal conversion coefficients (ICC's) for each transition were calculated with the program TICC. The multi-

pole order of each transition should, in principle, be known, but, in most cases this information does not exist. If this is the case the calculation was performed assuming the transition is 50% E2 plus 50% M1. Over a rather large energy range, this assumption is acceptable, since the two multipolarities exhibit nearly equal conversion coefficients. Also, in some instances experimentally measured ICC's may be available in which case these values can be substituted for the calculated coefficients. The actual transition intensity is then $(1+\alpha)I_\gamma$, where I_γ is the measured gamma intensity. This information was required as input to the program LEAF which was used to find the per cent beta branching to each level, given the amount of ground-state beta feeding. For the ^{93}Kr and ^{93}Rb decays the per cent delayed neutron branching must also be used to correct these branching percentages if they are to be expressed in absolute terms (per 100 decays). The log*ft* values for the observed beta feeding were then determined by means of the program LOGFT, making use of the output from LEAF and the known Q-value for the decay.

F. Assignment of Spins and Parities

Spin and parity assignments were made, whenever possible, on the basis of deduced log*ft* values and observed gamma-ray transitions. The rules for assignments based on deduced log*ft* values have been taken from a survey article by Raman and Gove (43). A summary of these is presented in Table 5.

Table 5. Rules for spin and parity assignments based on log*ft* values

Log*ft* Values	Spin Change	Parity Change
Z < 80 Log*ft* < 5.9	J = 0,1	No
Z > 80 Log*ft* < 5.1	J = 0,1	No
Logf_1t < 8.5	J = 0,1	Yes or No
Log*ft* < 11.0	J = 0,1 J = 2	Yes or No Yes
Log*ft* < 12.8	J = 0,1,2	Yes or No

In section I.B. the statements concerning relative intensities of transitions of different multipole order were direct results of the theory of electromagnetic radiation. In practice it is found that transitions are hindered by additional selection rules or enhanced by collective de-excitations. A compilation of experimentally determined hindrance and enhancement factors has been published by Gove (44). The resulting compilation is summarized in Table 6. It can be argued, on the basis of Gove's observations, that it is sufficient in virtually all cases (excluding known isomeric transitions) to limit transition multipolarities to E1, M1 or E2. E2 and M1 transitions will often compete because,

as noted, the M1's are often hindered while the E2's are usually enhanced.

Table 6. Rules for spin and parity assignments based on gamma-ray transitions.

Parity Changing: All observed E1 transitions emitted in the decay of bound nuclear states are hindered by a factor of 100 or more. These hindrance factors cover a wide range from 10^2 to 10^8 or more. Most M2 transitions are hindered by a factor between 2 and 5 x 10^3. Hence, an M2 gamma ray hindered by a factor of 10 can compete with an E1 hindered by 10^9. E3 hindrance factors cluster around 100 but some enhanced E3's are known. M4 gamma rays are very near single-particle estimates except for the special cases of ^{110}Ag and ^{182}Ta.
Parity Nonchanging: M1 transitions are hindered by a factor that is usually near 100. In contrast, the majority of E2 transitions are enhanced, although an appreciable number are hindered. M3 transitions are both hindered and enhanced so that no definite statements can be made about such transitions.

IV. EXPERIMENTAL RESULTS

The experimental results reported in this work are contained almost entirely in the tables and figures of this section. In the figures containing the observed gamma-ray spectra several intense peaks have been labelled according to energy. A perusal of the tables of observed coincidences indicates that, in most cases, coincidences are verified by gates on both coincident gammas. If a coincidence was only weakly present in a single gate it was termed a "possible" coincidence and denoted by an open circle in the decay scheme. The definite coincidences have been symbolized by a filled circle.

A. Decay of ^{93}Sr

An enhanced gamma-ray spectrum for the ^{93}Sr decay is shown in Figure 12. The 162 photopeaks observed in this spectrum are listed in Table 7. A ground-state beta feeding of 0% was adopted for this decay based on an earlier study by Bakhru and Mukherjee (25). In that study Bakhru and Mukherjee deduced from direct beta spectrum measurement that the ground state of ^{93}Y is not appreciably fed in beta decay. Included in the list of gamma-rays are several multiplets at energies of 167-169, 482-484, 590-594-596, 690-692, 717-718, 1266-1269, 1332-1334, 1978-1981, and 2984-2986 keV which had previously been reported tc be single gamma rays. There are

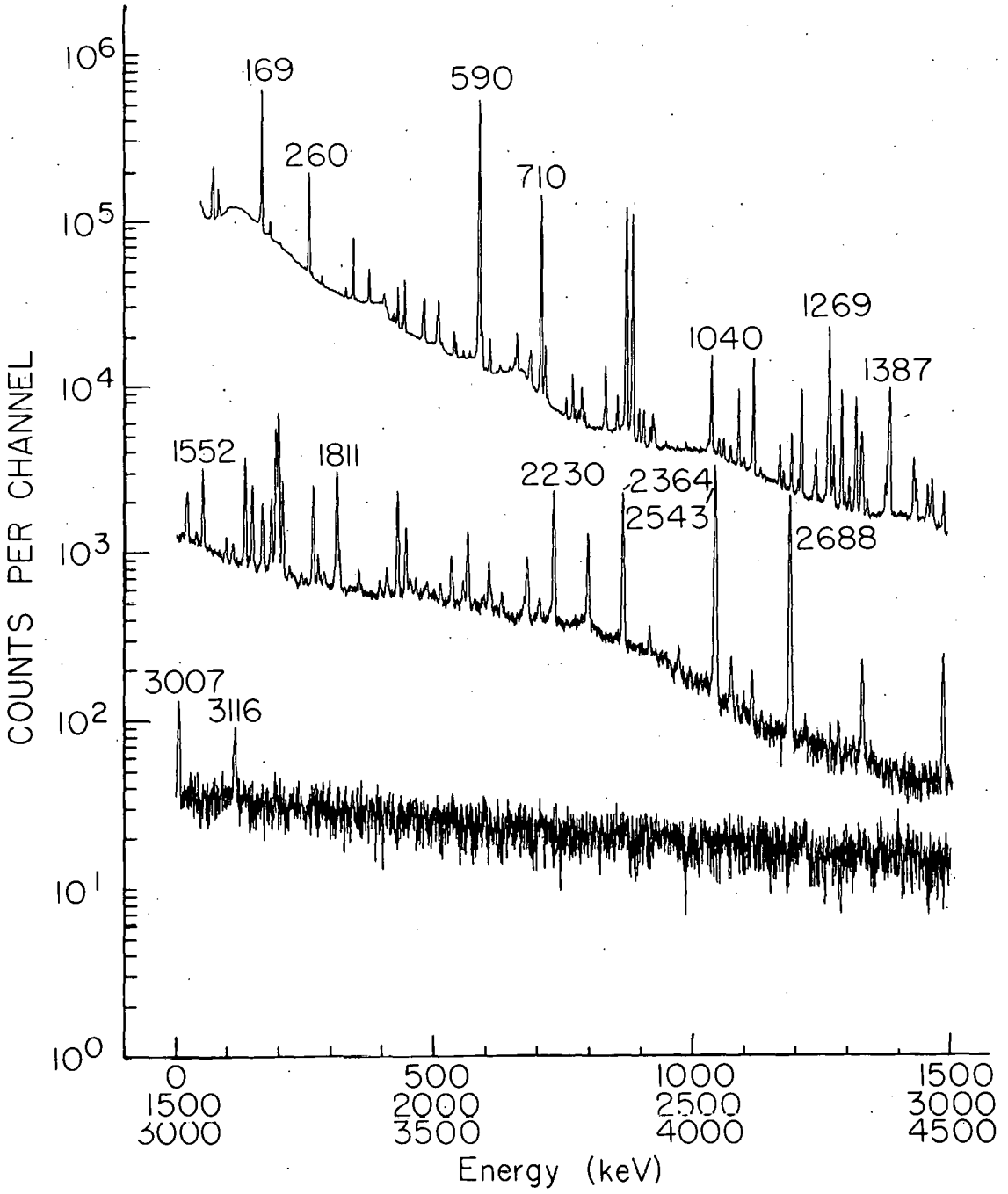

Figure 12. Gamma-ray spectrum for the decay of ^{93}Sr

Table 7. Gamma rays observed in the decay of ^{93}Sr.

Energy (keV)	Relative Intensity[1]	Intensity per 100 Beta Decays[2]	Assignment (keV)
166.57 ± 0.27	9.20 ± 2.38	0.61	2821 --> 2654
168.69 ± 0.05	270.59 ± 15.14	17.99	759 --> 590
260.12 ± 0.05	109.48 ± 5.76	7.28	1136 --> 876
285.65 ± 0.07	4.04 ± 0.28	0.27	876 --> 590
332.04 ± 0.07	5.19 ± 0.35	0.35	2688 --> 2356
342.88 ± 0.37	1.10 ± 0.37	0.07	2886 --> 2544
346.49 ± 0.05	48.21 ± 2.53	3.21	1647 --> 1301
377.36 ± 0.06	21.75 ± 1.37	1.45	1136 --> 759
406.71 ± 0.10	6.32 ± 0.56	0.42	1543 --> 1136
424.70 ± 0.13	3.78 ± 0.47	0.25	1301 --> 876
428.03 ± 0.21	2.22 ± 0.43	0.15	2784 --> 2356
432.67 ± 0.06	21.78 ± 1.29	1.45	1309 --> 876
440.80 ± 0.18	2.94 ± 0.56	0.20	2570 --> 2129
446.20 ± 0.06	34.72 ± 1.86	2.31	2094 --> 1647
481.96 ± 0.10	16.70 ± 1.49	1.11	2575 --> 2094
483.73 ± 0.08	24.46 ± 1.76	1.63	2575 --> 2091
486.74 ± 0.44	1.83 ± 0.66	0.12	2544 --> 2057
518.50 ± 0.15	1.94 ± 0.26	0.13	2575 --> 2057
541.89 ± 0.06	10.73 ± 0.63	0.71	1301 --> 759
545.81 ± 0.07	5.77 ± 0.40	0.38	1136 --> 590
559.92 ± 0.08	3.00 ± 0.28	0.20	1695 --> 1136
571.96 ± 0.16	3.07 ± 0.44	0.20	3116 --> 2544
586.47 ± 0.42	6.56 ± 2.34	0.44	2129 --> 1543
590.28 ± 0.05	1000.00 ± 54.51	66.50	590 --> 0
593.81 ± 0.18	16.37 ± 2.08	1.09	2688 --> 2094
596.15 ± 0.13	19.58 ± 2.18	1.30	2688 --> 2091
610.93 ± 0.06	15.96 ± 0.97	1.06	1912 --> 1301
630.97 ± 0.16	2.85 ± 0.36	0.19	2688 --> 2057
633.52 ± 0.28	1.57 ± 0.34	0.10	1911 --> 1278
650.56 ± 0.15	2.76 ± 0.34	0.18	1787 --> 1136
658.56 ± 0.11	6.24 ± 0.59	0.42	2570 --> 1912
663.58 ± 0.06	24.20 ± 1.41	1.61	2575 --> 1912

[1]Measured relative to the 590.3-keV transition (I_γ = 1000).
[2]Calculated from relative intensities using the factor 0.0665 on the basis of the decay scheme proposed and assuming 0% beta branching to the grcund state of ^{93}Y.

Table 7. (Continued)

Energy (keV)	Relative Intensity[1]	Intensity per 100 Beta Decays[2]	Assignment (keV)
687.79 ± 0.11	9.80 ± 0.91	0.65	1278 --> 590
690.06 ± 0.12	14.88 ± 1.18	0.99	2784 --> 2094
692.00 ± 0.35	3.28 ± 0.94	0.22	2784 --> 2091
710.40 ± 0.05	320.17 ± 16.76	21.29	1301 --> 590
716.79 ± 0.54	4.32 ± 2.34	0.29	1853 --> 1136
718.33 ± 0.12	21.71 ± 2.67	1.44	1309 --> 590
764.77 ± 0.52	0.44 ± 0.17	0.03	2821 --> 2057
771.19 ± 0.06	17.07 ± 1.01	1.14	1647 --> 876
776.07 ± 0.13	3.90 ± 0.40	0.26	1912 --> 1136
782.83 ± 0.15	3.15 ± 0.35	0.21	2091 --> 1309
785.45 ± 0.42	1.13 ± 0.31	0.08	2094 --> 1309
788.68 ± 0.08	11.30 ± 0.69	0.75	2575 --> 1787
791.10 ± 0.14	3.80 ± 0.40	0.25	2091 --> 1301
795.29 ± 0.12	3.44 ± 0.34	0.23	2886 --> 2091
831.30 ± 0.47	0.73 ± 0.30		
834.89 ± 0.05	24.62 ± 1.28	1.64	2688 --> 1853
837.85 ± 0.19	1.73 ± 0.24		
858.47 ± 0.07	10.67 ± 0.68	0.71	2770 --> 1912
875.73 ± 0.06	359.88 ± 19.59	23.93	876 --> 0
888.13 ± 0.05	325.11 ± 17.29	21.61	1647 --> 759
900.98 ± 0.07	10.16 ± 0.64	0.68	2688 --> 1787
910.18 ± 0.08	12.09 ± 0.74	0.80	1787 --> 876
922.70 ± 0.11	4.88 ± 0.45	0.32	2570 --> 1647
927.69 ± 0.08	9.40 ± 0.68	0.63	2575 --> 1647
930.91 ± 0.10	6.05 ± 0.54	0.40	2784 --> 1853
952.58 ± 0.23	1.65 ± 0.31	0.11	1543 --> 590
991.59 ± 0.21	1.84 ± 0.28	0.12	2778 --> 1787
1032.40 ± 0.47	1.53 ± 0.48	0.10	2575 --> 1543
1035.52 ± 0.26	3.04 ± 0.53	0.20	1912 --> 876
1040.63 ± 0.06	46.81 ± 2.58	3.11	2688 --> 1647
1046.42 ± 0.46	1.43 ± 0.45	0.10	3825 --> 2778
1050.61 ± 0.33	0.50 ± 0.21	0.03	3871 --> 2821
1055.13 ± 0.11	5.08 ± 0.37	0.34	2356 --> 1301
1064.37 ± 0.09	5.49 ± 0.41	0.37	2365 --> 1301
1077.86 ± 0.16	3.53 ± 0.39	0.23	2356 --> 1278
1094.00 ± 0.07	25.90 ± 1.50	1.72	1853 --> 759
1104.69 ± 0.23	2.15 ± 0.36	0.14	1695 --> 590
1117.10 ± 0.70	0.98 ± 0.40	0.07	3895 --> 2778
1122.48 ± 0.06	59.27 ± 3.12	3.94	2770 --> 1647
1136.77 ± 0.20	2.91 ± 0.31	0.19	2784 --> 1647

Table 7. (Continued)

Energy (keV)	Relative Intensity[1]	Intensity per 100 Beta Decays[2]	Assignment (keV)
1180.76 ± 0.17	3.59 ± 0.42	0.24	2057 --> 876
1196.23 ± 0.06	14.41 ± 0.79	0.96	1787 --> 590
1200.48 ± 0.74	0.38 ± 0.17		
1215.48 ± 0.07	36.74 ± 2.00	2.44	2091 --> 876
1239.15 ± 0.25	1.85 ± 0.39	0.12	2886 --> 1647
1243.41 ± 0.08	11.83 ± 0.72	0.79	2544 --> 1301
1249.22 ± 0.71	1.07 ± 0.37	0.07	3825 --> 2575
1261.30 ± 0.61	1.16 ± 0.46	0.08	2570 --> 1309
1266.38 ± 0.10	16.35 ± 1.18	1.09	2575 --> 1309
1269.47 ± 0.07	105.30 ± 5.46	7.00	2570 --> 1301
1277.99 ± 0.09	12.83 ± 0.88	0.85	1278 --> 0
1308.60 ± 0.09	5.87 ± 0.38	0.39	1309 --> 0
1321.24 ± 0.07	38.40 ± 2.00	2.55	1912 --> 590
1324.81 ± 0.69	0.76 ± 0.30	0.05	3895 --> 2570
1329.63 ± 0.32	1.01 ± 0.20	0.07	3116 --> 1787
1332.50 ± 0.50	7.40 ± 3.70	0.49	2091 --> 759
1334.50 ± 0.10	9.98 ± 0.74	0.66	2094 --> 759
1378.98 ± 0.10	5.22 ± 0.36	0.35	2688 --> 1309
1387.11 ± 0.07	51.11 ± 2.61	3.40	2688 --> 1301
1434.01 ± 0.08	13.34 ± 0.76	0.89	2570 --> 1136
1438.93 ± 0.09	7.42 ± 0.47	0.49	2575 --> 1136
1466.17 ± 0.31	1.47 ± 0.26	0.10	2057 --> 590
1469.50 ± 0.12	7.73 ± 0.52	0.51	2770 --> 1301
1483.34 ± 0.30	1.53 ± 0.26	0.10	2784 --> 1301
1492.13 ± 0.12	8.08 ± 0.53	0.54	2770 --> 1278
1506.49 ± 0.55	0.71 ± 0.23	0.05	3871 --> 2365
1511.77 ± 0.41	0.81 ± 0.20	0.05	2821 --> 1309
1520.05 ± 0.54	4.72 ± 0.95	0.31	2821 --> 1301
1538.71 ± 0.25	1.51 ± 0.28	0.10	2129 --> 590
1543.43 ± 0.56	0.60 ± 0.22	0.04	1543 --> 0
1551.59 ± 0.09	14.97 ± 0.91	1.00	2688 --> 1136
1609.77 ± 0.20	2.89 ± 0.28	0.19	4264 --> 2654
1634.05 ± 0.08	21.30 ± 1.22	1.42	2770 --> 1136
1641.97 ± 0.61	0.64 ± 0.21	0.04	2778 --> 1136
1647.53 ± 0.08	13.11 ± 0.76	0.87	2784 --> 1136
1652.20 ± 0.71	0.52 ± 0.20		
1668.68 ± 0.54	2.39 ± 1.32	0.16	2544 --> 876
1684.84 ± 0.13	10.50 ± 0.84	0.70	2821 --> 1136
1694.07 ± 0.09	38.05 ± 2.08	2.53	2570 --> 876
1699.06 ± 0.09	49.04 ± 2.62	3.26	2575 --> 876

Table 7. (Continued)

Energy (keV)	Relative Intensity[1]	Intensity per 100 Beta Decays[2]	Assignment (keV)
1706.59 ± 0.10	16.27 ± 1.00	1.08	3007 --> 1301
1742.13 ± 0.38	1.28 ± 0.23	0.08	3871 --> 2129
1765.36 ± 0.09	15.72 ± 0.82	1.04	2356 --> 590
1774.83 ± 0.16	2.38 ± 0.27	0.16	2365 --> 590
1786.56 ± 0.28	1.16 ± 0.18		
1811.45 ± 0.10	20.73 ± 1.16	1.38	2688 --> 876
1816.12 ± 0.19	3.45 ± 0.38	0.23	2575 --> 759
1894.10 ± 0.27	1.78 ± 0.26	0.12	2770 --> 876
1899.46 ± 1.04	0.52 ± 0.19	0.03	4264 --> 2365
1907.73 ± 0.23	2.59 ± 0.31	0.17	2784 --> 876
1928.79 ± 0.10	17.19 ± 0.95	1.14	2688 --> 759
1935.64 ± 0.73	0.50 ± 0.17		
1944.75 ± 0.12	8.23 ± 0.58	0.55	2821 --> 876
1952.40 ± 0.33	1.46 ± 0.25		
1972.15 ± 0.68	0.49 ± 0.18	0.03	3825 --> 1853
1978.15 ± 0.93	0.39 ± 0.18		
1981.41 ± 0.83	0.54 ± 0.20	0.04	3116 --> 1136
1984.85 ± 0.32	1.20 ± 0.19	0.08	2575 --> 590
2010.80 ± 0.25	1.79 ± 0.25	0.12	2886 --> 876
2054.68 ± 0.25	2.05 ± 0.27		
2063.64 ± 0.12	9.25 ± 0.57	0.62	2654 --> 590
2076.55 ± 0.69	0.88 ± 0.24		
2094.06 ± 0.57	1.08 ± 0.31		
2104.78 ± 0.15	4.61 ± 0.35		
2108.63 ± 0.37	1.30 ± 0.23	0.09	3895 --> 1787
2129.24 ± 0.52	1.51 ± 0.47	0.10	2129 --> 0
2172.02 ± 0.35	1.05 ± 0.19	0.07	4264 --> 2091
2179.49 ± 0.20	4.31 ± 0.60	0.29	2770 --> 590
2203.47 ± 0.70	1.26 ± 0.33		
2222.03 ± 0.84	0.64 ± 0.26		
2230.27 ± 0.12	22.84 ± 1.33	1.52	2821 --> 590
2296.13 ± 0.14	10.92 ± 0.72	0.73	2886 --> 590
2364.72 ± 0.11	23.22 ± 1.31	1.54	2365 --> 0
2416.33 ± 0.33	1.60 ± 0.29	0.11	3007 --> 590
2472.73 ± 0.31	1.12 ± 0.15	0.07	4120 --> 1647
2543.84 ± 0.11	44.52 ± 2.36	2.96	2544 --> 0
2574.20 ± 0.27	1.87 ± 0.29	0.12	2575 --> 0
2585.90 ± 0.62	0.40 ± 0.12	0.03	3895 --> 1309
2614.68 ± 0.27	1.32 ± 0.17		
2688.65 ± 0.12	31.32 ± 1.82	2.08	2688 --> 0

Table 7. (Continued)

Energy (keV)	Relative Intensity[1]	Intensity per 100 Beta Decays[2]	Assignment (keV)
2765.32 ± 0.62	0.61 ± 0.20		
2781.62 ± 0.37	0.76 ± 0.11		
2811.34 ± 0.67	0.31 ± 0.07	0.02	4120 --> 1309
2828.54 ± 0.20	2.52 ± 0.25		
2983.52 ± 0.42	0.66 ± 0.21	0.04	4120 --> 1136
2985.72 ± 0.21	2.92 ± 0.37	0.19	4264 --> 1278
2995.73 ± 0.64	0.29 ± 0.07	0.02	3871 --> 876
3006.86 ± 0.22	1.73 ± 0.17	0.12	3007 --> 0
3116.64 ± 0.35	1.02 ± 0.13	0.07	3116 --> 0

also approximately 80 gamma rays which are reported here but not in any previous studies of this decay. All except one of these gamma rays has an intensity less than 10.0 and as a result were probably too weak to have been observed elsewhere. The gamma ray with an intensity greater than 10.0 was also observed in the coincidence spectra reported in this work. All energies are in agreement with at least one of the previous Ge(Li) detector studies of this nuclide for which energy uncertainties are quoted (26,28). Relative intensities and transition assignments (for those gamma rays placed in the level scheme) are also provided in Table 7. A comparison of intensities obtained in this work and those in previous studies for all gamma rays having an intensity greater than 25 is made in Table 8. In general the intensities agree to within quoted uncertainties. Although 19 gamma rays are not placed in the level scheme, these gamma rays represent less than 1% of the observed gamma intensity.

Ten gamma rays previously reported only by Achterberg, et al. (28) were not observed in this study. However three of these gamma rays could not be placed in the level scheme proposed in that reference and four other gamma rays were used to define two new levels. Another gamma ray resulted from the reported resolution of a doublet at 1215 keV. In this work only one gamma ray was evident at this energy and its intensity was consistent with a single placement in coin-

Table 8. Comparison of intensities with other ^{93}Sr studies.

Energy	This Work	Achterberg et al. (31)	Herzog and Grimm (26)	Cavallini[1] et al. (22)
168.69[2]	271 ± 15	270 ± 30	254 ± 64	340
260.12	109 ± 6	105 ± 6	102 ± 10	130
346.49	48 ± 3	46 ± 3	40 ± 5	60
446.20	35 ± 2	32 ± 4	29 ± 3	40
590.28	1000 ± 55	1000 ± 60	1000 ± 81	1000
710.40	320 ± 17	290 ± 30	315 ± 25	310
875.73	360 ± 20	345 ± 30	358 ± 29	350
888.13	325 ± 17	335 ± 30	331 ± 27	310
1040.63	47 ± 3	41 ± 3	49 ± 4	60
1094.00	26 ± 2	29 ± 3	28 ± 3	20
1122.48[3]	59 ± 3	52 ± 5	58 ± 5	60
1215.48[4]	37 ± 2	35 ± 16	39 ± 4	40
1269.47	105 ± 5	109 ± 7	111 ± 10	110
1321.24	38 ± 2	39 ± 3	39 ± 6	40
1387.11	51 ± 3	45 ± 5	41 ± 8	80
1694.07	38 ± 2	34 ± 2	41 ± 4	40
1699.06	49 ± 3	58 ± 4	55 ± 5	60
2543.84	45 ± 2	42 ± 6	54 ± 4	50
2688.65	31 ± 2	31 ± 3	37 ± 3	30

[1] No intensity uncertainties were reported

[2] Intensities listed for the 168-keV gamma ray are not corrected for internal conversion

[3] Herzog and Grimm placed this gamma ray in two places based on their coincidence information

[4] Achterberg, et al. reported this transition as a doublet

cidence with the 875-keV gamma ray. Coincidence information also indicates that the 1122-keV gamma ray is definitely in coincidence with the gamma ray at 875 keV. However no evidence was seen to indicate its coincidence with the 260-keV gamma ray. As a result it is not placed twice as in the level scheme cffered by Herzog and Grimm (26).

All 72 of the coincidence gates resulted in either possible or definite coincidence information which is presented in Table 9. Based on this information it is possible to establish 28 of the 36 levels present in the ^{93}Sr decay scheme proposed in this study. The remaining levels were established entirely on the basis of energy sums. 144 gamma rays, representing more than 99% of the gamma-ray intensity, were placed in a level scheme comprised of 37 levels. This level scheme is presented in Figure 13.

B. Decay of ^{93}Rb

The enhanced gamma-ray spectrum for the ^{93}Rb decay is shown in Figure 14. In this spectrum 243 photopeaks were observed and are listed in Table 10. This table also includes relative intensities for all the gamma rays and transition assignments for those gamma rays that have been placed in the final level scheme. The absolute intensities, expressed per 100 beta decays, are calculated using a ground-state beta branching of 59 ± 3% which has been adopted from the study made by Achterberg, et al. and a delayed neutron probability

Table 9. Coincidences observed in the decay of ^{93}Sr.

Gate (keV)	Definite Coincidences (keV)	Possible Coincidences (keV)
168.7	590	
260.1	286, 560, 717, 776, 876, 1434, 1439, 1552, 1634, 1648, 1685	332, 789, 835, 992
285.6	260, 590	
332.0	1765	
346.5	590, 710, 1041, 1122	446, 482, 542, 876
377.4	1552, 1634, 1648	717, 1439, 1685
424.7	876	346
432.7	876, 1266	1379
446.2	346, 482, 594, 690, 710, 771, 888	286, 876
482.0	446, 888, 1334	346, 710
483.7	876, 1215	791
541.9	346, 1269	1470
545.8	590	
559.9		260, 377
590.3	169, 286, 346, 446, 611, 664, 688, 710, 718, 858, 1196, 1243, 1269, 1321, 1387, 1634, 1765, 2064, 2179, 2230, 2296	260, 332, 789, 901, 1036, 1266, 1466, 2416
593.8	446	346, 710

Table 9. (Continued)

Gate (keV)	Definite Coincidences (keV)	Possible Coincidences (keV)
596.2	876, 1215	1332
610.9	590, 664, 710, 858	
663.6	260, 590, 611, 710, 1321	876
687.8		590, 1492
690.1	446, 888	346
692.0		1215
710.4	346, 446, 482, 590, 611, 664, 1055, 1243, 1269, 1387, 1470, 1520	1041
716.8	260, 835, 876	
718.3	590, 1266	1379
771.2	446, 876	1122
776.1	260	
788.7	590, 910, 1196	876
791.1	590, 710	484
795.3	876, 1215	
834.9	260, 876, 1094	377, 717
858.5	590, 611, 1321	
875.7	260, 425, 433, 484, 717, 771, 795, 910, 1122, 1215, 1552, 1634, 1648, 1669, 1694, 1699, 1811, 1908, 1945	446, 594, 690, 789, 835, 1434, 1439, 1685

Table 9. (Continued)

Gate (keV)	Definite Coincidences (keV)	Possible Coincidences (keV)
888.1	446, 482, 690, 1041, 1122	1239
901.0	590, 910, 1196	
910.2	789, 876, 901	
922.7		888
927.7		771, 888
930.9	1094	
952.6	590	
1040.6	346, 710, 888	
1064.4	590, 710	
1094.0	835, 931	
1122.5	346, 771, 876, 888	572, 590
1196.2	590, 789, 901	
1215.5	484, 596, 692, 795, 876	
1239.2		888
1243.4	590, 710	
1266.4	433, 590, 876	718
1269.5	590, 710	542
1278.0		1492
1321.2	590, 664, 858	
1387.1	590, 710	542

Table 9. (Continued)

Gate (keV)	Definite Coincidences (keV)	Possible Coincidences (keV)
1434.0	260, 377, 876	
1438.9	260, 377	876
1469.5	590, 710	542
1492.1	590, 688	1278
1520.1	590, 710	
1551.6	260, 377	
1634.0	260, 377, 876	590
1647.5	260, 377	590, 876
1668.7		876
1684.8	260, 377	876
1694.1	876	
1699.1	876	
1765.4	332, 590	
1774.8		590
1811.5	876	
1944.7	876	
2063.6	590	
2230.3	590	
2296.1	590	

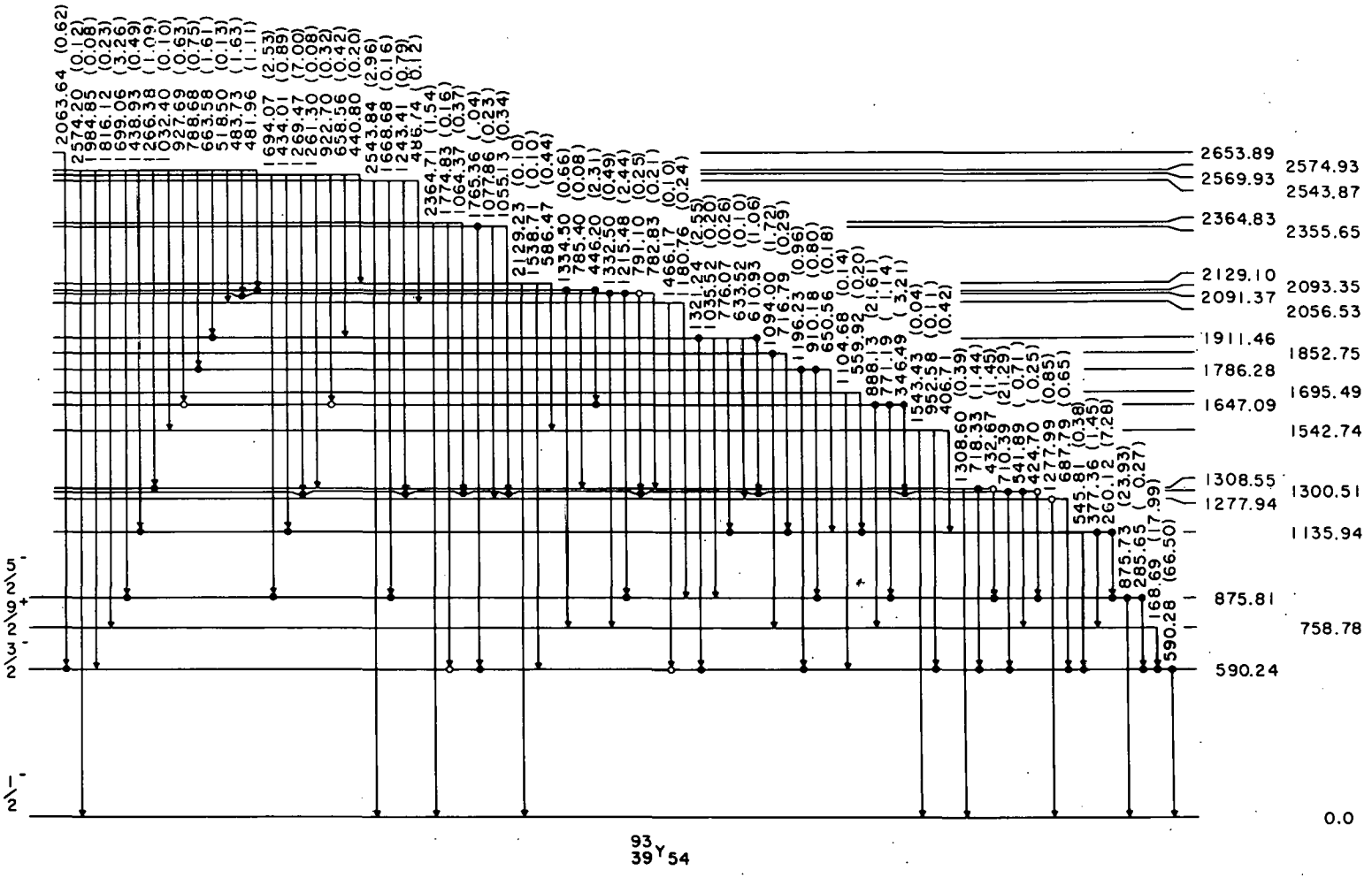

Figure 13. ^{93}Y level scheme

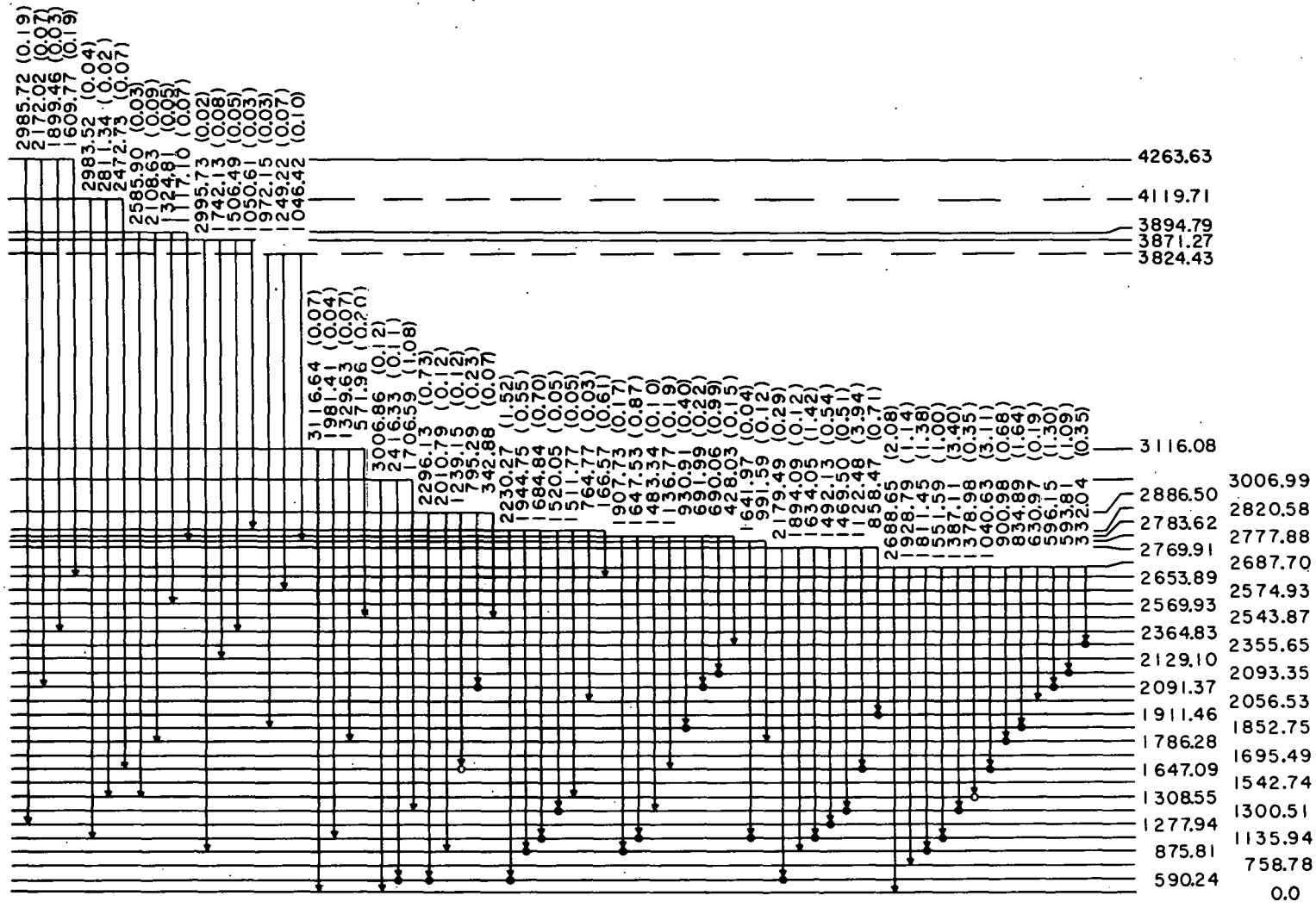

$^{93}_{39}Y_{54}$

Figure 13. (Continued)

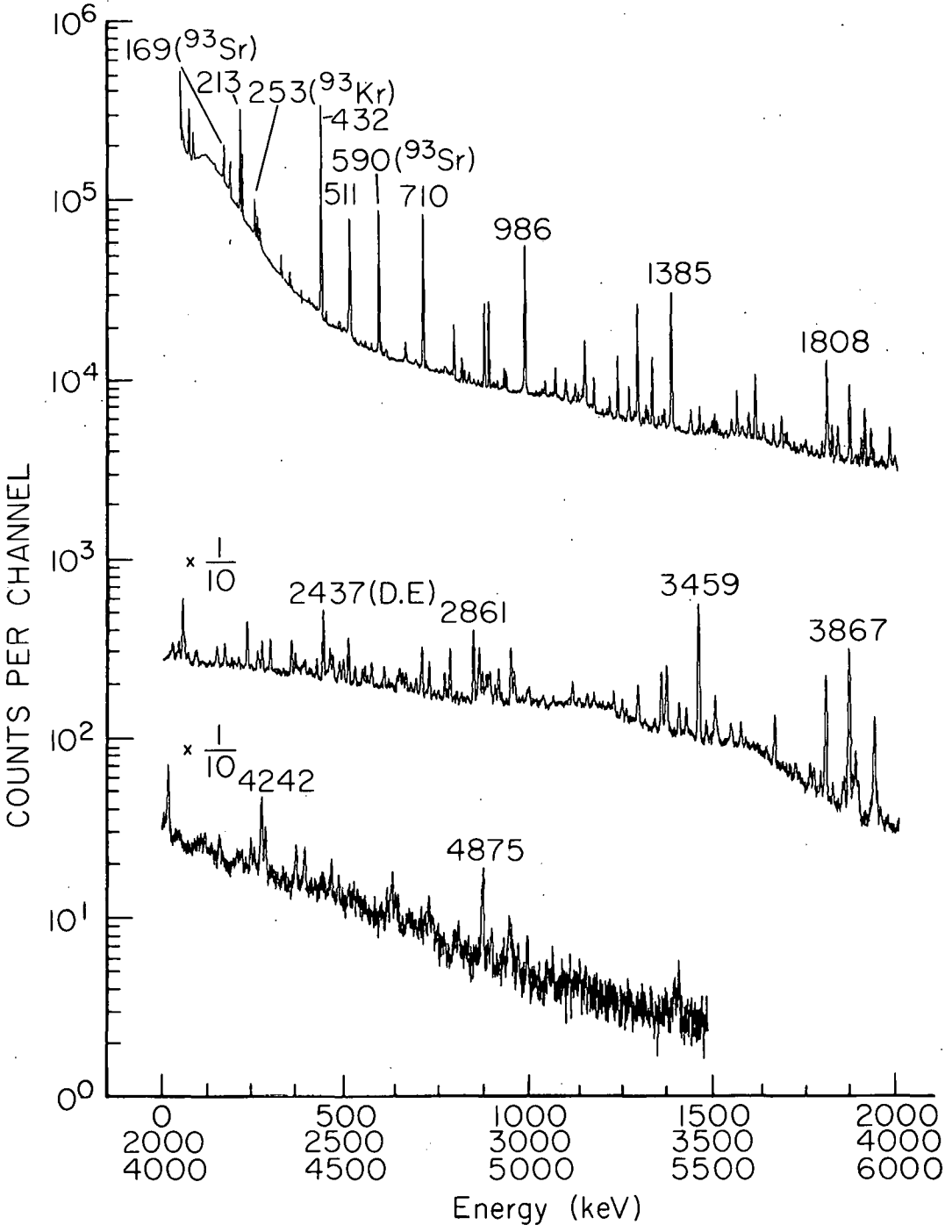

Figure 14. Gamma-ray spectrum for the decay of ^{93}Rb

Table 10. Gamma rays observed in the decay of ^{93}Rb.

Energy (keV)	Relative Intensity[1]	Intensity per 100 Beta Decays[2]	Assignment (keV)
163.40 ± 0.28	6.57 ± 1.46	0.08	2456 --> 2293
205.21 ± 0.55	6.26 ± 3.18	0.08	4714 --> 4509
213.39 ± 0.05	383.83 ± 21.89	4.69	213 --> 0
219.16 ± 0.06	158.05 ± 9.41	1.93	433 --> 213
351.74 ± 0.11	3.77 ± 0.37	0.05	3955 --> 3603
404.99 ± 0.18	3.11 ± 0.47	0.04	
432.51 ± 0.05	1000.00 ± 52.71	12.22	433 --> 0
473.83 ± 0.56	1.56 ± 0.72	0.02	4097 --> 3623
595.87 ± 0.13	12.68 ± 1.68	0.15	2869 --> 2273
602.56 ± 0.39	2.88 ± 0.86	0.04	4620 --> 4017
610.07 ± 0.43	10.06 ± 1.83	0.12	3867 --> 3256
661.64 ± 0.11	16.40 ± 2.80	0.20	4509 --> 3848
709.95 ± 0.05	308.00 ± 22.34	3.76	1142 --> 433
721.99 ± 0.17	2.87 ± 0.37	0.04	3955 --> 3233
768.36 ± 0.23	6.60 ± 1.08	0.08	1911 --> 1142
776.35 ± 0.43	3.03 ± 0.95	0.04	3233 --> 2456
793.65 ± 0.06	61.53 ± 3.32	0.75	1780 --> 986
822.41 ± 0.22	9.72 ± 1.71	0.12	1808 --> 986
831.18 ± 0.32	3.62 ± 0.84	0.04	4620 --> 3789
859.05 ± 0.18	4.78 ± 0.61	0.06	6273 --> 5414
867.74 ± 0.16	4.18 ± 0.47	0.05	3848 --> 2980
901.08 ± 0.18	6.32 ± 0.84	0.08	2771 --> 1870
905.64 ± 0.28	3.83 ± 0.79	0.05	2054 --> 1148
910.91 ± 0.14	8.16 ± 0.88	0.10	4714 --> 3804
929.04 ± 0.09	24.40 ± 1.66	0.30	1142 --> 213
934.70 ± 0.10	18.45 ± 1.39	0.23	1148 --> 213
981.14 ± 0.34	7.54 ± 1.65	0.09	5601 --> 4620
986.05 ± 0.06	391.01 ± 19.84	4.78	986 --> 0
990.86 ± 0.27	6.53 ± 1.27	0.08	2771 --> 1780
1035.07 ± 0.51	3.84 ± 1.21	0.05	2273 --> 1238
1054.68 ± 0.31	3.42 ± 0.71	0.04	2293 --> 1238
1059.36 ± 0.30	3.69 ± 0.72	0.05	2045 --> 986

[1] Measured relative to the 432.5-keV transition (I_γ = 1000).
[2] Calculated from relative intensities using the factor 0.0125 based on the decay scheme proposed with 59% beta branching to the ground state of ^{93}Sr and a delayed neutron probability of 1.65%.

Table 10. (Continued)

Energy (keV)	Relative Intensity[1]	Intensity per 100 Beta Decays[2]	Assignment (keV)
1068.51 ± 0.11	35.35 ± 2.89	0.43	3955 --> 2886
1077.60 ± 0.17	2.59 ± 0.30	0.03	5012 --> 3934
1096.71 ± 0.09	22.98 ± 1.45	0.28	1529 --> 433
1100.63 ± 0.12	10.36 ± 0.91	0.13	4991 --> 3891
1115.77 ± 0.22	5.44 ± 0.77	0.07	3233 --> 2117
1120.03 ± 0.44	4.19 ± 1.23	0.05	3891 --> 2771
1130.12 ± 0.16	10.97 ± 1.19	0.13	2273 --> 1142
1138.02 ± 0.31	11.58 ± 1.75	0.14	4336 --> 3198
1142.58 ± 0.12	18.14 ± 1.46	0.22	1142 --> 0
1148.18 ± 0.08	88.06 ± 4.94	1.08	1148 --> 0
1150.38 ± 0.13	26.72 ± 2.44	0.33	2293 --> 1142
1164.36 ± 0.25	5.16 ± 0.77	0.06	3623 --> 2460
1167.09 ± 0.47	2.57 ± 0.73	0.03	3623 --> 2456
1202.39 ± 0.74	2.71 ± 1.20	0.03	4991 --> 3789
1204.93 ± 0.74	2.87 ± 1.18	0.04	4461 --> 3256
1208.55 ± 0.19	8.94 ± 1.07	0.11	5012 --> 3804
1222.74 ± 0.38	3.96 ± 0.94	0.05	5012 --> 3789
1238.30 ± 0.08	84.58 ± 4.54	1.03	1238 --> 0
1283.99 ± 0.41	8.63 ± 2.02	0.11	3603 --> 2319
1286.97 ± 0.54	6.40 ± 1.98	0.08	2273 --> 986
1306.92 ± 0.19	6.64 ± 0.77	0.08	2293 --> 986
1315.64 ± 0.10	21.74 ± 1.48	0.27	2554 --> 1238
1332.97 ± 0.08	60.83 ± 6.09	0.74	2319 --> 986
1349.67 ± 0.21	8.11 ± 1.04	0.10	1563 --> 213
1359.92 ± 0.16	11.78 ± 1.14	0.14	6273 --> 4912
1365.36 ± 0.11	18.71 ± 1.37	0.23	2351 --> 986
1385.21 ± 0.08	328.18 ± 16.83	4.01	1385 --> 0
1388.66 ± 0.58	12.63 ± 2.55	0.15	2774 --> 1385
1397.71 ± 0.50	3.30 ± 0.94	0.04	2782 --> 1385
1405.37 ± 0.22	5.74 ± 0.74	0.07	2554 --> 1148
1437.10 ± 0.16	23.97 ± 2.05	0.29	1870 --> 433
1439.58 ± 0.54	5.22 ± 1.69	0.06	5775 --> 4336
1452.74 ± 0.66	2.94 ± 1.13	0.04	3233 --> 1780
1470.13 ± 0.22	10.93 ± 1.18	0.13	3789 --> 2319
1473.16 ± 0.59	3.10 ± 1.00	0.04	2460 --> 986
1479.08 ± 0.33	3.45 ± 0.67	0.04	2621 --> 1142
1483.96 ± 0.24	5.03 ± 0.69	0.06	4038 --> 2554
1491.25 ± 0.24	6.95 ± 0.95	0.08	6000 --> 4509
1494.85 ± 0.15	13.16 ± 1.13	0.16	3955 --> 2460
1501.18 ± 0.12	19.99 ± 1.34	0.24	2886 --> 1385

Table 10. (Continued)

Energy (keV)	Relative Intensity[1]	Intensity per 100 Beta Decays[2]	Assignment (keV)
1507.77 ± 0.14	13.60 ± 1.10	0.17	5385 --> 3877
1515.76 ± 0.33	5.37 ± 1.00	0.07	3867 --> 2351
1531.13 ± 0.68	3.68 ± 1.09	0.04	3804 --> 2273
1533.83 ± 0.26	8.05 ± 1.20	0.10	5631 --> 4097
1547.78 ± 0.15	16.28 ± 1.33	0.20	3867 --> 2319
1562.91 ± 0.11	57.64 ± 3.50	0.70	1563 --> 0
1566.19 ± 0.91	3.40 ± 1.62	0.04	1780 --> 213
1574.71 ± 0.22	7.13 ± 0.84	0.09	3867 --> 2293
1578.02 ± 0.27	8.78 ± 1.17	0.11	3623 --> 2045
1594.61 ± 0.12	33.34 ± 2.12	0.41	2980 --> 1385
1612.87 ± 0.11	96.24 ± 5.55	1.18	2045 --> 433
1635.20 ± 0.15	21.54 ± 1.76	0.26	2621 --> 986
1662.16 ± 0.15	20.98 ± 1.72	0.26	3955 --> 2293
1684.76 ± 0.13	31.62 ± 2.38	0.39	2117 --> 433
1690.88 ± 0.66	3.54 ± 1.20	0.04	4042 --> 2351
1726.28 ± 0.37	4.51 ± 0.93	0.06	2869 --> 1142
1736.29 ± 1.28	5.64 ± 2.83	0.07	3877 --> 2141
1738.39 ± 0.85	5.71 ± 3.67	0.07	2886 --> 1148
1743.18 ± 0.52	6.37 ± 1.81	0.08	3789 --> 2045
1745.72 ± 0.52	6.87 ± 1.78	0.08	4097 --> 2351
1749.61 ± 0.19	14.48 ± 1.34	0.18	3867 --> 2117
1753.62 ± 0.39	5.39 ± 1.06	0.07	5601 --> 3848
1793.62 ± 0.18	15.36 ± 1.43	0.19	3934 --> 2141
1803.55 ± 0.30	13.68 ± 1.97	0.17	4577 --> 2774
1808.50 ± 0.10	160.54 ± 8.36	1.96	1808 --> 0
1812.76 ± 0.21	14.32 ± 1.59	0.18	3198 --> 1385
1821.86 ± 0.13	33.02 ± 2.16	0.40	3867 --> 2045
1831.10 ± 0.22	11.85 ± 1.38	0.14	3877 --> 2045
1836.44 ± 0.57	16.30 ± 10.10	0.20	2980 --> 1142
1838.02 ± 0.41	26.68 ± 9.83	0.33	4620 --> 2782
1841.63 ± 0.65	4.74 ± 1.43	0.06	3404 --> 1563
1869.69 ± 0.11	109.21 ± 5.83	1.33	1870 --> 0
1882.90 ± 0.41	5.88 ± 1.21	0.07	4620 --> 2737
1886.62 ± 0.31	8.34 ± 1.25	0.10	2319 --> 433
1892.70 ± 0.24	10.02 ± 1.21	0.12	3804 --> 1911
1900.94 ± 0.12	26.45 ± 1.67	0.32	3955 --> 2054
1908.05 ± 0.56	5.58 ± 1.79	0.07	5775 --> 3867
1910.72 ± 0.12	66.44 ± 3.85	0.81	1911 --> 0
1918.98 ± 0.36	6.22 ± 1.16	0.08	2351 --> 433
1927.64 ± 0.12	42.53 ± 2.75	0.52	2141 --> 213

Table 10. (Continued)

Energy (keV)	Relative Intensity[1]	Intensity per 100 Beta Decays[2]	Assignment (keV)
1933.91 ± 0.29	14.84 ± 2.30	0.18	3804 --> 1870
1956.38 ± 0.27	9.95 ± 1.33	0.12	3867 --> 1911
1978.28 ± 0.15	46.25 ± 3.25	0.57	3848 --> 1870
1983.18 ± 0.90	3.99 ± 1.79	0.05	6000 --> 4017
1991.75 ± 0.26	9.64 ± 1.27	0.12	5396 --> 3404
1997.76 ± 0.65	3.44 ± 1.11	0.04	3867 --> 1870
2023.89 ± 0.44	7.02 ± 1.51	0.09	2456 --> 433
2026.88 ± 0.25	13.31 ± 1.66	0.16	2460 --> 433
2037.02 ± 0.82	3.90 ± 1.77	0.05	
2043.82 ± 0.17	17.51 ± 1.39	0.21	4912 --> 2869
2054.06 ± 0.12	77.19 ± 4.21	0.94	2054 --> 0
2058.78 ± 0.17	20.06 ± 1.66	0.25	3867 --> 1808
2068.36 ± 0.24	8.21 ± 0.92	0.10	3877 --> 1808
2087.43 ± 0.28	10.04 ± 1.35	0.12	3867 --> 1780
2147.63 ± 0.30	16.64 ± 2.20	0.20	4017 --> 1870
2168.24 ± 0.14	25.23 ± 1.80	0.31	4038 --> 1870
2170.36 ± 1.62	2.84 ± 2.75	0.03	4790 --> 2621
2206.21 ± 0.30	10.36 ± 1.45	0.13	6097 --> 3891
2229.44 ± 0.12	54.22 ± 2.99	0.66	4038 --> 1808
2256.17 ± 0.90	4.47 ± 2.92	0.05	3404 --> 1148
2258.43 ± 0.36	14.75 ± 2.70	0.18	4577 --> 2319
2262.03 ± 0.30	8.05 ± 1.12	0.10	4042 --> 1780
2270.20 ± 0.12	31.28 ± 1.80	0.38	3256 --> 986
2292.80 ± 0.13	30.74 ± 1.90	0.38	2293 --> 0
2327.50 ± 0.34	6.60 ± 0.98	0.08	3891 --> 1563
2333.97 ± 0.49	3.73 ± 0.84	0.05	4790 --> 2456
2349.58 ± 0.17	34.78 ± 2.68	0.43	2782 --> 433
2359.45 ± 0.16	18.65 ± 1.29	0.23	4912 --> 2554
2376.96 ± 0.33	7.78 ± 1.18	0.10	6000 --> 3623
2386.72 ± 0.23	12.93 ± 1.35	0.16	6277 --> 3891
2398.26 ± 0.33	7.03 ± 1.03	0.09	5631 --> 3233
2403.50 ± 0.57	3.68 ± 0.93	0.04	3789 --> 1385
2418.22 ± 0.22	19.10 ± 1.92	0.23	3404 --> 986
2451.67 ± 0.76	9.26 ± 2.21	0.11	
2454.97 ± 0.22	27.52 ± 2.71	0.34	3603 --> 1148
2461.98 ± 0.19	27.64 ± 2.39	0.34	3848 --> 1385
2491.20 ± 0.22	22.61 ± 2.28	0.28	3877 --> 1385
2505.20 ± 0.15	46.62 ± 2.96	0.57	3891 --> 1385
2523.73 ± 0.46	13.87 ± 5.46	0.17	2737 --> 213
2550.06 ± 0.22	15.41 ± 1.46	0.19	4461 --> 1911

Table 10. (Continued)

Energy (keV)	Relative Intensity[1]	Intensity per 100 Beta Decays[2]	Assignment (keV)
2557.51 ± 0.39	7.11 ± 1.23	0.09	2771 --> 213
2568.59 ± 0.20	21.94 ± 1.91	0.27	2782 --> 213
2602.38 ± 0.22	20.05 ± 1.88	0.25	5385 --> 2782
2614.09 ± 0.34	7.39 ± 1.09	0.09	5385 --> 2771
2620.22 ± 0.57	4.82 ± 1.12	0.06	4912 --> 2293
2624.78 ± 0.52	5.31 ± 1.13	0.06	5396 --> 2771
2638.06 ± 0.36	16.05 ± 2.12	0.20	3877 --> 1238
2646.56 ± 0.60	10.40 ± 3.04	0.13	3789 --> 1142
2652.62 ± 0.22	17.85 ± 1.75	0.22	4461 --> 1808
2661.08 ± 0.22	17.81 ± 1.70	0.22	3804 --> 1142
2674.16 ± 0.44	6.08 ± 1.16	0.07	6277 --> 3603
2704.97 ± 0.17	59.04 ± 4.37	0.72	3848 --> 1142
2724.60 ± 0.25	31.82 ± 4.63	0.39	3867 --> 1142
2733.96 ± 0.95	3.44 ± 1.31	0.04	3877 --> 1142
2766.48 ± 0.17	22.93 ± 1.70	0.28	2980 --> 213
2773.17 ± 0.41	6.97 ± 1.23	0.08	4336 --> 1563
2799.92 ± 0.43	8.65 ± 1.54	0.11	4038 --> 1238
2812.55 ± 0.54	6.23 ± 1.39	0.08	3955 --> 1142
2861.34 ± 0.15	63.60 ± 3.87	0.78	3848 --> 986
2869.23 ± 0.18	25.21 ± 1.88	0.31	2869 --> 0
2875.28 ± 0.60	5.98 ± 1.35	0.07	4017 --> 1142
2880.48 ± 0.22	21.86 ± 1.84	0.27	3867 --> 986
2886.26 ± 0.27	18.97 ± 1.95	0.23	2886 --> 0
2890.39 ± 0.26	23.46 ± 2.13	0.29	3877 --> 986
2903.58 ± 0.27	12.88 ± 1.49	0.16	6707 --> 3804
2954.93 ± 0.24	25.70 ± 2.70	0.31	4097 --> 1142
2958.11 ± 0.56	9.29 ± 2.42	0.11	5012 --> 2054
3027.58 ± 1.14	2.80 ± 1.19	0.03	6261 --> 3233
3104.10 ± 0.84	4.14 ± 1.41	0.05	4912 --> 1808
3113.85 ± 0.24	21.42 ± 1.99	0.26	6000 --> 2886
3129.22 ± 0.78	4.95 ± 1.52	0.06	
3133.14 ± 0.76	5.10 ± 1.53	0.06	4912 --> 1780
3172.09 ± 0.35	11.10 ± 1.47	0.14	5631 --> 2460
3211.55 ± 0.55	6.41 ± 1.34	0.08	4991 --> 1780
3226.37 ± 0.28	17.37 ± 1.80	0.21	6000 --> 2774
3296.10 ± 1.01	4.04 ± 1.72	0.05	5414 --> 2117
3337.95 ± 0.41	7.80 ± 1.26	0.10	5631 --> 2293
3366.63 ± 0.32	12.99 ± 1.63	0.16	4509 --> 1142
3370.97 ± 0.16	65.35 ± 3.67	0.80	3804 --> 433
3389.77 ± 0.88	3.52 ± 1.14	0.04	3603 --> 213

Table 10. (Continued)

Energy (keV)	Relative Intensity[1]	Intensity per 100 Beta Decays[2]	Assignment (keV)
3403.56 ± 0.18	26.29 ± 1.68	0.32	6273 --> 2869
3458.19 ± 0.16	213.89 ± 11.41	2.61	3891 --> 433
3477.39 ± 0.24	15.45 ± 1.32	0.19	4620 --> 1142
3486.93 ± 0.71	3.92 ± 1.00	0.05	6261 --> 2774
3501.92 ± 0.41	32.56 ± 6.91	0.40	3934 --> 433
3543.95 ± 0.80	8.56 ± 3.15	0.10	5414 --> 1870
3547.19 ± 0.89	7.65 ± 3.04	0.09	5601 --> 2054
3572.05 ± 0.25	17.09 ± 1.49	0.21	4714 --> 1142
3585.36 ± 0.46	6.14 ± 1.07	0.08	5631 --> 2045
3642.42 ± 0.59	5.60 ± 1.18	0.07	4790 --> 1148
3664.75 ± 0.19	31.52 ± 2.11	0.39	4097 --> 433
3706.58 ± 0.68	4.20 ± 0.96	0.05	6261 --> 2554
3721.59 ± 0.44	8.68 ± 1.37	0.11	3934 --> 213
3770.36 ± 0.34	10.20 ± 1.22	0.12	4912 --> 1142
3789.26 ± 0.34	8.66 ± 1.09	0.11	3789 --> 0
3803.98 ± 0.19	90.27 ± 5.32	1.10	3804 --> 0
3821.91 ± 0.44	5.62 ± 0.84	0.07	5385 --> 1563
3848.72 ± 0.66	6.14 ± 1.40	0.08	4991 --> 1142
3867.60 ± 0.17	148.04 ± 8.01	1.81	3867 --> 0
3876.73 ± 0.32	12.10 ± 1.30	0.15	3877 --> 0
3883.95 ± 0.22	25.92 ± 1.90	0.32	4097 --> 213
3890.49 ± 0.33	11.97 ± 1.31	0.15	3891 --> 0
3934.34 ± 0.18	55.80 ± 3.48	0.68	3934 --> 0
3941.65 ± 0.35	6.49 ± 1.25	0.08	6261 --> 2319
3954.24 ± 1.18	2.22 ± 0.85	0.03	3955 --> 0
4004.47 ± 0.76	4.54 ± 1.11	0.06	6277 --> 2273
4009.87 ± 1.20	3.00 ± 1.11	0.04	5396 --> 1385
4017.55 ± 0.21	23.64 ± 1.70	0.29	4017 --> 0
4156.56 ± 0.55	5.50 ± 1.06	0.07	5396 --> 1238
4242.07 ± 0.46	4.44 ± 0.70	0.05	5385 --> 1142
4250.90 ± 0.71	2.77 ± 0.67	0.03	6707 --> 2456
4271.23 ± 0.19	19.27 ± 1.26	0.24	5414 --> 1142
4281.87 ± 0.27	9.70 ± 0.83	0.12	4714 --> 433
4387.87 ± 0.37	6.73 ± 0.78	0.08	6707 --> 2319
4461.38 ± 0.43	4.44 ± 0.61	0.05	4461 --> 0
4481.20 ± 0.57	3.41 ± 0.60	0.04	6261 --> 1780
4615.36 ± 0.91	2.54 ± 0.76	0.03	6000 --> 1385
4626.96 ± 0.45	5.89 ± 0.82	0.07	5775 --> 1148
4644.95 ± 0.93	2.52 ± 0.77	0.03	5631 --> 986
4875.09 ± 0.26	10.11 ± 0.83	0.12	6261 --> 1385

Table 10. (Continued)

Energy (keV)	Relative Intensity[1]	Intensity per 100 Beta Decays[2]	Assignment (keV)
4890.02 ± 0.83	1.50 ± 0.34	0.02	
4899.36 ± 0.48	2.84 ± 0.36	0.03	6707 --> 1808
4947.45 ± 0.61	4.01 ± 0.71	0.05	6097 --> 1148
4953.88 ± 1.13	2.14 ± 0.52	0.03	6097 --> 1142
4971.81 ± 0.59	1.85 ± 0.35	0.02	
4996.76 ± 0.53	2.87 ± 0.54	0.04	
5138.94 ± 1.00	1.25 ± 0.36	0.02	
5154.63 ± 0.97	1.30 ± 0.38	0.02	
5164.78 ± 1.10	1.11 ± 0.37	0.01	
5396.72 ± 0.91	1.69 ± 0.41	0.02	5396 --> 0
5408.99 ± 0.70	2.30 ± 0.42	0.03	

of 1.65 ± 0.30% from the work of Talbert, et al. (10). A comparison between the energies presented in this work and those provided by Brissot, et al. (34) indicates that the values are consistent to within quoted errors in most cases. However, these values disagree in a systematic fashion with those reported by Achterberg, et al. (28). In a similar manner a comparison can be made among relative intensities quoted in these three works. Such a comparison is made in Table 11. Again the values agree quite well with those of Brissot, et al. but disagree systematically with those proposed by Achterberg, et al.

Of the 243 gamma rays determined to be ^{93}Rb photopeaks, approximately 52 have intensities greater than 10 and appear not to have been observed in other studies. This is partially due to the fact that Brissot, et al. reported in their article only the 69 transitions which had been placed in their final level scheme. They report they actually observed 162 transitions but failed to list those which had not been placed. An examination of the spectrum provided by Achterberg, et al. reveals why so few peaks were reported in that study. The most intense peak has a height of only 3.5 x 10^3 counts while the same peak in the spectrum reported here has a height of 10^6 counts. Since Brissot, et al. do not provide a spectrum for examanation, no similar comparison can be made with that work.

Table 11. Comparison of intensities with other ^{93}Rb studies

Energy	This Work	Achterberg et al. (31)	Brissot[1] et al. (28)
213.39	384 ± 22	385 ± 30	388
219.16	158 ± 9	137 ± 9	152
432.51	1000 ± 53	1000 ± 50	1000
709.95	308 ± 22[2]	250 ± 40	302
793.65	62 ± 3	49 ± 10	66
986.05	391 ± 20	342 ± 30	380
1148.18	88 ± 5	79 ± 5	109
1238.30	85 ± 5	71 ± 7	90
1332.97	61 ± 6	36 ± 5	
1385.21	328 ± 17	80 ± 50	338
1562.91	58 ± 4		62
1612.87	96 ± 6	93 ± 13	104
1808.50	161 ± 8	124 ± 11	152
1869.69	109 ± 6	85 ± 7	110
1910.72	66 ± 4	40 ± 11	74
2054.06	77 ± 4	63 ± 5	75
2229.44	54 ± 3	21 ± 5	55
2704.97	59 ± 4	42 ± 4	58
2861.34	64 ± 4		35
2869.23	64 ± 4		
3370.97	65 ± 4	40 ± 7	80
3458.19	214 ± 11	145 ± 19	255
3803.98	90 ± 5	45 ± 5	107
3867.60	148 ± 8	47 ± 13	174
3934.34	56 ± 3	39 ± 7	54

[1]The intensity uncertainties are reported to vary between 5 and 10% depending on the gamma ray intensity value.

[2]In order to eliminate the contamination resulting from the 710.4-keV gamma ray observed in the decay of ^{93}Sr, this intensity has been determined from the 432.5-keV coincidence gate.

Multiplets which had previously been reported as single peaks were also resolved at 1148-1150, 1746-1750, 1836-1838-1842, 1992-1998, and 2955-2958 keV. Ten gamma rays not observed in this work are placed in the level scheme offered by Brissot, et al. (34). Seven of these transitions are placed between levels also proposed in this work on the basis of different gamma rays. The other three, along with the 2230-keV gamma ray, are used to define a level at 4284 keV. In this work the 2230-keV gamma ray is placed elsewhere based on coincidence information and no level is present at 4284 keV. Achterberg, et al. (28) reported seven gamma rays not seen in this study. Six of these depopulate levels which are not evident in this study or that of Brissot, et al. The other gamma ray was not placed in their level scheme.

The coincidence information is compiled in Table 12. The coincidences observed in this work are consistent with the small number of coincidences reported by Achterberg, et al. (28). Although only five coincidence gates were examined by Brissot, et al. (34) a rather large amount of information was obtained in these gates. These coincidences are also consistent with the information reported here except for coincidences between the 1927-keV gamma ray and the 432- and 710-keV gamma rays. In this work the 1927-keV gamma ray appears to be in coincidence only with the 213-keV gamma ray. It is therefore placed as feeding this level. In the work

Table 12. Coincidences observed in the decay of ^{93}Rb.

Gate (keV)	Definite Coincidences (keV)	Possible Coincidences (keV)
213.4	219, 710, 929, 935, 1928, 2524	1350, 1612, 2350
219.2	213, 710, 1613, 2350	768, 1096
432.5	710, 1096, 1130, 1150, 1437, 1612, 1684	1831, 2026, 2350
710.0	213, 219, 432, 1150	768, 2646, 2661
793.7	986	2087, 2262
929.0	213	
934.7	213	
986.1	794, 1333, 1635, 2087	822, 1286, 1365, 1548, 2270
1068.5		1501
1096.7	432	213, 219
1130.2	432	710
1150.3	432, 710	
1238.2		1316
1315.6		1238
1333.0	986	1547
1349.7	213	
1365.4	986	
1385.2	1389, 2505	1501, 2491
1437.1		432

Table 12. (Continued)

Gate (keV)	Definite Coincidences (keV)	Possible Coincidences (keV)
1501.1		1385
1547.8	986, 1333	
1594.6		1385
1612.9	213, 219, 432, 1822	1831
1635.3	986	
1662.2		710, 1150
1684.8	432	
1808.5	2229	2059
1812.8	1385	
1821.9	432, 1613	
1869.7	1978	
1900.9		2054
1927.6	213	
1978.3	1869	
2026.9	432	
2058.8		1808
2087.4	794, 986	
2229.4	1808	
2262.0	794	
2349.6	213, 219, 432	
2418.2	986	

Table 12. (Continued)

Gate (keV)	Definite Coincidences (keV)	Possible Coincidences (keV)
2491.2	1385	
2505.2	1385	
2523.7	213	
2646.6	432, 710	
2661.1	432, 710	
2705.0	432, 710	213, 219
2724.6	432, 710	
2861.3	986	
2954.9	432, 710	
3371.0	213, 219, 432	
3458.2	213, 219, 432	
3501.9	213, 219, 432	
3664.7	432	

of Brissot, et al., the 1927-keV coincidence, along with the 1684-keV gamma ray, is used tc establish a new level at 3069 keV. Since the 1684-keV gamma ray is positioned elsewhere on the basis of coincidence information in this work the existence of this level seems unlikely. Brissot, et al. also list the coincidences 432-1837, and 986-2890 not seen in this study. However these two gamma rays were placed between the same levels in this study on the basis of energy sums alone. Information from 53 coincidence gates was used to build the final level scheme shown in Figure 15. This level scheme contains 74 levels based on the placement of 231 gamma rays representing approximately 99.5% of the total gamma intensity observed. In all, using this coincidence information, it is possible to verify 41 of the 73 excited levels in the level scheme proposed in this work. Since, in general, the gamma-ray intensities reported here agree with those reported by Brissot, et al. (34), the discrepancy between that work and the study of Achterberg, et al. appears to be resolved. Based on the gamma-ray information Brissot, et al. did present, it seems that their reported energies and intensities are in most cases correct.

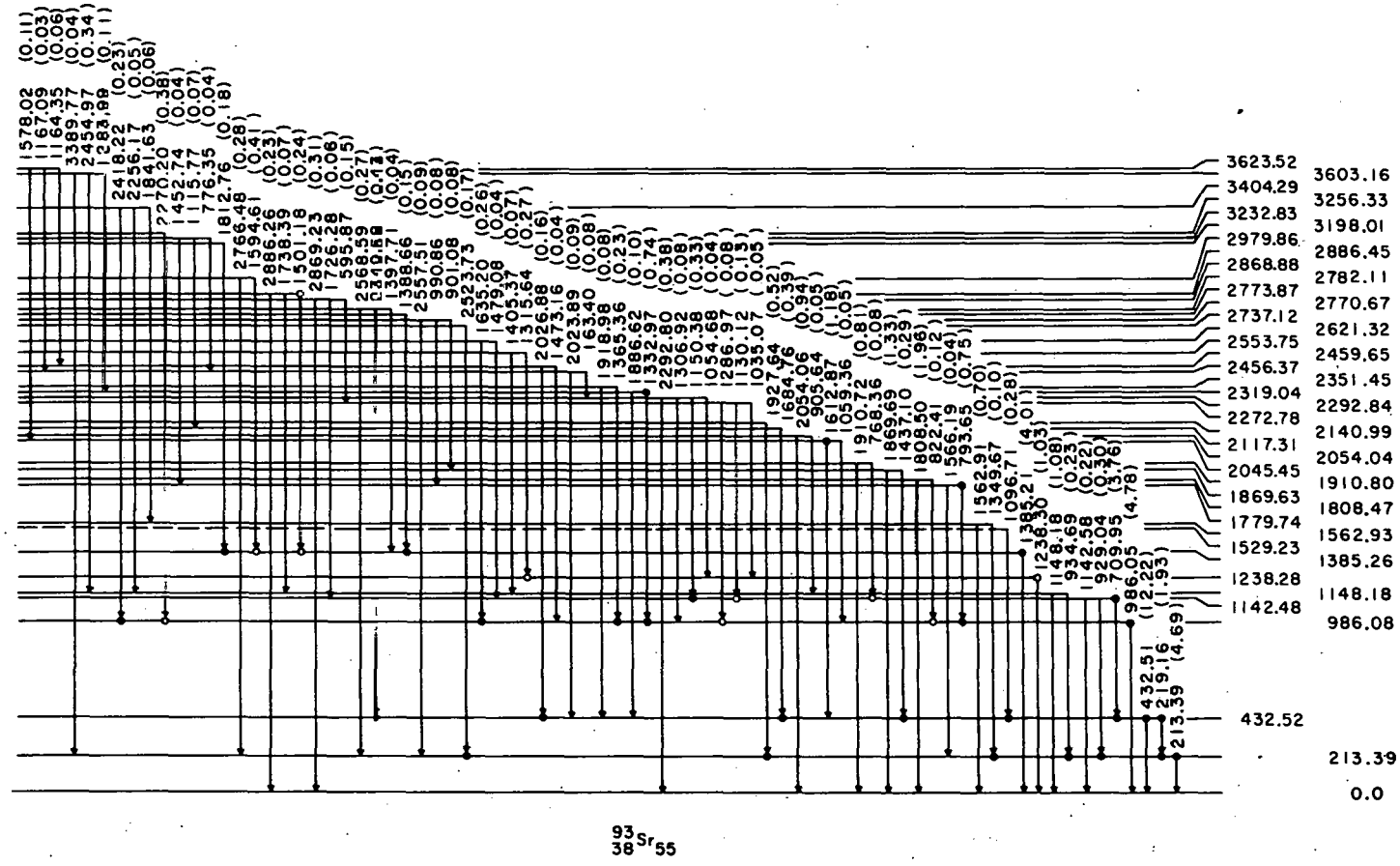

Figure 15. ^{93}Sr level scheme

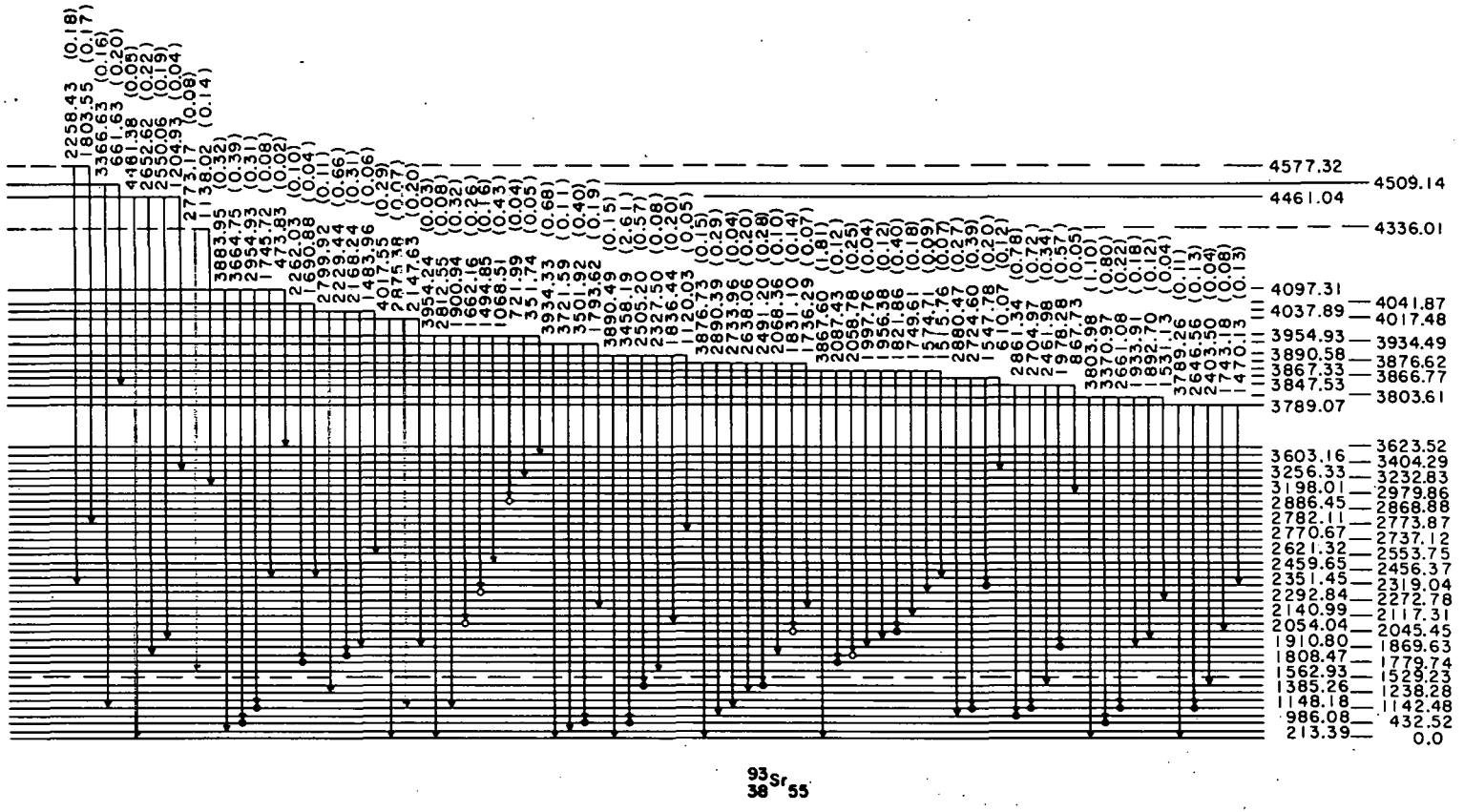

Figure 15. (Continued)

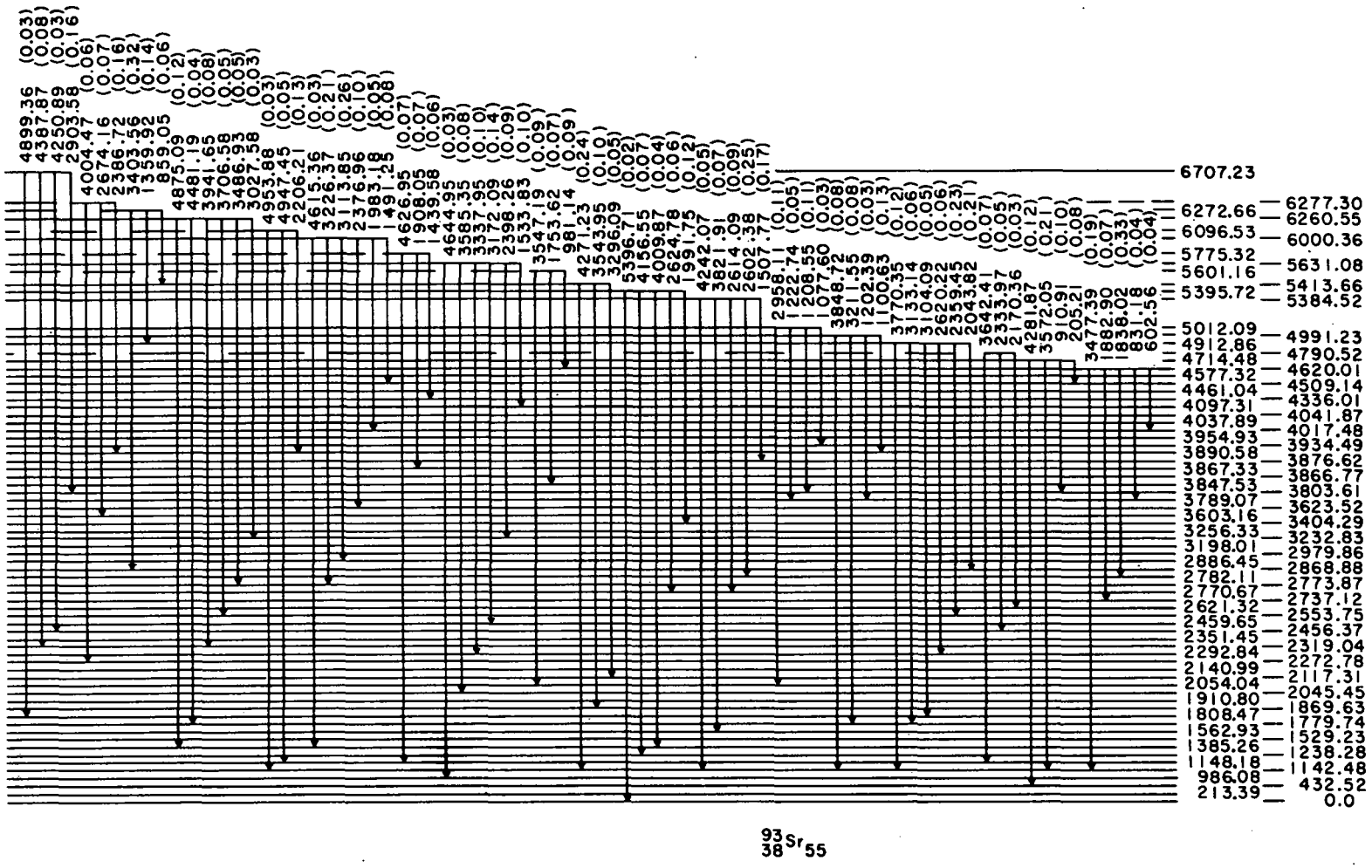

Figure 15. (Continued)

C. Decay of ^{93}Kr

The ^{93}Kr enhanced decay spectrum is shown in Figure 16. Due to the complexity of the low-energy region of this decay, a LEPS spectrum for the region 0-350 keV is also provided in Figure 17. The Au x-rays in this spectrum result from the presence of Au electrical contacts in the Ge(Li) detectors. The number of full-energy peaks in this spectrum was determined to be 217 and these gamma rays are listed in Table 13. A ground-state beta branching of 0% was adopted from the work of Achterberg, et al. (28). This branching value, in addition to a delayed neutron emission probability of 2.6 ± 0.5% (10), was used to calculate the absolute gamma-ray intensities quoted in Table 13. In this decay the most intense peak at 253 keV is actually a multiplet. As a result the intensities are all normalized relative to the second most intense peak at 323.9 keV. The energies agree, in most cases, to within errors quoted in the other articles published on the decay of this nuclide (28,34).

Although the intensities reported in this study agree fairly well with those proposed by Brissot, et al. (34), there are some important discrepancies. The first difference results from their failure to examine the low-energy region in satisfactory detail. Consequently the low-energy peaks at 57.1 and 70.6 keV were not detected. They also reported that the 252.8-keV gamma ray has an intensity which is approxi-

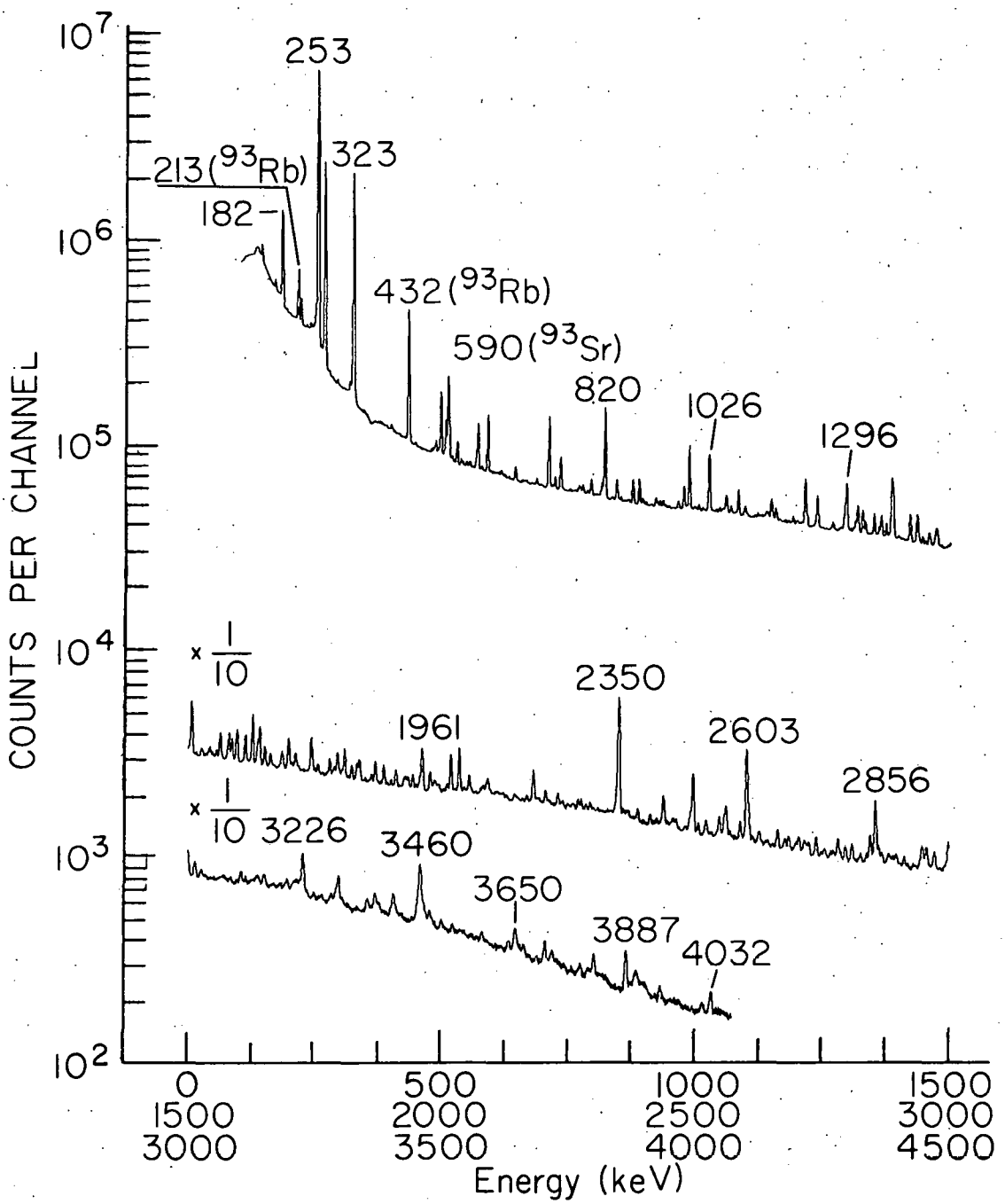

Figure 16. Gamma-ray spectrum for the decay of ^{93}Kr

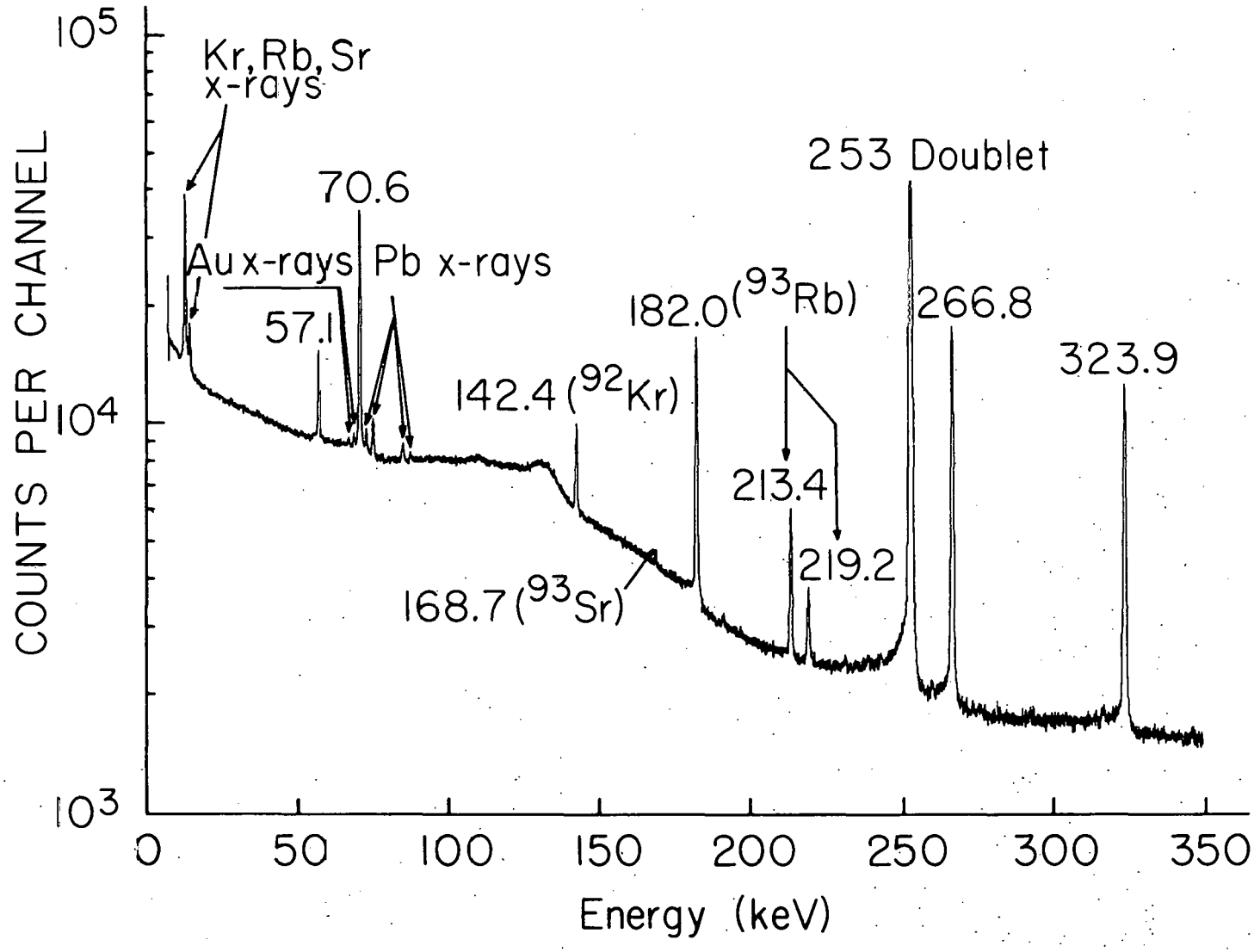

Figure 17. Low energy gamma-ray spectrum for the decay of ^{93}Kr

Table 13. Gamma rays observed in the decay of ^{93}Kr.

Energy (keV)	Relative Intensity[1]	Intensity per 100 Beta Decays[2]	Assignment (keV)
57.11 ± 0.05	10.70 ± 0.54	0.26	324 --> 267
70.57 ± 0.05	64.20 ± 3.21	1.55	324 --> 253
182.02 ± 0.05	223.33 ± 11.62	5.39	506 --> 324
191.06 ± 0.08	3.24 ± 0.32	0.08	2856 --> 2665
239.26 ± 0.22	6.61 ± 1.21	0.16	1880 --> 1641
252.51 ± 0.06	810.99 ± 42.14	19.58	506 --> 253
253.42 ± 0.05	1707.97 ± 88.76	41.24	253 --> 0
254.83 ± 0.05	28.86 ± 2.90	0.70	5920 --> 5665
266.83 ± 0.05	853.77 ± 43.05	20.53	267 --> 0
292.88 ± 0.08	3.75 ± 0.25	0.09	1850 --> 1558
316.72 ± 0.09	10.03 ± 0.77	0.24	4051 --> 3734
323.89 ± 0.05	1000.00 ± 50.17	24.15	324 --> 0
399.01 ± 0.12	4.85 ± 0.41	0.12	2609 --> 2210
401.51 ± 0.28	1.87 ± 0.34	0.05	1964 --> 1563
480.44 ± 0.20	3.59 ± 0.50	0.09	2169 --> 1689
491.93 ± 0.22	3.25 ± 0.49	0.08	3494 --> 3002
496.56 ± 0.05	75.24 ± 3.84	1.82	820 --> 324
519.78 ± 0.19	3.99 ± 0.54	0.10	3265 --> 2745
529.59 ± 0.05	20.43 ± 1.07	0.49	1350 --> 820
553.53 ± 0.20	3.17 ± 0.48	0.08	820 --> 267
555.41 ± 0.15	4.30 ± 0.51	0.10	3801 --> 3245
567.05 ± 0.11	6.92 ± 0.54	0.17	820 --> 253
570.16 ± 0.05	49.44 ± 2.53	1.20	2856 --> 2286
578.73 ± 0.17	3.50 ± 0.40	0.08	6070 --> 5492
616.51 ± 0.11	4.19 ± 0.32	0.10	5665 --> 5049
623.64 ± 0.16	2.14 ± 0.23	0.05	2265 --> 1641
643.18 ± 0.23	3.77 ± 0.86	0.09	2286 --> 1642
644.78 ± 0.09	11.16 ± 1.02	0.27	2609 --> 1964
686.51 ± 0.11	5.56 ± 0.42	0.13	2856 --> 2169
713.34 ± 0.36	2.31 ± 0.44	0.06	
716.89 ± 0.48	2.07 ± 0.53	0.05	
722.68 ± 0.08	11.30 ± 0.71	0.27	2286 --> 1563

[1]Measured relative to the 323.9-keV transition (I_γ = 1000).
[2]Calculated from relative intensities using the factor 0.0246 based on the decay scheme proposed with 0% beta branching to the ground state of ^{93}Rb and a delayed neutron emission probability of 2.6%.

Table 13. (Continued)

Energy (keV)	Relative Intensity[1]	Intensity per 100 Beta Decays[2]	Assignment (keV)
733.72 ± 0.05	36.39 ± 1.86	0.88	2084 --> 1350
737.24 ± 0.23	2.20 ± 0.31	0.05	1558 --> 820
770.70 ± 0.37	5.70 ± 0.95	0.14	4051 --> 3280
777.57 ± 0.10	8.26 ± 0.62	0.20	3063 --> 2286
820.45 ± 0.05	154.44 ± 8.04	3.73	820 --> 0
844.12 ± 0.06	23.27 ± 1.21	0.56	1350 --> 506
852.66 ± 0.12	3.85 ± 0.32	0.09	3063 --> 2210
891.46 ± 0.60	1.33 ± 0.39	0.03	2856 --> 1964
895.05 ± 0.13	7.18 ± 0.55	0.17	2745 --> 1850
898.03 ± 0.47	1.76 ± 0.42	0.04	5759 --> 4861
921.19 ± 0.10	9.42 ± 0.66	0.23	3777 --> 2856
965.01 ± 0.11	8.99 ± 0.71	0.22	2815 --> 1850
976.08 ± 0.06	29.37 ± 1.60	0.71	2665 --> 1689
1000.53 ± 0.34	1.85 ± 0.35	0.04	3265 --> 2265
1005.65 ± 0.09	6.77 ± 0.47	0.16	2856 --> 1850
1026.19 ± 0.05	90.32 ± 4.56	2.18	1350 --> 324
1046.57 ± 0.14	5.04 ± 0.45	0.12	2609 --> 1563
1051.69 ± 0.30	3.07 ± 0.51	0.07	1558 --> 506
1054.55 ± 0.23	4.45 ± 0.53	0.11	3265 --> 2210
1058.71 ± 0.17	12.76 ± 1.70	0.31	5920 --> 4861
1060.53 ± 0.13	15.93 ± 1.81	0.38	4861 --> 3800
1080.58 ± 0.69	1.69 ± 0.56	0.04	6572 --> 5492
1083.42 ± 0.06	33.81 ± 1.80	0.82	1350 --> 267
1097.14 ± 0.09	5.30 ± 1.00	0.13	1350 --> 253
1126.28 ± 0.33	2.79 ± 0.49	0.07	2815 --> 1689
1136.06 ± 0.34	3.24 ± 0.59	0.08	1642 --> 506
1139.17 ± 0.18	7.96 ± 0.70	0.19	3308 --> 2169
1157.09 ± 0.11	13.11 ± 1.02	0.32	5237 --> 4080
1191.49 ± 0.09	9.63 ± 0.62	0.23	3801 --> 2609
1214.98 ± 0.05	72.70 ± 3.77	1.76	2856 --> 1641
1235.53 ± 0.30	5.48 ± 0.87	0.13	3245 --> 2009
1238.76 ± 0.06	46.01 ± 2.49	1.11	1563 --> 324
1290.54 ± 0.23	9.90 ± 1.37	0.24	1558 --> 267
1296.08 ± 0.06	78.29 ± 4.13	1.89	1563 --> 267
1309.51 ± 0.21	4.33 ± 0.50	0.10	1563 --> 253
1313.44 ± 0.14	12.16 ± 0.99	0.29	3002 --> 1689
1318.38 ± 0.14	38.06 ± 3.48	0.92	1642 --> 324
1350.24 ± 0.06	30.98 ± 1.67	0.75	1350 --> 0
1360.26 ± 0.11	9.35 ± 0.65	0.23	3002 --> 1641
1364.77 ± 0.09	28.33 ± 1.96	0.68	1689 --> 324

Table 13. (Continued)

Energy (keV)	Relative Intensity[1]	Intensity per 100 Beta Decays[2]	Assignment (keV)
1374.78 ± 0.09	17.55 ± 1.17	0.42	3063 --> 1689
1382.67 ± 0.34	7.83 ± 1.62	0.19	3551 --> 2169
1387.92 ± 0.09	56.07 ± 3.81	1.35	1641 --> 253
1421.79 ± 0.06	39.97 ± 2.12	0.97	1689 --> 267
1435.35 ± 0.13	41.52 ± 3.10	1.00	1689 --> 253
1445.64 ± 0.18	8.36 ± 0.87	0.20	5496 --> 4051
1458.50 ± 0.09	16.44 ± 1.07	0.40	1964 --> 506
1471.32 ± 0.32	15.71 ± 1.68	0.38	4080 --> 2609
1505.76 ± 0.06	92.51 ± 4.81	2.23	2856 --> 1350
1508.41 ± 0.23	9.00 ± 1.28	0.22	3359 --> 1850
1525.89 ± 0.20	8.88 ± 1.00	0.21	1850 --> 324
1528.88 ± 0.30	5.98 ± 0.94	0.14	3494 --> 1964
1543.15 ± 0.11	14.19 ± 0.98	0.34	
1556.32 ± 0.12	10.32 ± 0.77	0.25	3245 --> 1689
1563.09 ± 0.06	39.22 ± 2.09	0.95	1563 --> 0
1576.61 ± 0.56	3.66 ± 0.96	0.09	3265 --> 1689
1586.89 ± 0.07	35.11 ± 1.95	0.85	3551 --> 1964
1596.20 ± 0.06	56.67 ± 2.99	1.37	1850 --> 253
1613.33 ± 0.08	14.30 ± 2.50	0.35	1880 --> 267
1616.85 ± 0.77	2.77 ± 0.99	0.07	4861 --> 3245
1627.10 ± 0.06	82.10 ± 4.36	1.98	1880 --> 253
1638.04 ± 0.19	20.86 ± 1.86	0.50	3280 --> 1642
1641.08 ± 0.06	59.71 ± 3.14	1.44	1641 --> 0
1651.87 ± 0.08	28.72 ± 1.67	0.69	3002 --> 1350
1662.74 ± 0.13	16.96 ± 1.27	0.41	2169 --> 506
1666.31 ± 0.58	3.43 ± 0.92	0.08	3308 --> 1642
1681.91 ± 0.71	3.98 ± 1.00	0.10	3245 --> 1563
1685.07 ± 0.20	22.68 ± 1.97	0.55	2009 --> 324
1687.44 ± 0.50	5.95 ± 2.05	0.14	3245 --> 1558
1697.84 ± 0.06	58.43 ± 3.22	1.41	1964 --> 267
1704.45 ± 0.18	10.54 ± 1.01	0.25	2210 --> 506
1710.78 ± 0.18	20.83 ± 2.19	0.50	1964 --> 253
1713.38 ± 0.28	12.81 ± 1.96	0.31	3063 --> 1350
1742.49 ± 0.08	53.28 ± 3.18	1.29	2009 --> 267
1745.28 ± 0.20	17.20 ± 1.82	0.42	3308 --> 1563
1755.88 ± 0.19	13.11 ± 1.29	0.32	2009 --> 253
1779.68 ± 0.08	23.78 ± 1.39	0.57	2285 --> 506
1785.80 ± 0.40	5.13 ± 0.98	0.12	4051 --> 2265
1788.96 ± 0.17	12.98 ± 1.17	0.31	2609 --> 820
1794.80 ± 0.08	35.98 ± 2.03	0.87	4080 --> 2286

Table 13. (Continued)

Energy (keV)	Relative Intensity[1]	Intensity per 100 Beta Decays[2]	Assignment (keV)
1798.25 ± 0.26	7.53 ± 0.95	0.18	4861 --> 3063
1803.71 ± 0.17	9.22 ± 0.84	0.22	5049 --> 3245
1822.26 ± 1.19	6.64 ± 11.35	0.16	3465 --> 1642
1823.76 ± 0.80	14.17 ± 11.42	0.34	3465 --> 1641
1840.12 ± 0.34	11.01 ± 3.40	0.27	4051 --> 2210
1850.10 ± 0.27	4.01 ± 0.55	0.10	1850 --> 0
1862.68 ± 0.12	11.04 ± 0.78	0.27	3551 --> 1689
1886.79 ± 0.08	28.99 ± 1.68	0.70	2210 --> 324
1929.71 ± 0.34	13.21 ± 1.95	0.32	3280 --> 1350
1943.54 ± 0.11	19.71 ± 1.32	0.48	2210 --> 267
1957.10 ± 0.18	14.49 ± 1.38	0.35	2210 --> 253
1961.83 ± 0.06	74.06 ± 3.91	1.79	2286 --> 324
1989.29 ± 0.26	11.66 ± 1.35	0.28	3631 --> 1642
1994.41 ± 0.21	10.79 ± 1.11	0.26	2815 --> 820
2011.68 ± 0.19	9.54 ± 0.91	0.23	2265 --> 253
2018.87 ± 0.07	58.27 ± 3.07	1.41	2286 --> 267
2035.36 ± 0.07	75.14 ± 3.89	1.81	2856 --> 820
2082.62 ± 0.14	12.27 ± 0.90	0.30	5860 --> 3777
2088.24 ± 0.19	11.34 ± 1.01	0.27	3777 --> 1689
2160.02 ± 0.46	2.83 ± 0.60	0.07	3801 --> 1641
2179.28 ± 1.17	3.97 ± 3.26	0.10	6260 --> 4080
2181.54 ± 0.12	48.16 ± 4.06	1.16	3002 --> 820
2235.44 ± 0.76	3.01 ± 0.92	0.07	5237 --> 3002
2239.21 ± 0.31	7.41 ± 1.00	0.18	2745 --> 506
2308.30 ± 0.52	3.14 ± 0.73	0.08	5860 --> 3551
2342.37 ± 0.79	7.28 ± 2.54	0.18	2609 --> 267
2349.96 ± 0.10	305.99 ± 15.77	7.40	2856 --> 506
2365.96 ± 0.64	5.34 ± 2.02	0.13	5860 --> 3494
2368.46 ± 0.59	5.69 ± 2.04	0.14	5920 --> 3551
2411.44 ± 0.15	12.82 ± 0.89	0.31	2665 --> 253
2424.26 ± 0.25	7.18 ± 0.76	0.17	3245 --> 820
2491.24 ± 0.31	19.35 ± 2.62	0.47	2815 --> 324
2496.05 ± 0.10	95.42 ± 4.98	2.30	3002 --> 506
2517.35 ± 0.56	3.23 ± 0.73	0.08	4080 --> 1563
2521.47 ± 0.16	19.61 ± 1.25	0.47	6572 --> 4051
2531.85 ± 0.28	5.39 ± 0.63	0.13	2856 --> 324
2548.02 ± 0.17	25.83 ± 1.99	0.62	2815 --> 267
2557.26 ± 0.16	24.28 ± 1.70	0.59	3063 --> 506
2561.33 ± 0.12	41.41 ± 2.42	1.00	2815 --> 253
2589.18 ± 0.15	21.20 ± 1.43	0.51	2856 --> 267

Table 13. (Continued)

Energy (keV)	Relative Intensity[1]	Intensity per 100 Beta Decays[2]	Assignment (keV)
2602.61 ± 0.11	173.98 ± 9.06	4.20	2856 --> 253
2606.65 ± 0.19	29.52 ± 2.43	0.71	5965 --> 3359
2663.49 ± 0.20	21.17 ± 2.22	0.51	5665 --> 3002
2678.04 ± 0.35	10.89 ± 1.90	0.26	3002 --> 324
2700.46 ± 0.32	9.09 ± 1.10	0.22	4051 --> 1350
2720.24 ± 0.35	8.32 ± 0.96	0.20	5965 --> 3245
2739.14 ± 0.12	21.10 ± 1.21	0.51	3063 --> 324
2755.62 ± 0.25	8.88 ± 0.92	0.21	
2772.85 ± 0.28	8.49 ± 0.92	0.21	
2782.26 ± 0.20	22.89 ± 1.81	0.55	
2796.56 ± 0.16	15.02 ± 1.03	0.36	3063 --> 267
2809.92 ± 0.12	18.34 ± 1.04	0.44	3063 --> 253
2826.62 ± 0.24	8.06 ± 0.81	0.19	5491 --> 2665
2838.48 ± 0.30	7.48 ± 0.89	0.18	5049 --> 2210
2846.03 ± 0.45	26.65 ± 12.00	0.64	
2852.62 ± 0.52	7.93 ± 1.77	0.19	3359 --> 506
2855.95 ± 0.11	90.35 ± 4.89	2.18	2856 --> 0
2913.49 ± 0.30	8.61 ± 1.04	0.21	3734 --> 820
2944.60 ± 0.40	7.29 ± 1.21	0.18	5759 --> 2815
2948.32 ± 0.19	25.14 ± 1.68	0.61	6725 --> 3777
2956.68 ± 0.16	24.78 ± 1.66	0.60	3777 --> 820
2972.22 ± 0.20	18.12 ± 1.75	0.44	
2998.45 ± 0.30	25.96 ± 6.14	0.63	3265 --> 267
3000.49 ± 0.54	13.50 ± 6.11	0.33	5665 --> 2665
3014.66 ± 0.45	12.91 ± 4.04	0.31	5759 --> 2745
3026.51 ± 0.30	7.16 ± 0.95	0.17	3280 --> 253
3097.65 ± 0.52	3.23 ± 0.85	0.08	
3105.40 ± 0.20	12.23 ± 0.98	0.30	3359 --> 253
3150.82 ± 0.48	8.71 ± 2.13	0.21	5965 --> 2815
3196.79 ± 0.66	6.02 ± 1.94	0.15	6260 --> 3063
3214.50 ± 0.29	8.86 ± 0.89	0.21	6070 --> 2856
3220.31 ± 0.31	7.44 ± 0.83	0.18	4861 --> 1641
3226.70 ± 0.15	41.42 ± 2.82	1.00	3494 --> 267
3229.89 ± 0.66	6.10 ± 1.95	0.15	4051 --> 820
3250.30 ± 0.27	6.50 ± 0.69	0.16	5860 --> 2609
3260.69 ± 0.48	3.64 ± 0.63	0.09	6725 --> 3465
3281.12 ± 0.66	3.32 ± 0.81	0.08	5492 --> 2210
3285.26 ± 0.34	7.34 ± 0.85	0.18	5496 --> 2210
3294.82 ± 0.76	8.64 ± 1.48	0.21	3801 --> 506
3298.31 ± 0.19	26.63 ± 2.12	0.64	3551 --> 253

Table 13. (Continued)

Energy (keV)	Relative Intensity[1]	Intensity per 100 Beta Decays[2]	Assignment (keV)
3303.90 ± 0.83	4.45 ± 1.32	0.11	4861 --> 1558
3307.19 ± 0.74	4.17 ± 1.44	0.10	3631 --> 324
3355.97 ± 0.54	8.66 ± 2.58	0.21	5965 --> 2609
3358.79 ± 1.02	5.02 ± 2.46	0.12	3359 --> 0
3379.74 ± 0.37	7.04 ± 0.96	0.17	5665 --> 2286
3408.09 ± 0.22	18.91 ± 1.42	0.46	5492 --> 2084
3412.72 ± 0.51	5.80 ± 1.05	0.14	5496 --> 2084
3445.11 ± 0.56	2.70 ± 0.54	0.07	6260 --> 2815
3453.31 ± 0.32	8.39 ± 0.99	0.20	3777 --> 324
3460.66 ± 0.63	29.28 ± 5.43	0.71	6725 --> 3265
3464.39 ± 1.24	13.08 ± 3.73	0.32	3465 --> 0
3467.20 ± 1.02	11.04 ± 5.23	0.27	3734 --> 267
3471.26 ± 0.53	6.33 ± 1.39	0.15	
3482.42 ± 0.45	4.94 ± 0.80	0.12	5492 --> 2009
3582.65 ± 0.26	6.27 ± 0.62	0.15	
3634.67 ± 0.30	7.89 ± 0.88	0.19	5920 --> 2286
3645.86 ± 0.52	9.74 ± 2.25	0.24	5496 --> 1850
3649.21 ± 0.43	12.71 ± 2.23	0.31	5860 --> 2210
3655.45 ± 0.46	5.72 ± 0.88	0.14	5920 --> 2265
3705.87 ± 0.16	12.27 ± 0.83	0.30	
3776.02 ± 0.30	6.14 ± 0.66	0.15	5860 --> 2084
3795.80 ± 1.08	1.55 ± 0.50	0.04	5965 --> 2169
3887.09 ± 0.43	5.26 ± 0.79	0.13	5237 --> 1350
4014.14 ± 1.08	2.49 ± 1.05	0.06	
4032.88 ± 0.20	8.77 ± 0.67	0.21	

mately three times that of the 253.5-keV member of this multiplet. This intensity apportionment is obviously not consistent with that from the fit of this multiplet shown in Figure 8. Finally, the gamma ray at 505.8 keV was reported to have an intensity of 100 as compared to an intensity of 34.0 ± 1.8 as reported in this work. In this work the 505.8-keV peak was assumed to be due entirely to sum peaking. This statement is supported by the correlation between source-to-detector distance and the intensity of this peak. Brissot, et al. (34) state that their detectors were positioned approximately 1 cm from the ^{93}Kr source. In this study the source-to-detector distance was approximately 2 cm. Since the intensity of a sum peak varies with the solid angle subtended by the detector, the intensity ratio of a sum peak observed in these two works should be approximately 4 : 1. The ratio is slightly less than this, as one would expect, because the distance should actually be measured from the source to the effective center of the Ge(Li) crystal. If this distance were included the ratio would be somewhat less than 4 : 1. This sum peak will have a rather large intensity because it is possible to sum two different intense cascades to obtain a peak at this energy. The intensity of this sum peak also agrees fairly well with the expected intensity based on the identification of a definite sum peak in the ^{93}Sr decay.

Brissot, et al. again report only the transitions placed in their final level scheme. They mention that they observed 114 transitions but energies are quoted for just 43 transitions which represent only 85% of the gamma intensity observed. Thus some of the 41 gamma rays with intensities greater than 10 not previously reported may also have been observed by Brissot, et al. As before, Achterberg, et al. (28) provide a spectrum which illustrates why such a large number of gamma rays were not observed in their study. The 324-keV peak has a height of only 7.5×10^3 counts while the same peak in the spectrum provided here has a height of almost 2.0×10^6 counts. Brissot, et al. do not provide any spectrum for this decay so again no comparison with their data can easily be made. Multiplets have also been resolved at 643-645, 1059-1061, 1136-1139, 1291-1296, 1711-1713, 1742-1745, 1795-1798, 2557-2561, 2603-2607 and 3227-3230 keV where previously only single peaks had been reported. Brissot, et al. do report peaks at energies of 1091.0 and 1613.8 keV which are comprised in large part of ^{93}Rb contamination peaks according to this study. These transitions have intensities in this work of 0.5 and 1.4, respectively while Brissot, et al. report intensities of 1.2 and 2.4 respectively. These gamma rays are placed between the same levels in both works.

Achterberg, et al. report 12 gamma rays which are not present in this study. Two of these, at 1077 and 2626 keV, are determined to be escape peaks while that at 1750 keV is partially an escape peak and partially a ^{93}Rb peak. The other nine gamma rays are placed using levels which are based largely on these transitions themselves and which are not present in the level schemes proposed in this work or that of Brissot, et al.

A comparison of intensities with those reported by Achterberg, et al. and Brissot, et al. is made in Table 14. As mentioned in the discussion of the ^{93}Rb decay, the intensities disagree in a systematic fashion. Since the deviation between intensities follows the same general pattern in both the ^{93}Rb and ^{93}Kr decays it appears that the disagreement must result from the efficiency curves used for the detectors. Because the results reported here agree, in general, with those of Brissot, et al. (34), it would seem that the intensities reported by Achterberg, et al. (28) are suspect. Doubt about the accuracy of these intensities is reinforced by two previous cases of intensity disparity with studies performed at IALE. In a recent study of the decays of ^{91}Kr and ^{91}Rb, Glascock (45) reported a similar pattern of intensity discrepancies. An earlier study of the decays of ^{138}Xe and ^{138}Cs by Carlson, et al. (46) provided the first evidence of an intensity disagreement with a similar study performed

Table 14. Comparison of intensities with other ^{93}Kr studies

Energy	This Work	Achterberg et al. (31)	Brissot[1] et al. (28)
70.57	64 ± 3	110 ± 40	
182.02	232 ± 12	223 ± 15	240
252.51	806 ± 42	1000 ± 100	1850
253.42	1698 ± 89	1505 ± 150	660
266.83	850 ± 43	855 ± 40	820
323.89	1000 ± 50	1000 ± 50	1000
496.56	75 ± 4	61 ± 5	86
820.45	154 ± 8	135 ± 10	180
1026.19	90 ± 5	62 ± 7	83
1214.98	73 ± 4	58 ± 7	
1296.08	78 ± 4	45 ± 4	84
1387.92	56 ± 4		83
1505.76	93 ± 5	64 ± 7	73
1596.20	57 ± 3		
1627.10	82 ± 4	56 ± 8	73
1641.08	60 ± 3	61 ± 7	58
1697.84	58 ± 3		43
1742.49	53 ± 3	32 ± 5	51
1961.83	74 ± 4	41 ± 5	56
2018.87	58 ± 3	27 ± 4	54
2035.36	75 ± 4	51 ± 7	59
2349.96	306 ± 16	164 ± 21	239
2496.05	95 ± 5	56 ± 10	69
2602.61	174 ± 9	104 ± 10	154
2855.98	90 ± 5	45 ± 10	76

[1] The intensity uncertainties are reported to vary between 5 and 10% depending on the gamma ray's intensity

at IALE (47). This last work is especially important since Achterberg, et al. (47) use the ^{138}Xe and ^{138}Cs decay transitions for on-line intensity calibration. If their intensity values for these transitions are inaccurate the intensities of the A = 93 decay transitions will also be incorrect. The total gamma-ray intensity of the 253-keV doublet is the same in both this work and that of Achterberg, et al. The partitioning of this intensity is rather different however. From the LEPS spectrum analysis, the intensity ratio for the two peaks is 2.1 while Achterberg, et al. report an intensity ratio of 1.5. The value reported in the present work was actually observed in three different experiments, the two low energy studies mentioned earlier and the final singles spectrum using a 60-cm^3 Ge(Li) detector. A third value for the intensity of the 505.8-keV peak, 75 ± 10, is also reported in the latter work. Such an intensity for this sum peak indicates a source-to-detector distance of between 1 and 2 cm; however, Achterberg, et al. did not report this distance in their article.

Gamma-gamma coincidence data were also accumulated for the ^{93}Kr decay. In contrast to the other two decays, however, the coincidences reported in this case vary quite a bit from one work to another. The coincidences observed in this study are compiled in Table 15. In spite of the different coincidences reported, only a few conflicts result. For ex-

Table 15. Coincidences observed in the decay of ^{93}Kr

Gate (keV)	Definite Coincidences (keV)	Possible Coincidences (keV)
57.1	182, 267	
70.6	182, 253	
182.0	253, 324, 2350	
252.5[1]	253	2350, 2496
253.0[2]	182, 253, 844, 1387, 1627, 2350, 2496, 2602	570, 1435, 1779
253.3[1]	182, 252	
266.8	570, 1083, 1296, 1421, 1697, 1742, 2018	1318, 1505, 1586, 1638, 2035
323.9	182, 496, 1026, 1238, 1318, 1685, 1961, 2035, 2350	976, 1365, 1471, 1505, 2496
496.6	324	
570.2	267, 324	253
820.4	2035	
1026.2	324, 1505	1651
1083.4	267	
1296.1	267	
1435.4		253

[1]Coincidence assignments based on LEPS - Ge(Li) coincidences

[2]Coincidences observed in gate on entire 253-keV doublet

Table 15. (Continued)

Gate (keV)	Definite Coincidences (keV)	Possible Coincidences (keV)
1458.5		253
1505.8	253, 267, 1026	324
1638.0		253, 267, 324
1697.8	267	
1742.5	267	
1779.7	253	570
1789.0		253, 267
1961.8	324	253
2035.4	324, 820	496
2350.0	253, 324	182
2496.0	253	324

ample the gamma rays at 529.6, 1215.0, 1364.8, 1421.8, 1710.8 and 2181.5 keV were placed in this work on the basis of energy sums alone but their placements are the same as those proposed on the basis of coincidence information reported in the other works (28,34). Similarly, gamma rays at 733.7, 921.2, 976.1, 1637.7 and 2956.7 keV were placed in a cascade consistent with the coincidences observed by the others. In the latter case, though, other gamma rays should also have been seen in these cascades. It should be noted that these gamma rays were either not placed by the authors reporting their coincidences or were also positioned such that other intermediate gamma rays should have been noted in the coincidence spectra.

The gamma ray at 570.2 keV was placed between the same levels in this work and in that of Brissot, et al. (34) on the basis of the same observed coincidences. Achterberg, et al. have placed this gamma ray as feeding the 505.9-keV level. If this is true they should also have seen the 182.1-keV gamma ray in the 570-keV coincidence gate. A gamma ray at 1060.3 keV is reported to be in coincidence with the 267-keV transition by Brissot, et al. Our placement of this gamma ray is in conflict with this observation but then so is the final placement of this gamma ray by Brissot, et al. Conflicting coincidences are reported for the 1961.8-keV gamma ray. In this work it can be placed on the basis of co-

incidence information, while Achterberg, et al. cannot place it using their reported coincidence. Finally Brissot, et al. report coincidences for the 1978.7- and the 3105.4-keV gamma rays. In both cases they were unable to place the gamma rays. The former gamma ray was removed in this work because it is the combination of a double escape peak for ^{93}Kr and a peak from the ^{93}Rb decay. The latter gamma ray was placed between levels which result in its "crossing-over" the gamma ray with which others reported it to be in coincidence. This last placement is the only one which is actually in contradiction with the coincidence information presented in other works. Approximately 98.5% of the total gamma-ray intensity observed has been placed in the final level scheme. This intensity percentage is based on the placement of 203 gamma rays in a level scheme consisting of 56 levels. The final level scheme for the ^{93}Kr decay is presented in Figure 18.

D. Beta Branchings and Logft Values

Once the gamma-ray placements in a level scheme were determined the program LEAF was used to find the best level energies and the per cent beta feedings. The program does not provide the best energies in the sense of an absolute minimization of chi-squared but it does provide a consistent method for determining level energies using gamma-ray energy information for gamma rays feeding each level as well as for those depopulating that level. The calculation also provides sta-

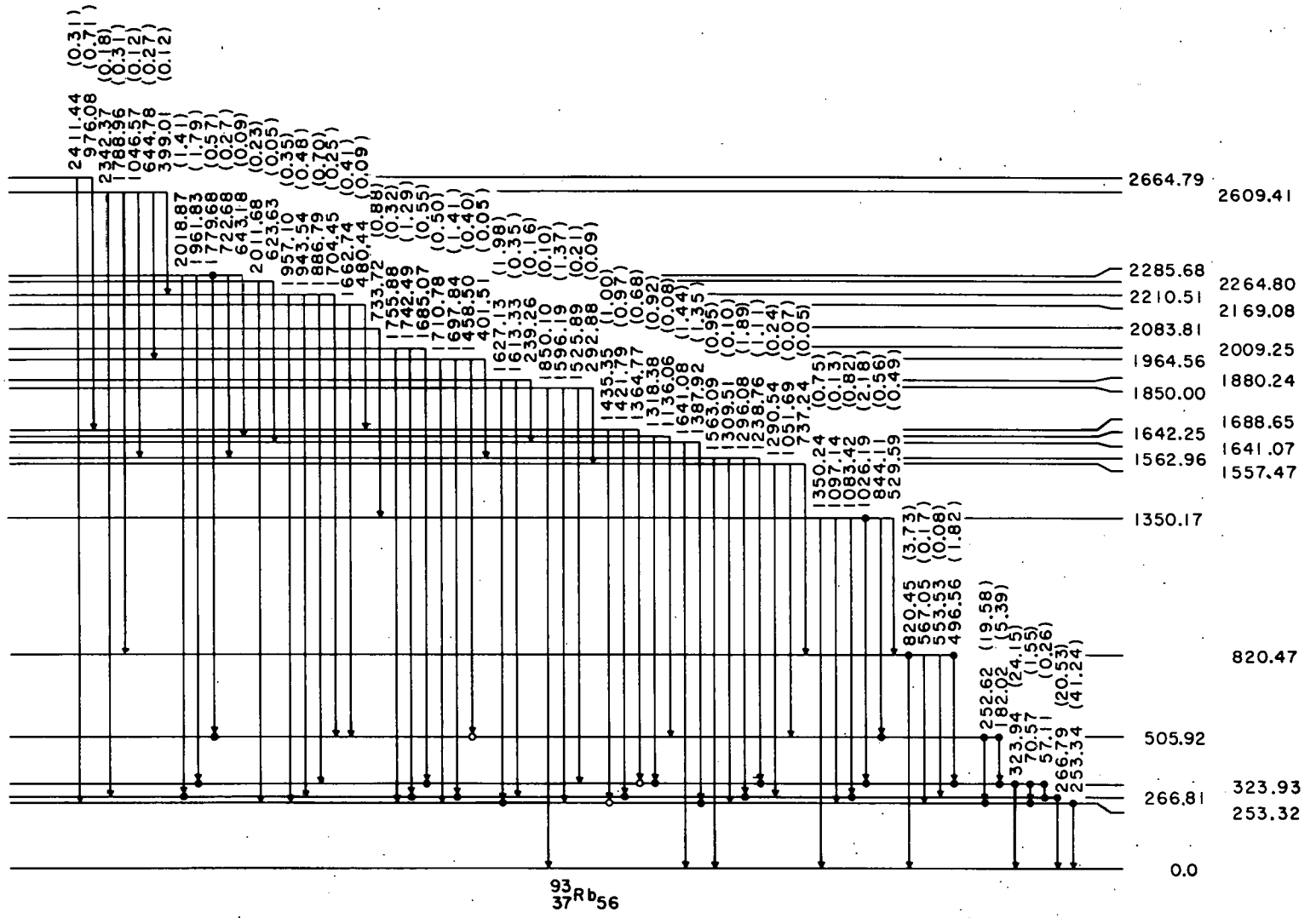

Figure 18. ^{93}Rb level scheme

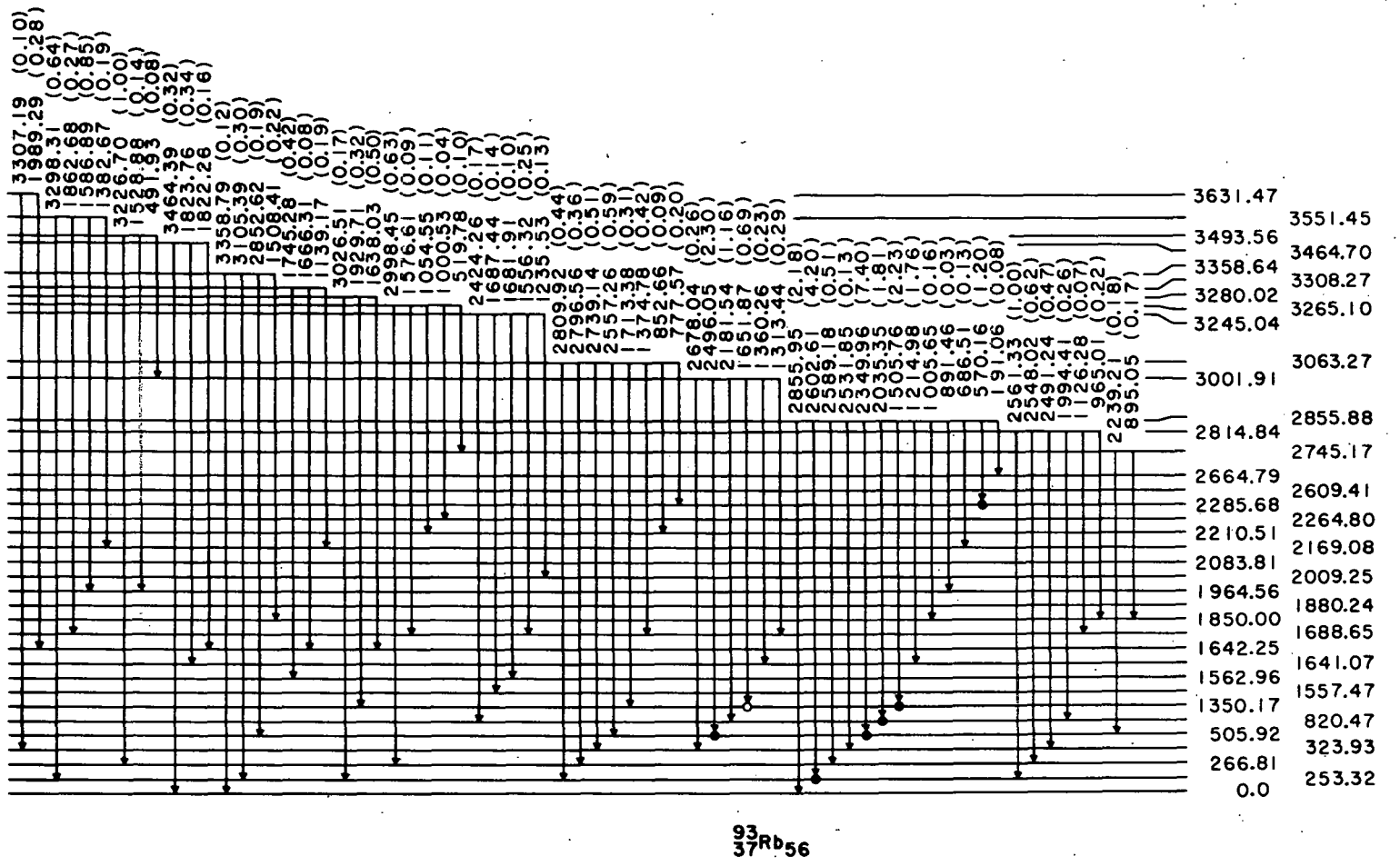

Figure 18. (Continued)

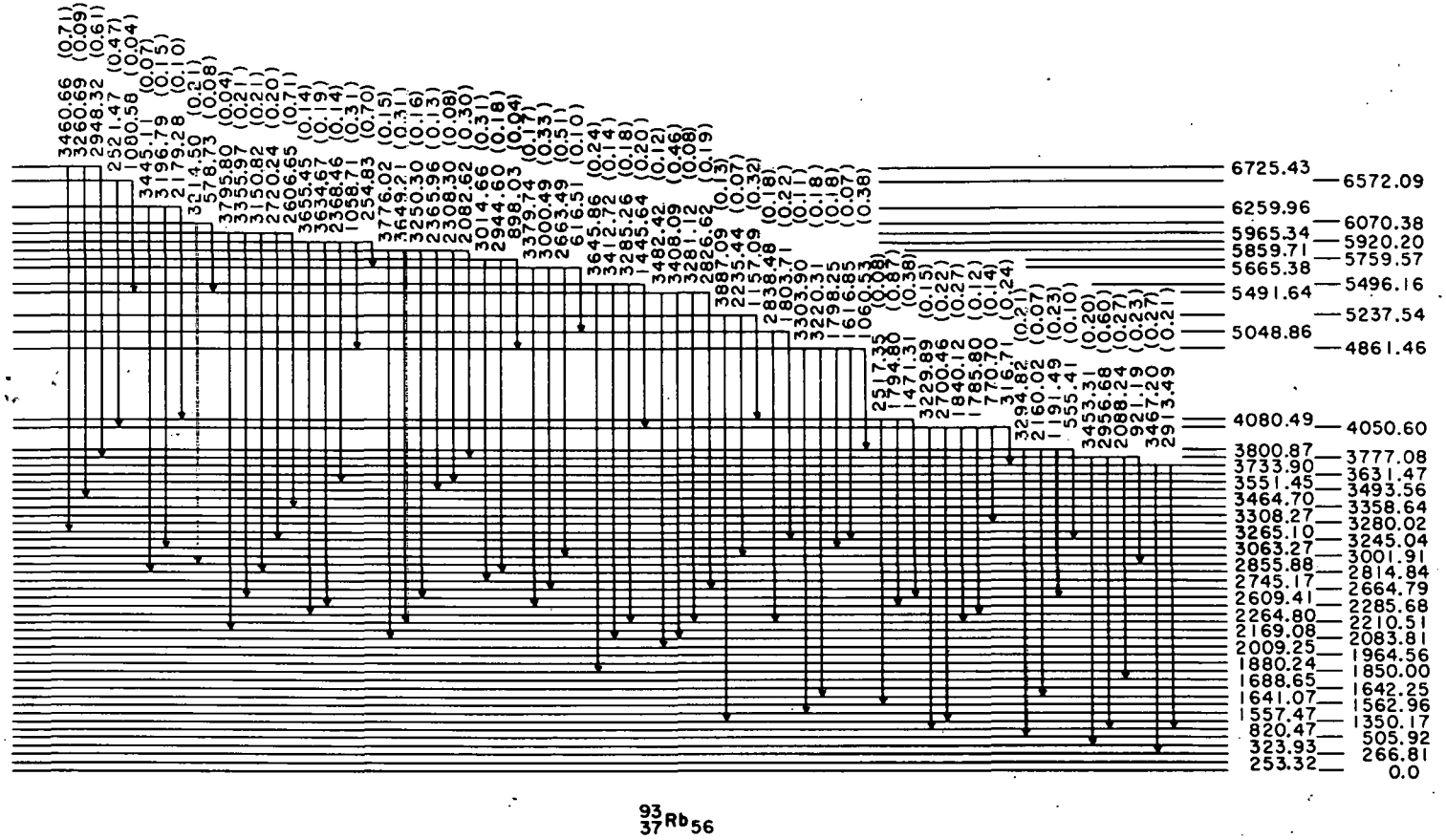

Figure 18. (Continued)

tistical uncertainties for the level energies. The absolute beta branching percentages were calculated in the program by making use of the level scheme intensity imbalances, the total ICC's for all transitions and the ground-state beta branchings. The resulting level energies, beta endpoint energies, and per cent beta branchings are provided in Tables 16, 17, and 18 for the ^{93}Sr, ^{93}Rb, and ^{93}Kr decays respectively.

The log*ft* values for each decay were determined by the program LOGFT. These values were calculated using the absolute beta branching percentages and the reported Q-values for each decay. The log*ft* values for the ^{93}Sr, ^{93}Rb, and ^{93}Kr decays are also provided in Tables 16, 17, and 18 respectively.

In Table 16 a log*ft* value of 1.6 is reported for beta feeding of the level at 4263.6 keV. This log*ft* value is unrealistically low but its uncertainty covers a wide range of more reasonable values. The uncertainty in this value is due largely to the uncertainty in the Q-value for the decay of ^{93}Sr. Because the log*ft* values depend strongly on energy, a small change in the Q-value results in a large change in the log*ft* value calculated for this level. In order to obtain a more reasonable lcg*ft* value for this level the Q-value must be very nearly 4.5 MeV. Therefore, the maximum

Table 16. Beta branchings and log*ft* values for ^{93}Sr decay.

γ Levels (keV)	Beta Endpoint Energy (MeV)	Per Cent Beta Branching	Log*ft*[1]
0.00	4.30	~0	-
590.24	3.71	~0	-
758.78[2]	3.54	6.57 ± 2.28	7.3 ± 0.2
875.81[2]	3.42	1.95 ± 1.40	7.8 ± 0.3
1135.94[2]	3.16	2.48 ± 0.47	7.5 ± 0.1
1277.94[2]	3.02	0.44 ± 0.10	8.2 ± 0.1
1300.51[2]	3.00	3.88 ± 1.22	7.2 ± 0.2
1308.55[2]	2.99	1.41 ± 0.20	7.7 ± 0.1
1542.74	2.76	~0	-
1647.09	2.65	15.47 ± 1.34	6.4 ± 0.1
1695.49[2]	2.60	0.35 ± 0.02	8.0 ± 0.1
1786.28[2]	2.51	0.25 ± 0.10	8.1 ± 0.2
1852.75	2.45	~0	-
1911.46[2]	2.39	1.46 ± 0.20	7.2 ± 0.1
2056.53	2.24	~0	-
2091.37	2.21	~0	-
2093.35	2.21	~0	-
2129.10[2]	2.17	0.36 ± 0.17	7.7 ± 0.2
2355.65	1.94	1.13 ± 0.09	7.0 ± 0.1
2364.83	1.94	2.01 ± 0.13	6.7 ± 0.1
2543.87	1.76	3.79 ± 0.24	6.3 ± 0.1
2569.93	1.73	11.51 ± 0.60	5.8 ± 0.1
2574.93	1.73	11.30 ± 0.52	5.8 ± 0.1
2653.89	1.65	~0	-
2687.70	1.61	17.91 ± 0.79	5.5 ± 0.1
2769.91	1.53	7.61 ± 0.38	5.7 ± 0.1
2777.88	1.52	~0	-
2783.62	1.52	3.13 ± 0.17	6.1 ± 0.1
2820.58	1.48	3.84 ± 0.26	6.0 ± 0.1
2886.50	1.41	1.28 ± 0.08	6.4 ± 0.1
3006.99	1.29	1.32 ± 0.09	6.2 ± 0.1
3116.08	1.18	0.38 ± 0.04	6.6 ± 0.2
3824.43	0.48	0.20 ± 0.04	5.4 ± 0.3
3871.27	0.43	0.19 ± 0.03	5.3 ± 0.4
3894.79	0.41	0.23 ± 0.04	5.1 ± 0.4
4119.71	0.18	0.14 ± 0.02	4.2 ± 0.8
4263.63	0.04	0.50 ± 0.04	1.6 ± 3.6

[1]Calculated using a Q-value of 4.3 ± 0.2 MeV and a half-life of 7.32 ± 0.10 min.

[2]Logf_1t > 8.5, so first-forbidden unique transitions cannot be excluded.

Table 17. Beta branchings and log*ft* values for ^{93}Rb decay.

Sr Levels (keV)	Beta Endpoint Energy (MeV)	Per Cent Beta Branching	Log*ft*[1]
0.00	7.23	59.00 ± 3.00	5.8 ± 0.1
213.39[2]	7.02	0.42 ± 0.31	7.9 ± 0.3
432.52[2]	6.80	1.80 ± 0.74	7.2 ± 0.2
986.08[2]	6.24	0.46 ± 0.28	7.7 ± 0.3
1142.48[2]	6.09	1.95 ± 0.34	7.0 ± 0.1
1148.18[2]	6.08	0.52 ± 0.10	7.6 ± 0.1
1238.28[2]	5.99	0.30 ± 0.07	7.8 ± 0.1
1385.26[2]	5.84	1.54 ± 0.25	7.0 ± 0.1
1529.23[2]	5.70	0.28 ± 0.03	7.7 ± 0.1
1562.93[2]	5.67	0.50 ± 0.07	7.4 ± 0.1
1779.74[2]	5.45	0.27 ± 0.06	7.6 ± 0.1
1808.47[2]	5.42	0.75 ± 0.13	7.2 ± 0.1
1869.63[2]	5.36	0.14 ± 0.10	7.9 ± 0.3
1910.80[2]	5.32	0.45 ± 0.07	7.4 ± 0.1
2045.45[2]	5.18	0.40 ± 0.09	7.4 ± 0.1
2054.04[2]	5.18	0.26 ± 0.14	7.6 ± 0.2
2117.31[2]	5.11	0.09 ± 0.04	8.0 ± 0.2
2140.99[2]	5.09	0.26 ± 0.06	7.5 ± 0.1
2272.78	4.96	∿0	-
2292.84[2]	4.94	0.23 ± 0.06	7.5 ± 0.1
2319.04	4.91	∿0	-
2351.45[2]	4.88	0.11 ± 0.04	7.8 ± 0.1
2456.37	4.77	∿0	-
2459.65	4.77	∿0	-
2553.75	4.68	∿0	-
2621.32[2]	4.60	0.26 ± 0.05	7.3 ± 0.1
2737.12[2]	4.49	0.10 ± 0.07	7.7 ± 0.3
2770.67[2]	4.46	0.07 ± 0.03	8.1 ± 0.4
2773.87	4.46	∿0	-
2782.11[2]	4.45	0.16 ± 0.13	7.5 ± 0.3
2868.88	4.36	∿0	-
2886.45	4.34	∿0	-
2979.86[2]	4.25	0.62 ± 0.06	6.8 ± 0.1
3198.01[2]	4.03	0.03 ± 0.03	8.0 ± 0.4

[1]Calculated using a Q-value of 7.23 ± 0.10 MeV and a half-life of 5.86 ± 0.13 sec.

[2]Logf_1t > 8.5, so first-forbidden unique transitions cannot be excluded.

Table 17. (Continued)

Sr Levels (keV)	Beta Endpoint Energy (MeV)	Per Cent Beta Branching	Log*ft*[1]
3232.83	3.99	∿0	-
3256.33[2]	3.97	0.07 ± 0.04	7.1 ± 0.1
3404.29[2]	3.82	0.22 ± 0.05	7.0 ± 0.1
3603.16	3.63	0.36 ± 0.06	6.7 ± 0.1
3623.52[2]	3.61	0.09 ± 0.03	7.3 ± 0.1
3789.07	3.44	0.36 ± 0.06	6.6 ± 0.1
3803.61	3.43	2.06 ± 0.20	5.9 ± 0.1
3847.53	3.38	2.14 ± 0.21	5.8 ± 0.1
3866.77	3.36	0.96 ± 0.11	6.2 ± 0.1
3867.33	3.36	2.94 ± 0.28	5.7 ± 0.1
3876.62	3.35	1.07 ± 0.11	6.1 ± 0.1
3890.58	3.34	3.18 ± 0.33	5.6 ± 0.1
3934.49	3.30	1.31 ± 0.15	6.0 ± 0.1
3954.93	3.27	1.33 ± 0.13	6.0 ± 0.1
4017.48	3.21	0.47 ± 0.06	6.4 ± 0.1
4037.89	3.19	1.12 ± 0.11	6.0 ± 0.1
4041.87	3.19	0.14 ± 0.02	6.9 ± 0.1
4097.31	3.13	1.00 ± 0.10	6.0 ± 0.1
4336.01	2.89	0.16 ± 0.04	6.7 ± 0.1
4461.04	2.77	0.49 ± 0.05	6.1 ± 0.1
4509.14	2.72	0.19 ± 0.06	6.5 ± 0.1
4577.32	2.65	0.49 ± 0.06	6.2 ± 0.1
4620.01	2.61	0.56 ± 0.13	5.9 ± 0.1
4714.48	2.52	0.50 ± 0.06	5.9 ± 0.1
4790.52	2.43	0.15 ± 0.04	6.4 ± 0.1
4912.86	2.32	0.58 ± 0.07	5.7 ± 0.1
4991.23	2.24	0.31 ± 0.04	5.9 ± 0.1
5012.09	2.22	0.30 ± 0.01	5.9 ± 0.1
5384.52	1.85	0.61 ± 0.06	5.3 ± 0.1
5395.72	1.83	0.30 ± 0.04	5.6 ± 0.1
5413.66	1.82	0.32 ± 0.05	5.5 ± 0.1
5601.16	1.63	0.25 ± 0.05	5.4 ± 0.1
5631.08	1.60	0.51 ± 0.06	5.1 ± 0.1
5775.32	1.45	0.20 ± 0.04	5.3 ± 0.1
6000.36	1.23	0.72 ± 0.08	4.5 ± 0.1
6096.53	1.13	0.20 ± 0.03	4.9 ± 0.1
6260.55	0.97	0.37 ± 0.04	4.4 ± 0.1
6272.66	0.96	0.51 ± 0.05	4.2 ± 0.1
6277.30	0.95	0.28 ± 0.04	4.5 ± 0.1
6707.23	0.52	0.30 ± 0.03	3.5 ± 0.2

Table 18. Beta branchings and log*ft* values for ^{93}Kr decay.

Rb Levels (keV)	Beta Endpoint Energy (MeV)	Per Cent Beta Branching	Log*ft*[1]
0.00	7.51	~0	-
253.34[2]	7.26	3.01 ± 2.47	6.5 ± 0.4
266.82	7.24	7.20 ± 1.13	6.1 ± 0.1
323.95	7.19	12.87 ± 1.36	5.8 ± 0.1
506.02	7.00	12.57 ± 1.22	5.8 ± 0.1
820.48[2]	6.69	0.57 ± 0.27	7.0 ± 0.2
1350.18	6.16	~0	-
1557.50	5.95	~0	-
1562.97	5.95	3.02 ± 0.16	6.1 ± 0.1
1641.08	5.87	~0	-
1642.28	5.87	~0	-
1688.67[2]	5.82	0.19 ± 0.12	7.2 ± 0.3
1850.02[2]	5.66	0.76 ± 0.10	6.6 ± 0.1
1880.25	5.63	2.49 ± 0.14	6.1 ± 0.1
1964.58	5.55	1.06 ± 0.12	6.4 ± 0.1
2009.27	5.50	1.90 ± 0.11	6.1 ± 0.1
2083.84[2]	5.43	0.14 ± 0.06	7.3 ± 0.2
2169.10	5.34	~0	-
2210.53[2]	5.30	0.45 ± 0.13	6.7 ± 0.1
2264.81	5.25	~0	-
2285.71	5.22	1.51 ± 0.16	6.1 ± 0.1
2609.43	4.90	~0	-
2664.81	4.85	0.42 ± 0.16	6.5 ± 0.2
2745.21	4.76	~0	-
2814.85	4.70	2.18 ± 0.14	5.8 ± 0.1
2855.90	4.65	21.39 ± 0.79	4.8 ± 0.1
3001.95	4.51	4.28 ± 0.22	5.4 ± 0.1
3063.29	4.45	2.60 ± 0.12	5.6 ± 0.1
3245.06	4.26	0.20 ± 0.08	6.6 ± 0.2
3265.12	4.24	0.26 ± 0.20	6.5 ± 0.3
3280.05	4.23	0.86 ± 0.08	6.0 ± 0.1
3308.28	4.20	0.69 ± 0.06	6.1 ± 0.1
3358.67[2]	4.15	0.11 ± 0.10	6.8 ± 0.4
3464.72	4.05	0.73 ± 0.40	6.0 ± 0.2

[1]Calculated using a Q-value of 7.51 ± 0.05 MeV and a half-life of 1.289 ± 0.012 sec.

[2]Logf_1t > 8.5, so first-forbidden unique transitions cannot be excluded.

Table 18. (Continued)

Rb Levels (keV)	Beta Endpoint Energy (MeV)	Per Cent Beta Branching	Logft[1]
3493.57	4.02	1.09 ± 0.09	5.8 ± 0.1
3551.47	3.96	1.73 ± 0.11	5.5 ± 0.1
3631.50	3.88	0.38 ± 0.05	6.2 ± 0.1
3733.92	3.78	0.23 ± 0.13	6.3 ± 0.2
3777.10	3.73	0.40 ± 0.07	6.1 ± 0.1
3800.89	3.71	0.23 ± 0.06	6.3 ± 0.1
4050.62	3.46	0.46 ± 0.11	5.9 ± 0.1
4080.51	3.43	0.91 ± 0.11	5.5 ± 0.1
4861.48	2.65	0.57 ± 0.08	5.3 ± 0.1
5048.89	2.46	0.30 ± 0.03	5.4 ± 0.1
5237.57	2.27	0.52 ± 0.04	5.0 ± 0.1
5491.67	2.02	0.72 ± 0.06	4.7 ± 0.1
5496.18	2.01	0.75 ± 0.07	4.7 ± 0.1
5665.40	1.84	0.40 ± 0.18	4.8 ± 0.2
5759.60	1.75	0.53 ± 0.10	4.6 ± 0.1
5859.73	1.65	1.11 ± 0.09	4.1 ± 0.1
5920.23	1.59	1.49 ± 0.11	3.9 ± 0.1
5965.36	1.54	1.37 ± 0.11	3.9 ± 0.1
6070.40	1.44	0.30 ± 0.02	4.5 ± 0.1
6259.98	1.25	0.31 ± 0.09	4.2 ± 0.1
6572.10	0.94	0.51 ± 0.04	3.5 ± 0.1
6725.45	0.78	1.40 ± 0.14	2.8 ± 0.1

value for this Q-value should be preferred. This disagrees with the Q-value adopted in the recent compilation on the A = 93 mass chain (48), where a value of 4.1 MeV was adopted on the basis of systematics.

Finally, in Table 18 the last two levels listed are assigned log*ft* values which are rather low. However, since these levels have confidence indices of 2 and 3 respectively, it may be that these levels do not actually exist. As a result no attempt will be made in this study to explain why these unusually low values were observed.

V. DISCUSSION

The original shell model of Mayer and Jensen (49) resulted in level orderings which were the same for both protons and neutrons. Above N,Z = 38 the ordering of the nucleon single-particle states was found to be;

$2p_{1/2}$, $1g_{9/2}$, $1g_{7/2}$, $2d_{5/2}$, $2d_{3/2}$, $3s_{1/2}$, . . .

However, the ordering of the neutron single-particle states is now known to differ from this scheme and has the sequence;

$2p_{1/2}$, $1g_{9/2}$, $2d_{5/2}$, $3s_{1/2}$, $1g_{7/2}$, $2d_{3/2}$, . . .

for the region near A = 90 (50). This ordering results from solving the Schroedinger equation for the case of a single particle in a spherical potential well with spin-orbit coupling. The solutions of this equation indicate that as A increases the separation between the $1g_{7/2}$ orbit and $2d_{5/2}$ orbit decreases faster than the separation between the $3s_{1/2}$ and $2d_{5/2}$ orbits. Experimental evidence (51) also exists to indicate that this trend does occur and that, in fact, the $1g_{7/2}$ orbit falls faster than the theory indicates. As a result the level ordering for the neutron single-particle states above N = 50 may be either

$2d_{5/2}$, $1g_{7/2}$, $3s_{1/2}$, $2d_{3/2}$, . . .

or

$1g_{7/2}$, $2d_{5/2}$, $3s_{1/2}$, $2d_{3/2}$, . . .

This ordering will be important in determining the ground-state spin and parity of ^{93}Sr and ^{93}Kr.

A. Level Structure of ^{93}Y

If we assume that ^{88}Sr is an inert core for this nuclide we are left with a single proton and four neutrons outside this core. The shell model predicts that the low-lying configurations for the level scheme of ^{93}Y should be;

$\pi(2p_{1/2})\nu(2d_{5/2})^{4}_{0}$ $1/2^-$

$\pi(1g_{9/2})\nu(2d_{5/2})^{4}_{0}$ $9/2^+$

$\pi[(2p_{3/2})^{-1}(2p_{1/2})^{2}_{0}]\nu(2d_{5/2})^{4}_{0}$ $3/2^-$

$\pi[(1f_{5/2})^{-1}(2p_{1/2})^{2}_{0}]\nu(2d_{5/2})^{4}_{0}$ $5/2^-$

$\pi(2p_{1/2})\nu(2d_{5/2})^{5}_{2}$ $3/2^-,\ 5/2^-$

$\pi[(1f_{7/2})^{-1}(2p_{1/2})^{2}_{0}]\nu(2d_{5/2})^{4}_{0}$ $7/2^-$

with the resulting spin and parity possibilities given above. Since the $1g_{7/2}$ orbit is observed to lie very near the $2d_{5/2}$ orbit the neutron configuration admixtures $\nu[(2d_{5/2})^{2}_{0}(1g_{7/2})^{2}_{0}]$ and $\nu(1g_{7/2})^{4}_{0}$ probably contribute significantly and may, in fact, be the dominant configurations for describing these levels. Regardless of the neutron configuration however, these same spin and parity possibilities will result from coupling the odd particle or hole to the 0^+ and 2^+ even-particle excitations. Therefore, for the sake of simplicity, the neutron configuration will be assumed to be $(2d_{5/2})^{4}$.

^{93}Y ground-state ($J^{\pi} = 1/2^-$): The reaction studies of Preedom, et al. (27) and Muller (52) indicate a spin-parity assignment of $1/2^-$ for this ground state. This spin-parity

assignment is consistent with the trend established by other odd-A yttrium isotopes. Such a state can be explained in terms of the seniority-one state formed by coupling the $2p_{1/2}$ proton to the 0^+ state of the neutron configuration. The above assignment is also ccnsistent with the lack of beta feeding to this level in the decay of ^{93}Sr which presumably has a $(7/2^+)$ ground state, as discussed below.

590.2-keV level ($J^\pi = 3/2^-$): The reaction studies previously cited indicate a $3/2^-$ spin-parity assignment for this level. Internal conversion coefficient measurements by several authors (22,26,28) as well as the half-life measurement by Casella, et al. (29) have established the E3 character of the 169-keV transition feeding this level. Based on this information and the $9/2^+$ spin and parity of the 759-keV level it is possible to restrict the spin-parity value for this level to $3/2^-$. Again this is consistent with the lack of beta feeding from the $(7/2^+)$ ground state of ^{93}Sr. An $L_p = 1$ distribution was measured for this level in the ^{94}Zr(d,^{3}He) reaction study (27). Thus this state is most likely the result of coupling a $2p_{3/2}$ proton hole to the ground state of the neutron configuration. Vervier (13) calculates that a second $3/2^-$ state should be observed at an energy of approximately 0.8 MeV from the coupling of a $p_{1/2}$ proton to the 2^+ state of the neutron configuration. The possibility of configuration mixing between these two states could be responsi-

ble for the depressed energy of the $3/2^-$ hole state as compared with its energy in the ^{89}Y level scheme. Such mixing would also result in an increased energy for the $3/2^-$ state predicted by Vervier.

758.8-keV level ($J^\pi = 9/2^+$): This level was observed in the reaction work of Freedom, et al. (27) and given a spin-parity assignment of $9/2^+$. The shell model predicts such a low-lying $9/2^+$ level and a level with this spin and parity was previously observed in the level schemes of ^{89}Y and ^{91}Y at approximately the same energy. Also this level was the only $L_p = 4$ transfer detected in the reaction study of Ref. 27. Excitation of the odd proton to the nearby $1g_{9/2}$ orbit accompanied by the even neutron ground-state coupling would explain such a state. Because the log*ft* value determined from the beta feeding of this level was used to determine the spin and parity of the ^{93}Sr ground state it is, of course, consistent with that assignment.

875.8-keV level ($J^\pi = 5/2^-$): The spin-parity assignment for this level was based on both previously cited reaction studies. This identification is in agreement with the intense ground-state transition and the weaker first excited-state transition which are observed to depopulate this level. In both reaction studies the angular distribution for this level was fit with an $L_p = 3$ distribution indicating that the dominant proton configuration is a $1f_{5/2}$ proton-hole state.

Again Vervier has predicted a $5/2^-$ state at approximately 1.0 MeV formed from coupling a $2p_{1/2}$ proton with the 2^+ state of the neutron configuration. If we assume that configuration mixing occurs, the two levels will repel each other and possibly account for the lowered energy of the $5/2^-$ hole state and the increased energy of the level predicted by Vervier.

1135.9-keV level ($J^\pi = 7/2^-$): This level was observed in the reaction study by Muller (52) where it was determined to have a possible spin and parity of $7/2^-$. From the ^{93}Sr decay, we can limit the spin and parity values to $5/2^+$, $7/2^-$ on the basis of gamma-ray transitions and beta feeding. An $L_p = 3$ distribution was determined for this level so that it most likely contains a component resulting from a $1f_{7/2}$ proton-hole configuration. Because of the overlap with $7/2^-$ value determined in the reaction study this value has been chosen. There is another $7/2^-$ state at 1300.5 keV but it was not observed in the reaction studies and its energy agrees quite well with that expected (13) for a state resulting from the coupling of a $2p_{1/2}$ proton with the 4^+ state of the neutron configuration. However, because there is significant beta feeding to the level at 1300.5-keV it seems that the latter level would have to contain an admixure of this $7/2^-$ proton hole state.

1277.9-keV level (J^{π} = 3/2$^-$,5/2$^-$): Preedom, et al. (27) observe a doublet at 1.28 MeV with possible spins of 1/2$^-$ or 3/2$^-$ and 5/2$^-$ while Muller (52) is able to limit the spins of this multiplet to 3/2$^-$ and 5/2$^-$ at an energy of 1.302 MeV. In the present work there are three levels at energies of 1278, 1300 and 1309 keV. Since the 1300-keV level can be limited to the spin-parity possibilities (5/2$^+$,7/2$^-$) cn the basis of gamma-ray transitions to the first and second excited states this level is not a member of the doublet observed in the reaction studies. As a result, the levels at 1278 and 1309 keV are limited to spin-parity values of 3/2$^-$ and 5/2$^-$. The same restrictions are proposed on the basis of gamma-ray transitions and beta feeding so that no further limitation is possible. Fcr the 3/2$^-$ level an L_p = 1 distribution was observed in both reaction studies while an L_p = 3 distribution was observed for the 5/2$^-$ level. If the spin-parity assignment is 3/2$^-$ then the level can be described as containing admixtures of the configurations obtained from coupling a $2p_{1/2}$ proton to the 2$^+$ state of the even neutron configuration and coupling a $2p_{3/2}$ proton hole to the ground state of the same neutron configuration. The 5/2$^-$ level probably contains a large admixture of the configuration resulting from coupling a $1f_{5/2}$ proton hole state to the ground state of the neutron configuration while the dominant config-

uration results from coupling a $2p_{1/2}$ proton hole state to the ground state of that same neutron configuration.

1300.5-keV level ($J^{\pi} = 7/2^-$): As discussed above the spin-parity assignment for this level can be limited to $5/2^+$ or $7/2^-$ on the basis of the ^{93}Sr decay scheme. The $7/2^-$ possibility was chosen because of the excellent energy agreement with a $7/2^-$ level calculated by Vervier to be at approximately 1.32 MeV. If this assignment is correct the level can be described as resulting from coupling a $2p_{1/2}$ proton to the 4^+ state of the neutron configuration. But in order to account for the beta feeding to this level, an admixture of the $7/2^-$ hole state would have to be postulated. It is not obvious from the present study that such an admixture exists.

1308.6-keV level ($J^{\pi} = 3/2^-$ or $5/2^-$): This level is assumed to be the second member of the doublet near 1300 keV observed in both reaction studies. As before, the gamma-ray transitions and beta feeding impose $3/2^-$ or $5/2^-$ limitations on possible spin-parity values and no definite choice can be made between these possibilities.

1542.7-keV ($J^{\pi} = 3/2^-$ or $5/2^-$): Since no beta feeding to this level is observed, the spin-parity values possible are determined by the gamma-ray transitions to the ground state ($1/2^-$) and the level at 1136-keV ($7/2^-$).

1647.1-keV level ($J^{\pi} = 5/2^+, 7/2\pm, 9/2^-$): This level was observed in the reaction study by Muller but no statement was

made concerning its spin or parity. The values quoted here for the spin and parity were established by intense gamma-ray transitions tc the first- and second-excited states and a log*ft* value of 6.4 for beta feeding to this level. Vervier calculated an energy of approximately 1.63 MeV for a $9/2^-$ level, which may be associated with this level, because of this energy similarity. If this assignment is correct the level would be described by the configuration resulting from coupling a $2p_{1/2}$ proton to the 4^+ state of the even neutron configuration. Again, however, there is a rather large percentage of beta feeding to this level which contradicts its assumed collective character. Because of these complications it is impossible to limit the possibilities for the spin and parity of this level.

The levels at 1695.5 keV, 1786.3 keV and 1911.5 keV could only be limited to the J^π possiblities of $(3/2^-, 5/2\pm, 7/2^-)$. These values were all determined on the basis of gamma-ray transitions to the $3/2^-$ first excited state and log*ft* values between 7.2 and 8.1. Muller reports a level at 1.89 MeV with a spin-parity value of $(5/2^-)$ which is probably the level reported here at 1911 keV. Therefore a value of $5/2^-$ is preferred for this level. Muller alsc reports a $(9/2^-)$ level at 1.72 MeV which was not observed in this work.

The other four levels below 2.10 MeV could not be limited to fewer than four values for the spin nor could the parity of the levels be determined. However, the level at 2056 keV may be the $5/2^-$ level observed at this same energy by Muller. Because of this energy equivalence, a spin-parity assignment of $5/2^-$ for this level will be assumed.

2129.1-keV level ($J^\pi = 3/2^-$ or $5/2^-$): The possible values for the spin-parity of this level were established by the gamma-ray transition feeding the $1/2^-$ ground state and a log*ft* value of 7.7.

2355.6-keV level ($J^\pi = 5/2\pm, 7/2^-$): The spin-parity values for this level were determined by an intense gamma-ray transition to the $3/2^-$ first-excited state and a log*ft* value of 7.0. Muller reports a doublet at 2.37 MeV composed of states with spin-parity values of $3/2^-$ and $9/2^-$. Since neither of these values lies in the range given above it appears that a different level was observed in the present work.

2364.8-keV level ($J^\pi = 5/2^-$): The single value of $5/2^-$ for the spin-parity of this level was established by an intense ground-state transition and a log*ft* value of 6.7. Since a strong argument prchibits the spin-parity assignment of $3/2^-$ this level cannot be a member of the doublet observed by Muller at an energy of 2.37 MeV.

2543.9-keV level ($J^{\pi} = 5/2^-$): Again the single value of $5/2^-$ for the spin and parity was based on an intense ground-state transition and a log*ft* value of 6.3. This level was reported in both previously cited reaction studies but Muller was unable to determine its J value. He did, nonetheless, determine from the distribution for this level that $L_p > 1$ while Preedom, *et al.* (27) observed an $L_p = 1$ distribution for this level. If $L_p > 1$, then the $5/2^-$ assignment is possible and in agreement with the observed log*ft* value.

The levels at 2569.9 keV and 2574.9 keV both have intense transitions to the $5/2^-$ level at 875.8 keV and a log*ft* value of 5.8. Because of the allowed character of these beta transitions the parity of these levels must be positive but the spin may be either 5/2 or 7/2. The level at 2553.9 keV is not beta fed and too few gamma-ray transitions are observed to provide reasonable limits for the spin and parity values possible for this level.

2687.7-keV level ($J^{\pi} = 5/2^+$): As a result of the intense ground-state transition depopulating this level, the spin is limited to $J \leq 5/2$. Because the log*ft* value for this level is 5.4 it is also true that $5/2 \leq J \leq 9/2$ and the parity is positive. These considerations lead to the final spin-parity assignment of $5/2^+$.

The spin of the levels at 2769.9 keV, 2820.6 keV, 2886.5 keV and 4263.6 keV can be limited to the values of 5/2 and

7/2. Of these levels, the first and the last have positive parity as determined by allowed beta feeding of these levels. The levels at 2820 keV and 2886 keV most likely correspond to the levels at 2.84 MeV and 2.91 MeV observed by Muller. In that work no spin-parity assignments were made for these two levels so that only their existence is verified. Preedom, et al. report a level at 2.93 MeV which may be the level reported by Muller at 2.91 MeV. In the study by Preedom, a spin-parity assignment of either $1/2^-$ or $3/2^-$ is made. Since the 2886-keV level has a log*ft* value of 6.4, a strong argument limits the possible values for this level to $(5/2\pm,7/2\pm,9/2\pm)$. The difference in possible spin values between these studies prohibits any positive statements on the spin or parity of this level, which may not be that observed in the reaction studies.

The level at 2777.9 keV is not beta fed and is depopulated only by two rather weak gamma-ray transitions. As a result a large range of spin-parity assignments are possible. The level at 2783.6 keV is limited in spin to the values (5/2,7/2,9/2) because of beta feeding with a log*ft* value of 6.1. The 3007.0-keV level is assigned a spin-parity value of $(5/2^-)$ because of the presence of a ground-state transition and a log*ft* value of 6.2.

3116.1-keV level ($J^\pi = 5/2^-$): This level was observed by Muller in his reaction study and determined to have possi-

ble spin-parity values of $(5/2^-, 7/2^-)$. Because a ground-state transition is known to depopulate this level and the level is fed in beta decay with a log*ft* value of 6.6 a spin-parity assignment of $(5/2^-)$ is made.

Finally, the levels at 3824.4 keV, 3871.3 keV, 3894.8 keV and 4119.7 keV have the range of spin-parity values $(5/2^+, 7/2^+, 9/2^+)$. This conclusion results from beta feeding to these levels with log*ft* values which are less than 5.9.

In an effective interaction calculation for the levels of ^{93}Y, Vervier assumed that the odd proton is either a $2p_{1/2}$ or a $1g_{9/2}$ and that the neutrons are all $2d_{5/2}$. By coupling the odd proton to the possible excitations of the even neutron configuration he obtained sequences of positive and negative parity states. The energies of the levels in each sequence were determined by the energy separation of the 0^+, 2^+, and 4^+ states in ^{94}Zr. The relative positions of the two sequences was then determined from the single-particle energy difference for a $2p_{1/2}$ and a $1g_{9/2}$ proton. The resulting level scheme does not agree very well with the experimental level scheme reported in the present work. Due to a lack of experimental information Vervier was unable to include any proton hole states in his calculation. Since the reaction studies indicate that these configurations are dominant even at fairly low energies the calculation would appear to be of limited value. It does, however, appear to predict fairly

accurately the energies of the $7/2^-$ and $9/2^-$ states formed from coupling the $2p_{1/2}$ proton to the 4^+ state of the even neutron configuration. As has been noted above, the significant beta feedings of these levels disagrees with such collective character. Therefore, the energy agreement observed is probably entirely coincidental. This calculation was repeated, as part of this study, using the energy separation of the 0^+, 2^+, and 4^+ levels in ^{92}Sr. That calculation gives a better fit for the $3/2^-$ and $5/2^-$ levels but it also predicts extremely large energies for the $7/2^-$ and $9/2^-$ levels. Since the $3/2^-$ and $5/2^-$ levels are now known to result from different configurations this calculation results in even poorer agreement with experiment.

These results indicate that instead of changing the neutron excitation energies the correct approach would be to enlarge the configuration space used in the calculation. If the proton-hole configurations $\pi[(2p_{3/2})^{-1}(2p_{1/2})^2]$ and $\pi[(1f_{5/2})^1(2p_{1/2})^2]$ were included, configuration mixing between the resulting states might lead to the reduced energies observed for the $3/2^-$ and $5/2^-$ levels. This approach would also provide the larger number of low-lying negative parity states which is observed experimentally.

B. Level Structure of ^{93}Sr

As in the discussion of the ^{93}Y level scheme we will assume that ^{88}Sr acts as an inert core. For the ^{93}Sr nucleus

the protons are assumed to complete a shell closure at Z = 38. Therefore the odd neutron will determine the character of the low-lying levels. The shell model predicts that the most likely odd neutron configurations would be those given below;

$\nu(2d_{5/2})^5$ $5/2^+$

$\nu[(2d_{5/2})^4_0(3s_{1/2})]$ $1/2^+$

$\nu[(2d_{5/2})^4_0(1g_{7/2})]$ $7/2^+$

$\nu[(2d_{5/2})^2_0(1g_{7/2})^3]$ $7/2^+$

$\nu[(2d_{5/2})^4_0(2d_{3/2})]$ $3/2^+$

with the resulting spin and parity values listed. Again it should be mentioned that since the $1g_{7/2}$ orbit probably lies very close in energy to the $2d_{5/2}$ orbit, configuration mixing with such neutron configurations should also be included. For example, the $\nu(2d_{5/2})^5$ configuration probably contains admixtures of the configurations $\nu[(2d_{5/2})^3(1g_{7/2})^2]$ and $\nu[(2d_{5/2})(1g_{7/2})^4]$. These mixings will, of course, also lead to a multiplicity of the states mentioned above. For the sake of simplicity we will again denote the even neutron configurations by $\nu(2d_{5/2})^4$.

^{93}Sr Ground-state ($J^\pi = 7/2^+$): Beta feeding to the 758.8-keV ($9/2^+$) and 875.8-keV ($5/2^-$) levels in ^{93}Y with logft values of 7.3 and 7.8 respectively limit the possible spin-parity values to ($5/2^-, 7/2\pm, 9/2^+$). Since all the low-lying states are expected to be positive parity from the

shell model, it seems reascnable to limit the possibilities to $(7/2^+,9/2^+)$. In the initial discussion of Section V it was mentioned that the $1g\ 7/2$ level was descending toward the $2d\ 5/2$ level as proton and neutron pairs are added to the ^{88}Sr nucleus. Evidently the $1g\ 7/2$ level has fallen far enough to lie below the $2d\ 5/2$ level although it is surprising to see this occur for such a low neutron number (N = 55). It may also be that a second $7/2^+$ state, resulting from the promotion of a pair of neutrons from the $2d\ 5/2$ to the $1g\ 7/2$ orbit, is present at fairly low energy. The configuration interaction between these twc states would result in a lowered energy for the lower lying $7/2^+$ state. If this repulsion were large enough it could explain the observed $7/2^+$ ground state. A value of $5/2^+$ would be much more likely on the basis of the shell model but inconsitent with the log$\underline{ft}$ values measured. The internal conversion coefficient for the 169-keV E3 transition depopulating the $9/2^+$ level in ^{93}Y can determine whether or not this level is beta fed. If the internal conversion coefficient were small enough this level would not be beta fed while the 590.2-keV $(3/2^-)$ level would be. This would result in possible J^π values of $(3/2^+,5/2^+)$. For this to cccur, however, the internal conversion coefficient would have to be 0.563. Four internal conversion coefficient measurements have now been made (22,26,28,34), the average of which exactly equals the theoretical value cf

0.920 determined by Hager and Seltzer (53) for E3 multipolarity. The extremely low value for α necessary to assign a J^{π} value of $5/2^{+}$ for the ground state of ^{93}Sr therefore seems highly unlikely. Also, over 99% of the gamma-ray intensity observed has been placed in the level scheme. Consequently, even if all the unplaced gamma rays are placed feeding the 758.9-keV level an intensity imbalance would still exist and the level would have to be fed in beta decay.

No reaction studies have been made of the levels of ^{93}Sr so it is not possible to assign spins and parities on the basis of comparison with such works. Furthermore, although Achterberg, et al. (28) have proposed multipolarities for the 213.4-, 219.2-, and 432.5-keV transitions, these values are suspect because of the low-lying odd-parity level which results. If the 219.2- and 432.5-keV transitions are both E1 the level at 432.5 keV must have negative parity. The presence of such a low-lying negative-parity state cannot be explained on the basis of the spherical potential shell model. A negative-parity state at this low energy is also inconsistent with the predominance of positive-parity states in this energy region in other odd-A strontium isotopes. In an earlier work on the decay of ^{91}Kr, Achterberg, et al. (54) had reported a positive-parity state in the level scheme of ^{91}Rb. The parity was based on the supposed E1 multipolarity of the transition depopulating that level. In a later study,

Wohn, et al. (55) established that the multipolarity of this transition was M1 and not E1 and that therefore no change in parity occurs. It appears that such a situation has occurred again, especially since the internal conversion coefficients used to make the multipolarity assignments are based on the absence of conversion electron peaks rather than a fit of the conversion peaks themselves. Hence spin and parity assignments will be made without making use of the proposed E1 multipolarity of these two transitions. In order to make some reasonable assumptions for the spins and parities of the levels in ^{93}Sr it will therefore be necessary to determine the ground-state spin and parity of ^{93}Rb. In the discussion of the next section it will be argued that the most likely spin-parity assignment for this ground state is $(5/2^-)$.

213.4-keV level ($J^\pi = 5/2^+, 7/2^+, 9/2^+$): Using the known (28) E2 plus M1 character of the 213.4-keV gamma-ray transition depopulating this level, it is possible to limit the range of spin-parity values to $(5/2^+, 7/2^+, 9/2^+)$. This level is also fed in beta decay with a log*ft* value of 7.9 which limits the spin-parity assignment to a range of values including all of the above spin and parities. Thus, no further restriction on the spin can be made. Since the $2d_{5/2}$ and $1g_{7/2}$ orbits appear to be very close in energy the spin-parity assignment $5/2^+$ would be favored.

Because the ground state is the only level limited to a single value for the spin and parity very little else can be said concerning spin-parity assignments for the other levels of ^{93}Sr. The few statements that can be made concerning spin-parity assignments, given the total lack of supportive reaction data, are compiled in Table 19.

Table 19. Spin-parity assignments for ^{93}Sr level scheme.

J^{π} Assignments	Level Energies (keV)
(3/2±,5/2±,7/2±)	2979.9, 3603.2, 3866.8, 4017.5, 4037.9, 4041.9, 4097.3, 4336.0, 4509.1, 4577.5, 4620.0, 4714.5, 4790.5, 4991.2, 5012.1
(3/2$^+$,5/2±,7/2±)	3789.1, 3803.6, 3876.6, 3934.5, 3954.9, 4461.0
(3/2$^-$,5/2$^-$,7/2$^-$)	3847.5, 4913.0, 5384.5, 5413.7, 5601.2, 5631.1, 5775.3, 6000.4, 6096.5, 6260.5, 6272.8, 6277.3, 6707.2
(5/2$^-$,7/2$^-$)	3867.3, 3890.6, 5395.7

The levels having spin-parity possibilities of 3/2±, 5/2±,7/2± were fed in beta decay with logf_1t values less than 8.5. The levels with spin-parity possibilities 3/2$^+$,5/2±,7/2± were also fed in beta decay with logf_1t less than 8.5 but in addition were depopulated by a ground-state transtion. Those levels fed in beta decay with logft < 5.9 could be limited to the spin possibilities 3/2, 5/2, 7/2 with

negative parity. If a ground-state transition is observed to depopulate such a level the spin was further restricted to 5/2, 7/2. The only single-particle states which appear to be identified are the ground state and the first excited state. One would also expect to see low-lying single-particle states with spins and parities of $1/2^+$ and $3/2^+$ but until more definite statements can be made about the spin-parity assignments of the levels in ^{93}Sr no further identification will be possible.

C. Level Structure of ^{93}Rb

In terms of the ^{88}Sr inert core the active nucleons in the ^{93}Rb nucleus consist of a proton hole and six neutrons. For the low-lying states the neutrons are assumed to be coupled to zero so that the dominant configurations for these levels should result from the possible proton hole states. Based on the shell model the most likely nucleon configurations are

$\pi(2p_{3/2})^{-1}\nu(2d_{5/2})^6$ $3/2^-$

$\pi(1f_{5/2})^{-1}\nu(2d_{5/2})^6$ $5/2^-$

$\pi(1f_{7/2})^{-1}\nu(2d_{5/2})^6$ $7/2^-$

with the resulting spin and parity values given above. For simplicity the even neutron configurations have again been denoted as $2d_{5/2}$. As before there are probably large admixtures of the neutron configurations $(2d_{5/2})^4(1g_{7/2})^2$, $(2d_{5/2})^2(1g_{7/2})^4$, and $(1g_{7/2})^6$. In fact, the last configura-

tion may be the dominant neutron configuration.

^{93}Rb Ground-state ($J^{\pi} = 5/2^-$): On the basis of the shell model the most likely nucleon configuration for the ground state arises from coupling the proton hole state to the ground-state neutron configuration. In the ^{87}Rb, ^{89}Rb, and ^{91}Rb (51,56,54) level schemes the ground state is $3/2^-$ and the first first excited state is $5/2^-$. However, the separation between these levels is decreasing as the number of neutrons is increased. Therefore the ^{93}Rb ground state may be either $3/2^-$ or $5/2^-$ based on these systematics. Since the $7/2^+$ ground state of ^{93}Sr is beta fed in the decay of ^{93}Rb with a log*ft* value of 5.8, the possible spin values for the ^{93}Rb ground state are 5/2, 7/2, and 9/2. The log*ft* value also indicates positive parity but, since all the shell model states are of negative parity, this assignment is unlikely. It may be that the percentage of ground-state feeding is somewhat less since Brissot, *et al.* (34) report 42% rather than 59% as reported by Achterberg, *et al.* (28). This difference in ground-state feeding is important since Achterberg, *et al.* argue that their large percentage of ground-state feeding, along with the observed density of low-lying levels, indicates positive parity for the first five levels. These positive-parity states are then the basis for their observation that the ^{93}Rb nucleus is deformed. The uncertainty in the log*ft* value would therefore extend beyond

the limiting value of 5.9 for parity-changing decays. Based on these arguments a ground-state spin-parity assignment of $(5/2^-)$ is made.

The ground-state spin and parity for ^{93}Kr will be determined by the odd neutron since the even-proton configuration is assumed to be coupled tc a total angular momentum of zero. On the basis of the shell model the neutron configuration will probably be either $\nu[(2d_{5/2})^6(1g_{7/2})]$ or $\nu[(1g_{7/2})^6(2d_{5/2})]$ which indicates a spin-parity assignment of $7/2^+$ or $5/2^+$ respectively. However, the other N = 57 isotones for which ground-state spin and parity assignments have been made (57,58) are known to have a $1/2^+$ ground state. It also appears that the ground-state spin of ^{95}Sr is less than 5/2 since feeding to the ground state of ^{95}Y $(1/2^-)$ has been reported (33). This assignment would also be consistent with the lack of beta feeding tc the $5/2^-$ ground state of ^{93}Rb while the other values are not. As a result it seems that a spin-parity of $1/2^+$ is most reasonable. This assignment will be used to predict spins and parities for the levels of ^{93}Rb. Such a spin-parity assignment might result from the neutron configuration $\nu[(1g_{7/2})^6(3s_{1/2})]$ or $\nu[(2d_{5/2})^6(3s_{1/2})]$.

253.3-keV level ($J^\pi = 3/2^-, 5/2^-$): The intense transition depopulating this level has been determined to have an M1 multipolarity (28) which limits the spin-parity to $3/2^-$, $5/2^-$, or $7/2^-$. Beta feeding to this level with a log$\underline{ft}$ value

of 6.5 then limits the spin to $3/2 \leq J \leq 7/2$. The intersection of these two groups limits the spin-parity assignment to the possibilities given abcve. Because the other odd-A rubidium isotopes have ground-state spin and parity of $3/2^-$ there is probably a low-lying level in ^{93}Rb with this same spin and parity. As a result, the $3/2^-$ value is preferred for this level. Such a state probably results from coupling a $2p_{3/2}$ proton hole to the ground state of the even neutron configuration.

266.8-keV level ($J^\pi = 1/2^-, 3/2^-$): The ground-state transition depopulating this level is reported to have an E2 multipolarity (28). The parity of this level is therefore negative and the spin is less than or equal to 9/2. Since this level is also fed in beta decay with a log*ft* value cf 6.1 the spin must be less than 5/2. These two arguments lead to the final spin-parity assignments listed. The $1/2^-$ value is favored since such an assignment could result from promoting the odd proton tc the $2p_{1/2}$ orbit.

324.0-keV level ($J^\pi = 3/2^-$): This level is depopulated by an M1 transition (28) so that the spin-parity values possible are $(3/2^-, 5/2^-, 7/2^-)$. It is also fed in beta decay with a log*ft* value of 5.9 which implies a spin change cf zero or one. The only value possible for the spin and parity is therefore $3/2^-$.

506.0-keV level ($J^{\pi} = 1/2^-, 3/2^-$): Two M1 transitions are reported (28) to depopulate this level. These two transitions limit the spin to less than 7/2, and because both feed negative parity levels, the parity of this level must also be negative. Beta feeding with a log$\underline{ft}$ value of 5.9 limits the possibilities to $(1/2\pm, 3/2\pm)$. Combining these arguments we find the possible values listed above.

Since only the ground state and the third excited state can be limited to a single spin-parity possibility, feeding of these levels, along with beta feeding of the levels of interest, will determine the other spin-parity assignments. Most of these arguments would therefore be repetitive. In order to avoid this redundancy the assignments are presented in Table 20 followed by the arguments leading to those assignments.

The levels assigned spin-parity values of $(1/2^-, 3/2\pm, 5/2^-)$ were fed in beta decay with log$\underline{f}_1\underline{t}$ values greater than 8.5. The possible values which result from this feeding would be $(1/2\pm, 3/2\pm, 5/2^-)$. A ground-state transition also depopulates these levels so that the $1/2^+$ possibility is very unlikely. The levels assigned the possibilities $(1/2^-, 3/2\pm)$ were fed in beta decay with log$\underline{f}_1\underline{t} < 8.5$ so that the $5/2^-$ is eliminated. A ground-state transition again depopulates these levels and eliminates the $1/2^+$ possibility. The possible values of $(1/2\pm, 3/2\pm, 5/2^-)$ were based entirely

Table 20. Spin-parity assignments for ^{93}Rb level scheme.

J^{π} Assignments	Level Energies (keV)
$(1/2^-,3/2\pm,5/2^-)$	820.48, 1850.02, 3358.67
$(1/2^-,3/2\pm)$	1562.97, 3464.72
$(1/2\pm,3/2\pm,5/2^-)$	1688.67, 2083.84, 2210.53
$(1/2\pm,3/2\pm)$	1880.25, 1964.58, 2009.27, 2285.71, 2664.81, 3245.06, 3265.12, 3280.05, 3308.28, 3631.50, 3733.92, 3777.10, 3800.89, 4050.62
$(1/2^+,3/2^+)$	2814.85, 3001.95, 3063.29, 3493.57, 3551.47, 4080.51, 4861.48, 5048.89, 5237.57, 5491.67, 5496.18, 5665.40, 5759.60, 5859.73, 5920.23, 5965.36, 6070.40, 6259.98, 6572.10, 6725.45

on beta feeding with logf_1t values greater than 8.5. The possibilities $(1/2\pm,3/2\pm)$ were also determined entirely by beta feeding but in this case the logf_1t values were less than 8.5. The last group of levels has possible spin-parity assignments of $(1/2^+,3/2^+)$ based on beta feeding with logft values less than 5.9. Only the level at 2855.9 keV can be limited to a single spin-parity possibility. This assignment is based on beta feeding with a logft value less than 5.9 and a gamma-ray transition to the ground state. The only single-particle states which appear to be observed are the ground state and the first two excited states. The other low-lying states generally have negative parity and probably result

from coupling these single-particle states to the excitations of the even neutron configuration. Not much more can be said about the description of these states until the proton and neutron configurations are better known for this mass region.

VI. CONCLUSIONS

The level schemes for ^{93}Y, ^{93}Sr, and ^{93}Rb all provide greater detail for the decays of ^{93}Sr, ^{93}Rb, and ^{93}Kr than was presented in previous articles on these decays (26,28,34). In some cases, especially that of the ^{93}Rb decay, these details have a significant effect on the beta feeding of previously established levels. Changes in these beta feeding percentages, along with a re-evaluation of the Q-value information available, result in corresponding changes in the log*ft* values for these decays. Because of the changes in log*ft* values which occur it is possible to argue that it is consistent to assign negative parity for the low-lying levels in ^{93}Rb, to conform to the predictions of the shell model. The positive parity proposed by Achterberg, *et al.* (28) requires that they postulate the existence of a deformed nucleus in the case of ^{93}Rb.

Changes in the Q-values reported for the decays of ^{93}Sr and ^{93}Kr have also resulted from the present work. Based on the log*ft* values for the high-lying levels in ^{93}Sr it has been shown that a Q-value of 4.5 MeV is favored. A re-evaluation of the beta decay information provided by Clifford, *et al.* (21) has made it possible to calculate a more reliable Q-value for the decay of ^{93}Kr.

Further work is needed before reliable comparisons can be made with the single-particle shell model for this mass region. Measurement of the ground-state spins of ^{93}Kr, ^{93}Rb, and ^{93}Sr would be extremely useful in any comparison with the values predicted by the shell model. Once the ground-state spin-parity assignments have been made it would be helpful if ICC and angular correlation studies could be performed. This information would aid in the assignment of spins and parities for the excited levels observed in these decay schemes. New measurements of the internal conversion coefficients are especially needed for the 219.2-keV and 432.6-keV transitions in ^{93}Sr in order to determine if the 432-keV level they depopulate is actually a negative-parity state as suggested by Achterberg, et al. (28).

VII. APPENDIX A: EXPERIMENTAL NOTES

The gamma-ray energies used to determine the calibrations for the mixed spectra are presented in Table 21. The energies quoted are a weighted average of the values quoted by Greenwood, et al. (59,60,61), Multhauf and Tirsell (62), and Gunnink, et al. (63). The intensities quoted for these gamma rays by Gunnink, et al. (63), Camp and Meredith (64), Aubin, et al. (65), and Edwards et al. (66) were used to establish the detector efficiency curve required for the area-to-intensity conversion.

Table 21. Gamma-ray calibration sources.

Nuclide	Gamma-Ray Energies (keV)
^{56}Co	846.753, 1037.817, 1175.071, 1238.255, 1360.176, 1771.307, 1810.701, 1963.675, 2015.135, 2034.709, 2113.049, 2212.862, 2598.399, 3009.523, 3201.884, 3253.342, 3272.915, 3451.068, 3547.842
^{57}Co	122.063, 136.473
^{60}Co	1173.210, 1332.475
^{182}Ta	31.736, 42.715, 67.750, 84.680, 100.105, 116.418, 152.434, 156.387, 179.393, 198.356, 222.110, 229.322, 264.072, 1121.273, 1189.023, 1221.377, 1230.990, 1257.391, 1273.705, 1289.127, 1373.807, 1387.376
^{226}Ra	186.14, 241.96, 295.20, 351.92, 609.27, 665.40, 742.48, 768.35, 785.80, 806.16, 934.06, 1120.28, 1155.17, 1238.13, 1280.98, 1377.64, 1401,44, 1407.98, 1509.22, 1661.24, 1729.55, 1764.49, 1838.33, 1847.44, 2118.52, 2204.14, 2447.63

VIII. APPENDIX B: COMPUTER PROGRAMS

A. DISKRITE

Each data set was initially transferred from the analyzer memory to a seven-track magnetic tape. This tape was used to provide the input data for the various computer programs utilized in the data analysis. In order to provide a more durable and easily accessed form for the input data, the data sets were transferred from the magnetic tape to a private disk pack stored at the Iowa State Computation Center. The program DISKRITE was designed to perform the transfer of these data sets. It was also possible to correct individual channels and compensate for gain shifts before adding data sets using this program. The gain shift correction is linear, that is, if a peak occurs in channel X in one spectrum and channel X' in another the two are assumed to be related by the equation

$$X' = AX + B.$$

The values of A and B are calculated by the program based on the locations of a high- and a low-energy peak in each spectrum. The channel numbers of each data set are then shifted to make the peak locations correspond to those given for the first data set read in.

B. SKEWGAUS

The program SKEWGAUS was used to fit the large number of peaks observed in the Ge(Li) detector spectra data collected for this study. A recent report by W. C. Schick, Jr. (67) explains this program and its use in great detail so that only a sketch of this program will be presented here. The basic form for the function which is assumed to fit the Ge(Li) detector peaks is a Gaussian with an exponential tail on the low energy side. Because of the increased complexity resulting from several sources the complete function used is different for each of the three regions listed below:

Region I $(x < x_0 - \tau)$:

$$f = h[1 - t + a(-z-v)^N]\exp[v(v + 2z)] + ht$$

Region II $(x_0 - \tau < x < x)$:

$$f = h(1 - t)\exp(-z^2) + ht$$

Region III $(x_0 < x)$:

$$f = h(1 + bz^M)\exp(-z^2)$$

where

$$z = (x - x_0)/(\sqrt{2}\sigma)$$

$$v = \tau/(\sqrt{2}\sigma)$$

$$\sigma = (FWHM)/\sqrt{8\ln 2}\ .$$

The variable parameters used here are h, the peak height; x_0, the peak centrcid; FWHM, the full width at half maximum of the Gaussian; τ, the distance from the centroid to the junction of regions I and II; t, the ratio of the tail

height to peak height; a, the lower skewness parameter; and b, the upper skewness parameter.

In most cases the upper and lower skewness parameters were not needed and were set equal to zero. The tail parameter was used only for a few intense low-energy peaks. The values of FWHM and τ were linearized as functions of energy based on the best fits of several intense peaks in the spectrum.

Initial estimates are required for all parameters but if the fit includes only one peak the program calculates these estimates itself. If more than one peak is to be fit the user need only supply estimates for the peak centroids. The peak background may be assumed to be either linear or quadratic and may be fit separately or along with the peak. A standard nonlinear least squares method is used to find the best fit to the data points. Punched card output consisting of peak height, centroid, area and their associated errors can be obtained for input to the program DRUDGE.

C. DRUDGE

The program DRUDGE is a secretary program used to carry out the number-crunching of converting peak centroids and areas to energies, intensities and uncertainties. The energy calibration is calculated by the program using a series of points specified by (channel, energy) pairs. The nonlinearity of the detectors, amplifiers, and ADC's can be accounted

for by comparing the "true" gamma-ray energies with the least square energies, E(LSQ), determined from the energy calibration line. The difference between these two values is E(NONLIN). A nonlinearity curve is input to the program in the form of a series of points (E(LSQ),E(NONLIN)). This curve is then used by the program to correct for such nonlinearity.

A table of detector efficiency as a function of energy must be input to the program in order to complete the area-to-intensity conversion. Since a 1/4" thick plastic disk is used to protect the end of the Ge(Li) detector a table of relative attenuations versus energy is also required as input to the program. Between the input points a log-log interpolation is used to determine the detector efficiency and external attenuation.

The gamma-ray energy uncertainties are determined from the expression

$$\Delta E = \mathrm{SQRT}((2\sigma_x)^2 + (\sigma_a^2 - \sigma_{ab}^2 x + \sigma_b^2 x^2) + \sigma_e^2)$$

where σ_x is the standard deviation of the centroid, σ_e is the uncertainty in the energy nonlinearity, σ_a^2, σ_b^2, and σ_{ab}^2 are the uncertainties and covariance of the least square line parameters. The gamma-ray intensity uncertainties are determined assuming the uncertainty in the peak area is due mostly to errors in the peak height. As a result the expression

used is

$$\Delta I = A * SQRT((2\sigma_H/H)^2 + (0.05)^2)$$

where a 5% detector efficiency uncertainty is assumed.

D. BUFFTAPE

The program BUFFTAPE is used to run gates on the buffer tapes on which the coincidence information is stored. Information exists on the tapes in the form of A/B pairs of channels. The program allows the user to gate on either the A or the B members of the pairs. Up to 255 bands can be run during a single execution of the program. A maximum of 10^5 counts can be stored in a single channel of the output spectrum provided by this program.

E. LVLSURCH

This program was used to extend the decay schemes using the energies of previously known levels and the energies of the unplaced gamma rays. Possible new levels are found which have transitions with old levels and then a search is made to place gamma-ray transitions between new levels.

The criteria required for placing a gamma-ray transition were 1) that it match the energy difference between two levels to within the limit (DEL), 2) that it not have been placed previously, 3) that it have no crossover (coincidence) violations with previous placements. A new level is kept only if 1) its energy lies between the limits ELL and EHH and

is at least 2*DEL distant from other levels, 2) is defined by at least LNIT transitions, and 3) has at least one transition depopulating the level.

F. Auxiliary Programs

The program TICC was used to calculate the total internal conversion coefficients for the gamma-ray transitions observed in this study. The program is a modified version of the spline interpolation used by Hager and Seltzer (53). It also allows the user to calculate internal conversion coefficients for transitions of mixed multipolarity.

LEAF is a secretary type program used to calculate level energies and the per cent beta branching to each level. A list of gamma-ray energies and intensities, internal conversion coefficients, and the per cent ground-state beta feeding are required as input to the program. The gamma-ray energies are used to determine the level energies and the gamma-ray intensity imbalances determine the beta branching.

The program BRUTAL was used to locate peaks in the coincidence spectra and calculate their energies and intensities. In order to complete the peak location-to-energy and area-to-intensity conversions the program requires the input of the energy calibration and a detector efficiency curve. The intensity of each peak in the "gate" spectrum is then compared with its intensity in the "background" spectrum in order to determine if there is a significant change in inten-

sity. Since it is possible for the program to miss peaks, especially in the regions where the background count is low, each spectrum was also checked visually to insure that all the peaks were found. The details on the execution of this program have been reported by Gunnink, et al. (68); therefore they will not be repeated here.

The program LOGFT was used to calculate the Fermi function for each of the levels fed in beta decay. The half-life of the parent nucleus, the atomic number and atomic weight of the daughter nucleus, and the Q-value for the decay are required as input to the program. Using this information along with the energy and per cent beta feeding of each level the program calculates the logft values for both statistical and first forbidden unique shapes. It is also possible to correct for atomic screening, and this has been done for the logft values reported here. This correction has the greatest effect for high energy levels lying close to the Q-value for beta decay.

IX. LITERATURE CITED

1. J. Chadwick, "Possible existence of a neutron," Nature 129, 312 (1932).

2. E. Fermi, "Possible production of elements of atomic number higher than 92," Nature 133, 898 (1934).

3. O. Hahn and F. Strassman, "Uber den Nachweis und das Verhalten der bei der Bestrahlung des Urans mittels Neutronen entstehenden Erdalkalimetalle," Naturwiss. 27, 11 (1939).

4. O. Hahn and F. Strassman, "Nachweis der Entstehung aktiver Bariumisotope aus Uran und Thorium durch Neutronenbestrahlung; Nachweis weiterer aktiver Bruchstucke bei der Uranspaltung," Naturwiss. 27, 89 (1939).

5. L. Meitner and O. R. Frisch, "Disintegration of uranium by neutrons: a new type of nuclear reaction," Nature 143, 239 (1939).

6. O. R. Frisch, "Physical evidence for the division of heavy nuclei under neutron bombardment," Nature 143, 276 (1939).

7. V. S. Ramamurthy and R. Ramanna, "Mass and charge distributions in fission," in Proceedings of the Second IAEA Symposium on the Physics and Chemistry of Fission, (IAEA, Vienna, 1969), p. 41.

8. R. Vandenbosch and J. R. Huizenga, Nuclear Fission, (Academic Press, Inc., New York, 1973).

9. E. A. C. Crouch, "Calculated independent yields in thermal neutron fission of ^{233}U, ^{235}U, ^{239}Pu, ^{241}Pu, and in fission of ^{232}Th, ^{238}U, and ^{240}Pu," United Kingdom Atomic Energy Authority Report AERE-R-6056, (1969, unpublished).

10. W. L. Talbert, Jr., A. B. Tucker, and G. M. Day, "Delayed neutron emission in the decays of short-lived separated isotopes of gasecus fission products," Phys. Rev. 177, 1805 (1969).

11. K. H. Bhatt and J. B. Ball, "Nuclear spectroscopy of the isotopes of Nb, Mo, and Tc," Nucl. Phys. 63, 286 (1965).

12. T. A. Hughes, "Nuclear structure of ^{88}Sr and ^{89}Sr," Phys. Rev. 181, 1586 (1969).

13. J. Vervier, "Effective nucleon-nucleon interactions in Y, Sr, Nb, Mo and Tc isotopes," Nucl. Phys. 75, 17 (1966).

14. N. Auerbach, "Particle-core coupling in ^{89}Sr," Phys. Lett 270, 127 (1968).

15. S. Cohen, R. D. Lawson, and M. H. MacFarlane, "The effective interaction and identical-nucleon seniority for nuclei near ^{90}Zr," Phys. Lett. 10, 195 (1964).

16. I. Talmi and I. Unna, "Energy levels and configuration interaction in ^{90}Zr and related nuclei," Nucl. Phys. 19, 225 (1960).

17. J. M. Eisenberg and W. Greiner, Nuclear Theory, Vol. 1, (North-Holland Publishing Co., Amsterdam, 1970).

18. S. A. E. Johansson, "Gamma de-excitation of fission fragments," Nucl. Phys. 64, 147 (1965).

19. E. Cheifetz, R. C. Jared, S. G. Thompson, J. B. Wilhelmy, "Angular momentum of primary products formed in the spontaneous fission of ^{252}Cf," Phys. Rev. C5, 2041 (1972).

20. J. W. Grueter, K. Sistemich, P. Armbruster, J. Eidens, and H. Lawin, "Identification of μs-isomers among primary fission products," Phys. Lett. 33B, 474 (1970).

21. J. W. Grueter, Kernforschungsanlange Julich, Institut fur Neutronenphysik, Report No. Jul-879-NP, (1972, unpublished).

22. P. Cavallini, F. Schussler, and A. Moussa, "Niveau excite metastable dans l'yttrium 93," C. R. Acad. Sc. Paris 272, 394 (1971).

23. C. Lieber, "Die Spaltprodukte aus der Bestrahlung des Urans mit Neutronen: die Strontium-Isotope," Naturwiss. 27, 421 (1939).

24. G. C. Carlson, W. C. Schick, Jr., W. L. Talbert, Jr., and F. K. Wohn, "Half-lives of some short-lived mass separated gaseous fission products and their daughters," Nucl. Phys. A125, 267 (1969).

25. H. Bakhru and S. K. Mukherjee, "The decay of ^{93}Sr and the gamma spectrum of ^{93}Y," Nucl. Phys. 61, 56 (1965).

26. W. Herzog and W. Grimm, "Der Zerfall des ^{93}Sr," Z. Physik 257, 424 (1972).

27. B. M. Preedom, E. Newman, and J. C. Hiebert, "(d,^{3}He) Reactions on the even-even Zirconium isotopes," Phys. Rev. 166, 1156 (1967).

28. E. Achterberg, F. C. Iglesias, A. E. Jech, J. A. Moragues, D. Otero, M. I. Perez, A. N. Proto, J. J. Rossi, and W. Scheuer, "Levels of ^{93}Rb, ^{93}Sr, and ^{93}Y fed in the decays of ^{93}Kr, ^{93}Rb, and ^{93}Sr," Phys. Rev. C10, 2526 (1974).

29. V. R. Casella, J. D. Knight, and R. A. Naumann, "E3 isomers of ^{93}Y and ^{101}Ag," Nucl. Phys. A239, 83 (1975).

30. K. Fritze and T. J. Kennett, "The identification of fission-product ^{92}Rb and ^{93}Rb," Can. J. Phys. 38, 1614 (1960).

31. C. R. Dillard, R. M. Adams, H. Finston and A. Turkevich, "Determination of gas half-lives by the charged wire technique (11)," in The Fission Products, edited by C. D. Coryell and N. Sugarman, (National Nuclear Energy Series, Division IV, 1951).

32. J. R. Clifford, W. L. Talbert, Jr., F. K. Wohn, J. P. Adams, and J. R. McConnell, "Decay energies of gaseous fission products and their daughters for A = 88 to 93," Phys. Rev. C7, 2535 (1973).

33. M. I. Macias-Marques, R. Foucher, M. Caillian, and J. Belhassen, "Mass-differences in the neutron-rich Sr region," CERN Report No. 70-30, Vol. 1, 321 (1970).

34. R. Brissot, F. Schussler, E. Monnand, and A. Moussa, "Niveaux de ^{93}Rb et ^{93}Sr alimentes dans les desintegrations de ^{93}Kr et ^{93}Rb," Nucl. Phys. A238, 149 (1975).

35. G. T. Garvey, I. Kelson, W. J. Gerace, R. L. Jaffe, and I. Talmi, "Set of nuclear-mass relations and a resultant mass table," Rev. Mod. Phys. Suppl. 41, S1 (1969).

36. P. A. Seeger, "Deformable mass formula and fission data," in Atomic Masses and Fundamental Constants, edited by J. H. Sanders, (Plenum Press, London, 1972).

37. A. H. Wapstra and N. B. Gove, "The 1971 atomic mass evaluation," Nucl. Data A9, 265 (1971).

38. E. L. Brady and N. Sugarman, "Short-lived Krypton and Xenon isotopes," in The Fission Products, edited by C. D. Coryell and N. Sugarman, (National Nuclear Energy Series, Division IV, 1951).

39. B. Selikson and J. M. Siegel, "Note on the mass number of 10h $Y^{(93)}$," in The Fission Products, edited by C. D. Coryell and N. Sugarman, (National Nuclear Energy Series, Division IV, 1951).

40. L. E. Glendenin, C. D. Coryell, and R. R. Edwards, "Distribution of nuclear charge in fission," in The Fission Products, edited by C. D. Coryell and N. Sugarman, (National Nuclear Energy Series, Division IV, 1951).

41. J. R. McConnell and W. L. Talbert, "The TRISTAN on-line isotope separator facility," (To be published in Nucl. Instrum. and Methods).

42. J. H. Norman, W. L. Talbert, and D. M. Roberts, "Optimizing activity separation in fission product decay chains," U. S. Atomic Energy Commission Report IS-1893 (Iowa State Univ., Ames) 1968.

43. S. Raman and N. B. Gove, "Rules for spin and parity assignments based on logft values," Phys. Rev. C7, 1995 (1973).

44. N. B. Gove, "Beta and gamma transition probabilities," in Nuclear Spin-Parity Assignments, edited by N. B. Gove and R. L. Robinson, (Academic Press, New York, 1966).

45. M. D. Glascock, "Gamma-ray decay schemes for ^{91}Kr and ^{91}Rb," Ph. D. thesis, Iowa State University, (1975, unpublished).

46. G. H. Carlson, W. L. Talbert, and J. R. McConnell, "Decay of mass-separated ^{138}Xe and ^{138}Cs," Phys. Rev. C9, 283 (1974).

47. E. Achterberg, F. C. Iglesias, A. E. Jech, J. A. Moragues, D. Otero, M. L. Perez, A. N. Proto, J. J. Rossi, W. Scheuer, and J. F. Suarez, "Levels of ^{138}Cs fed in the beta decay of ^{138}Xe," Phys. Rev. C7, 365 (1973).

48. D. C. Kocher, "Nuclear Data Sheets for A = 93," Nuclear Data Sheets, B8, 527 (1972).

49. M. G. Mayer and J. H. D. Jensen, Elementary Theory of Nuclear Structure, (John Wiley and Sons, Inc., New York, 1955).

50. A. Bohr and B. R. Mottelson, Nuclear Structure, Vol. 1, (W. A. Benjamin, Inc., New York, 1969).

51. D. J. Horen and W. B. Ewbank, Nuclear Level Schemes A = 45 through A = 257 from Nuclear Data Sheets, edited by Nuclear Data Group, Oak Ridge National Laboratory, (Academic Press, New York, 1973).

52. R. Muller, "Die Drei-Nukleonen-Transfer-Reaktion an den geraden Zirkon-Isotopen," Ph.D. thesis, Technischen Universitat Munchen, (1973, unpublished).

53. R. S. Hager and E. C. Seltzer, "Internal conversion tables, part I: K-, L-, M-shell conversion coefficients for Z = 30 to Z = 103," Nuclear Data 4, 41 (1968).

54. E. Achterberg, F. C. Iglesias, A. E. Jech, J. A. Moragues, D. Otero, M. L. Perez, A. N. Proto, J. J. Rossi, and W. Scheuer, "Levels of ^{91}Rb and ^{91}Sr fed in the decay of ^{91}Kr and ^{91}Rb," Phys. Rev. C9, 229 (1974).

55. F. K. Wohn, W. L. Talbert, Jr., R. S. Weinbeck, M. D. Glascock, and J. K. Halbig, "Internal-conversion coefficient determination of odd parity for the 108.8-keV first-excited state of ^{91}Rb," Phys. Rev. C11, 1455 (1975).

56. E. A. Henry, W. L. Talbert, Jr., and J. R. McConnell, "Gamma-ray decay schemes for ^{89}Kr and ^{89}Rb," Phys. Rev. C7, 222 (1973).

57. L. R. Medsker, "Nuclear Data Sheets for A = 97," Nuclear Data Sheets 10, 1 (1973).

58. L. R. Medsker, "Nuclear Data Sheets for A = 99," Nuclear Data Sheets 12, 431 (1974).

59. R. C. Greenwood, R. G. Helmer, and R. J. Gehrke, "Precise comparison and measurement of gamma-ray energies with Ge(Li) detector I. 50-420 keV," Nucl. Instrum. and Methods 77, 141 (1970).

60. R. G. Helmer, R. C. Greenwood, and R. J. Gehrke, "Precise comparison and measurement of gamma-ray energies with a Ge(Li) detector II. 400-1300 keV," Nucl. Instrum. Methods 96, 173 (1971).

61. R. C. Greenwood, R. G. Helmer, and R. J. Gehrke, private communication (1974).

62. L. Multhauf and K. G. Tirsell, private communication (1974).

63. R. Gunnink, J. B. Niday, R. P. Anderson, and R. A. Meyer, "Gamma-ray energies and intensities," USAEC Report No. UCID-15439, (1969, unpublished).

64. D. C. Camp and G. L. Meredith, "The decays of ^{56}Co and ^{66}Ga and precise gamma-ray intensities," Nucl. Phys. A166, 349 (1971).

65. G. Aubin, J. Barrette, M Barrette, and S. Monaro, "Precision measurements of gamma-ray intensities and energies in the decay of $^{152\ 154}$Eu, ^{56}Co, ^{110}Ag, and ^{125}Sb," Nucl. Instrum. Methods 76, 93 (1969).

66. W. F. Edwards, F. Boehm, J. Rogers, and E. J. Seppi, "Relative intensities for gamma rays following the decay of ^{182}Ta and ^{183}Ta," Nucl. Phys. 63, 97 (1965).

67. W. C. Schick, Jr., "SKEWGAUS: A FORTRAN program for fitting peaks in semidonductor spectra," U. S. Atomic Energy Commission Report IS-3460, (1974, unpublished).

68. R. Gunnink, H. B. Levy, and J. B. Niday, "Identification and determination of gamma emitters by computer analysis of Ge(Li) spectra," U. S. Atomic Energy Commission Report UCID-15140, (1967, unpublished).

X. ACKNOWLEDGEMENTS

The author would like to express his sincere appreciation for the assistance provided by the following people in completing this work:

Dr. W. L. Talbert, Jr. for initially suggesting a study of the A = 93 decay chain and providing the guidance necessary to complete that study. He also devoted a great deal of time and interest to provide constructive comments and criticisms during the writing of this thesis. The lucidness of this work is largely due to his continued efforts.

Dr. W. C. Schick for stimulating my interest in the field of nuclear physics and for his help and suggesticns while data accumulation and analysis were being performed.

Drs. J. C. Hill and F. K. Wohn for helpful discussions and comments throughout this study.

My colleagues, Drs. J. A. Morman, J. F. Wright, L. J. Alquist, and M. D. Glascock for providing many useful suggestions and some remarks that were not so useful.

J. R. McConnell, D. R. Lekwa, M. A. Cullison, and A. R. Landin for their efforts in work with the TRISTAN facility. The latter two along with E. Struble and D. Berglund are to be thanked for their efforts to point out to me the statistical probability of being dealt a double flush.

All of the other members of Nuclear Physics Group VII for their assistance.

Finally, my love and thanks to Mary Jean whose unending support and assistance made it possible for me to bridge troubled waters. Without her the completion of this work would be meaningless.